

# **MODELING CO<sub>2</sub> SEQUESTRATION AND ENHANCED GAS RECOVERY IN COMPLEX UNCONVENTIONAL RESERVOIRS**

Foteini Vasilikou

Dissertation submitted to the faculty of the Virginia Polytechnic Institute and State  
University in partial fulfillment of the requirements for the degree of

Doctor of Philosophy  
In  
Mining Engineering

Michael E. Karmis, Co-Chair

Nino S. Ripepi, Co-Chair

Zacharias G. Agioutantis

Gerald H. Luttrell

Kramer D. Luxbacher

May 06, 2014

Blacksburg, VA

Keywords: coalbed methane, carbon dioxide, reservoir modeling, unconventional  
reservoirs

©2014, Foteini Vasilikou

# MODELING OF CO<sub>2</sub> SEQUESTRATION AND ENHANCED GAS RECOVERY IN COMPLEX UNCONVENTIONAL RESERVOIRS

Foteini Vasilikou

## ABSTRACT

Geologic sequestration of CO<sub>2</sub> into unmineable coal seams is proposed as a way to mitigate the greenhouse gas effect and potentially contribute to economic prosperity through enhanced methane recovery.

In 2009, the Virginia Center for Coal and Energy Research (VCCER) injected 907 tonnes of CO<sub>2</sub> into one vertical coalbed methane well for one month in Russell County, Virginia (VA). The main objective of the test was to assess storage potential of coal seams and to investigate the potential of enhanced gas recovery. In 2014, a larger scale test is planned where 20,000 tonnes of CO<sub>2</sub> will be injected into three vertical coalbed methane wells over a period of a year in Buchanan County, VA.

During primary coalbed methane production and enhanced production through CO<sub>2</sub> injection, a series of complex physical and mechanical phenomena occur. The ability to represent the behavior of a coalbed reservoir as accurately as possible via computer simulations yields insight into the processes taking place and is an indispensable tool for the decision process of future operations. More specifically, the economic viability of projects can be assessed by predicting production: well performance can be maximized, drilling patterns can be optimized and, most importantly, associated risks with operations can be accounted for and possibly avoided.

However, developing representative computer models and successfully simulating reservoir production and injection regimes is challenging. A large number of input parameters are required, many of which are uncertain even if they are determined experimentally or via in-situ measurements. Such parameters include, but are not limited to, seam geometry, formation properties, production constraints, etc.

Modeling of production and injection in multi-seam formations for hydraulically fractured wells is a recent development in coalbed methane/enhanced coalbed methane (CBM/ECBM) reservoir modeling, where models become even more complex and demanding. In such cases model simulation times become important.

The development of accurate simulation models that correctly account for the behavior of coalbeds in primary and enhanced production is a process that requires attention to detail, data validation, and model verification. A number of simplifying assumptions are necessary to run these models, where the user should be able to balance accuracy with computational time.

In this thesis, pre- and post-injection simulations for the site in Russell County, VA, and preliminary reservoir simulations for the Buchanan County, VA, site are performed. The concepts of multi-well, multi-seam, explicitly modeled hydraulic fractures and skin factors are incorporated with field results to provide accurate modeling predictions.

## **DEDICATION**

This dissertation is dedicated to my beloved mother Alkioni Vasilikou, my father Constantinos Vasilikos and my brother Ioannis Vasilikos, M.D., Ph.D., who never left my side and taught me that “where there’s a will, there’s a way.”

## **ACKNOWLEDGMENTS**

There are no words to express my gratitude to all the people who have supported me in this challenging period of my life. I sincerely thank Professor Michael Karmis for his guidance and advice in all aspects of my educational and professional life. Without his support I wouldn't be here.

I would like to thank Dr. Nino Ripepi for his support during the past three years. He has been an excellent advisor and teacher and helped me overcome many difficulties along this journey.

I cannot thank enough Professor Zach Agioutantis for his skill, teaching, motivation, guidance and patience. Professor Agioutantis has been an amazing mentor.

I would like to express my gratitude to Dr. Kray Luxbacher for her advice and guidance, and to Professor Gerry Luttrell who was the first person to welcome me to the Mining Engineering Department and guide my studies.

A special thank you to Steve Schafrik, whose exceptional technical and coding skills were of utmost importance in this effort.

I would also like to thank Dr. Cigdem Keles for her valuable help and support with the reservoir modeling.

Finally, a big "Thank you" to everyone at the Virginia Center for Coal and Energy Research who has contributed with their support in this work and especially my dear friend and advisor Dr. John Craynon.

I would also like to express my love for my amazing mother Alkioni, who never left my side and crossed the Atlantic Ocean numerous times to be by my side; to my cousin, Dr. Demetrios Vavvas, who has been a father, an advisor and a friend to me; and to my brother Ioannis for his constant love and support.

I am thankful to my friends Christos, Constantinos and Korina for always being there for me.

## TABLE OF CONTENTS

<b>Abstract</b>	<b>ii</b>
<b>Dedication</b>	<b>iv</b>
<b>Acknowledgments</b>	<b>v</b>
<b>Table of Contents</b>	<b>vi</b>
<b>List of Tables</b>	<b>ix</b>
<b>List of Figures</b>	<b>x</b>
<b>Preface</b>	<b>xiii</b>
<b>The Application of Constitutive Laws to Model the Dynamic Evolution of Permeability in Coal Seams for the Case of CO<sub>2</sub> Geologic Sequestration and Enhanced Coal Bed Methane Recovery</b>	<b>1</b>
Abstract	1
Introduction	2
Coalbed Characteristics	3
Coalbed Methane and Enhanced Coalbed Methane Production Mechanisms	5
Permeability Models	6
Discussion on Implementation of Permeability Models for Reservoir Simulation	17
Conclusions	19
Acknowledgements	20
Nomenclature	20
References	21
<b>Experiences in Reservoir Model Calibration for Coal Bed Methane Production in Deep Coal Seams in Russell County, Virginia</b>	<b>27</b>
Abstract	27
Introduction	28
Geology	30
Well Stimulation	31

Production History _____	34
Modeling _____	35
<i>Description of Production Model</i> _____	35
Results and Discussion _____	40
Conclusions _____	44
Acknowledgments _____	45
References _____	45
<b>Model Verification of Carbon Dioxide Sequestration in Unmineable Coal Seams with Enhanced Coalbed Methane Recovery _____</b>	<b>47</b>
Abstract _____	47
Introduction _____	48
Field Description _____	49
<i>Field Site Layout</i> _____	50
CO <sub>2</sub> Injection _____	50
<i>Injection Logging</i> _____	51
<i>Monitoring Well Results</i> _____	52
Reservoir Modeling _____	52
<i>Theoretical Considerations for the Skin Factor and         the Hydraulic Fracture Approach</i> _____	53
<i>The Importance of Relative Permeability</i> _____	54
<i>History Match</i> _____	55
Results and Discussion _____	56
Conclusions _____	59
Acknowledgments _____	59
References _____	60
<b>Reservoir Simulations for Coal Bed Methane (CH<sub>4</sub>) Production and Carbon Dioxide (CO<sub>2</sub>) Injection in Deep Coal Seams in Buchanan County, Virginia _____</b>	<b>62</b>
<i>Reservoir Model Calibration for Coal Bed Methane Production     from Deep Coal Seams in Buchanan County, Virginia</i> _____	62
Abstract _____	62

Introduction _____	63
Geology _____	63
Well Stimulation _____	65
Production History _____	65
Description of Reservoir Model _____	67
<i>18- Layer Models</i> _____	68
<i>5-Zone Model</i> _____	73
Results and Discussion _____	74
<i>Initial Volumetrics</i> _____	74
<i>Production Mechanism</i> _____	79
Conclusions _____	81
<b><i>CO<sub>2</sub> Injection Model for Enhanced Coalbed Methane</i></b>	
<b><i>Recovery in Deep Coal Seams in Buchanan County, VA</i></b> _____	82
Abstract _____	82
Development of Reservoir Models _____	82
Results and Discussion _____	89
<i>S Models</i> _____	90
<i>L Models</i> _____	96
Conclusions _____	103
Acknowledgements _____	103
References _____	104
<b>Summary and Conclusions _____</b>	<b>107</b>
Further Work _____	110
Recommendations for Transferring Lessons Learned	
from Coalbed Methane Modeling to Shale Gas Modeling _____	111

## LIST OF TABLES

Table 1 - BD114 Stimulated Coal Seams (VaDMME, 2002) _____	33
Table 2 - Parameters and Material Properties Used in the Reservoir Model _____	37
Table 3 - Optimal Parameters Determined for the Dingle-Well Runs _____	40
Table 4 - Parameter Range Used as Input in the CMOST Model Runs _____	42
Table 5 - Optimal Parameters After CMOST Runs and Manual Adjustments for the Multi-Well Runs _____	43
Table 6 - Parameters and Material Properties Used in the 18-Layer Reservoir Model _____	70
Table 7 - Set of Parameters Varied in Simulations for Cases C1 to C11 _____	71
Table 8 - Input Parameters for Modeling Hydraulic Fractures in Scenarios H1, H2, H3, H4 ____	73
Table 9 - Parameters and Material Properties Used in the 5-Zone Reservoir Model _____	74
Table 10 - Reference Names and Production Start Dates for the Coalbed Methane Wells Included in the Simulations _____	83
Table 11 - Layers Number, Coal Seam Names, Thicknesses and Top Elevations for the Geologic Structure Assumed for the Study Area _____	85
Table 12 - Input Parameters for the Combined and Four-Well Models _____	86
Table 13 - CO <sub>2</sub> Flowback at the Injectors and CO <sub>2</sub> Breakthrough at the Offset Well for the (S) Models for Projection Time to Year 2023 _____	95
Table 14 - Cumulative CH <sub>4</sub> Production for the (S) Models for the Base (S1), Skin (S2) and Hydraulic Fractures (S3) Scenarios for Projection Time to Year 2023 _____	95
Table 15 - Cumulative Gas Production (CGP) for All Wells for Cases, L1a, L1b, L2a, L1c _	101
Table 16 - CO <sub>2</sub> Flowback and Breakthrough for Cases, L1a, L1b, L2a, L1c _____	102

## LIST OF FIGURES

Figure 1 - Face and Butt Cleats _____	4
Figure 2 - The Matchstick Model _____	8
Figure 3 - Different Modes of Coupled Simulation (a, b, c) and Uncoupled Simulation (d) ____	10
Figure 4 - Uniaxial Strain Model _____	11
Figure 5 - Fracture Aperture Changes with Swelling/Shrinkage _____	11
Figure 6 - Matchstick Model with Bridging Between Coal Blocks _____	16
Figure 7 - Domain Discretization _____	18
Figure 8 - Case Study Area Showing Injection Wells _____	18
Figure 9 - Initial Attempts for Coupled Simulation Using an External Geomechanics Package (Vasilikou et al., 2012) _____	19
Figure 10 - Location of Field Test Site (Ripepi et al, 2009) _____	29
Figure 11 - Layout of Injection and Offset Wells (Karmis et al., 2008) _____	29
Figure 12 - (A) Rose Diagram Showing Face and Butt Cleat Orientation (B) Rotation by 35° Clockwise _____	31
Figure 13 - Gas Production History at the Injection and the Offset Wells _____	34
Figure 14 - 3D View of Model Grid and Wells _____	36
Figure 15 - Relative Permeability Curves Used in the Single Well Runs (Gash et al. 1993, Mavor et al. 1953) (SWT: Water Relative Permeability or Water Saturation Fraction; SLT: Gas Relative Permeability or Gas Saturation Fraction) (see Table 2) _____	38
Figure 16 - Face Cleat Permeability Regions for Single-Well Models and Combined Model _	39
Figure 17 - Butt Cleat Permeability Regions for Single-Well Models and Combined Model __	39
Figure 18 - History Match on Gas and Water Rates for Well BD-115 (RU-132) Under a Single Well Run. The Bottom Hole Pressure is Also Shown _____	41
Figure 19 - History Match of Gas and Water Rates for Well BD-115 (RU-132) for the Combined Run. The Bottom Hole Pressure is Also Shown _____	41
Figure 20 - Relative Permeability Curves as Determined by the Optimization Algorithm for Two of the Eight Production Wells (SWT: Water Relative Permeability or Water Saturation Fraction; SLT: Gas Relative Permeability or Gas Saturation Fraction) _____	43

Figure 21 - History Match on Gas and Water Rates for Well BD-115 (RU-132) for the Combined Run with Optimized Input Parameters. The Bottom Hole Pressure is Also Shown	44
Figure 22 - (A) Rose Diagram Showing Face and Butt Cleat Orientation (B) Rotation by 35° degrees clockwise	51
Figure 23 - Typical Relative Permeability Curves for Two Wells	54
Figure 24 - Relative Permeability Curves for the HF and SF Models	55
Figure 25 - Face Cleat Permeability Variation for the Base Model	56
Figure 26 - Typical HF Discretization for All Wells	56
Figure 27 - Cumulative Water Production vs. Measured Data for Well BC-115 (RU-123) for All Models	57
Figure 28 - Gas Rate and Cumulative Gas during CO <sub>2</sub> Injection into Well BD 114 (RU 84)	58
Figure 29 - CO <sub>2</sub> Plume around Injection Well Immediately After Injection Has Been Completed In the HF Model	58
Figure 30 - Daily Gas Production Rate of the Injection Wells	66
Figure 31 - Daily Water Production Rate of the Injection Wells	67
Figure 32 - (A) 18-Layer Model, (B) 5-Zone Model	68
Figure 33 - History Matching of Monthly Gas Rate and Cumulative Gas for Well DD7 Up to Year 2013	69
Figure 34 - Langmuir Adsorption Isotherms for Langmuir Volume Constants 500, 650, 800 scf/ton and Langmuir Pressure Constants 100 and 333 psi; Maximum and Minimum Pore Pressures in the Reservoir for Pressure Gradients 0.315 and 0.36 psi/ft	71
Figure 35 - Different Scenarios for the Relative Permeability Curves to Water and Gas	72
Figure 36 - Original Gas in Place in the Model and Initially Adsorbed Gas on the Coal Matrix for All Cases (C)	76
Figure 37 - Original Water in Place for All Cases (C)	76
Figure 38 - Coal Matrix Volume per Layer Starting from the Shallowest (Layer 1) to the Deepest (Layer 18) Seam for Cases C3 and C11	77
Figure 39 - Minimum and Maximum Pore Pressures per Layer for Two Different Pressure Gradients Used In C Cases	77
Figure 40 - Initially Adsorbed Gas per Layer for Cases C3, C5 and C8	78
Figure 41 - Originally Adsorbed Gas per Layer for the 5-Zone Model	80

Figure 42 - Originally Adsorbed Gas per Layer for the 18-Layer Model _____	81
Figure 43 - Relative Permeability Curves to Water and Gas as Determined Through History Matching Gas Production for All the Wells in the Study Area _____	89
Figure 44 - Gas Rate at Surface Conditions for the Three Injectors, DD7, DD7A, and DD8 throughout History Matching, Injection and Forecasting to Year 2023 _____	90
Figure 45 - (A) Cumulative Gas Production per Layer Up to Year 2013 and (B) CO <sub>2</sub> Adsorption per Layer during Injection and Post Injection Up to Year 2023 for Scenario S3 _____	93
Figure 46 - CO <sub>2</sub> Adsorption Profile in gmole/ft <sup>3</sup> at Layer 4 for Scenarios (A) S1 Base, (B) S2 Skin and (C) S3 Hydraulic Fractures Scenario _____	94
Figure 47 - Gas Mass Rate of Injected CO <sub>2</sub> at Surface Conditions Versus Time for the Injection Scenarios L1 and L2 _____	97
Figure 48 - Pressure-Temperature Phase Diagram for CO <sub>2</sub> and Bottom Hole Pressures at Injection Well DD7 for Injection Plans L1a, L1b, and L1 _____	98
Figure 49 - Cumulative Gas Production of All the Wells in the Study Area for All Cases Examined for the (L) Models _____	99

## **PREFACE**

This research effort comprises the four major tasks summarized below. These tasks are addressed in a set of scholarly works which are either published or will be submitted for publication.

### **Task 1. Investigation of dynamic evolution permeability models**

The main objectives for Task 1 are to:

- a) Critically review permeability change models which are proposed in the literature for coalbeds with respect to primary and enhanced production.
- b) Implement a permeability change model in single well models by coupling a reservoir simulator and appropriate geomechanical code.

### **Task 2. Sensitivity analysis for numerical models**

The main objectives for Task 2 are to:

- a) Perform sensitivity analyses to study the behavior of the reservoir models when production and injection occur in multiple zones.
- b) Examine the response of the reservoir models with respect to varying input parameters that affect the volumetrics properties.
- c) Validate well and reservoir characteristics in the models that have an effect on the production mechanism.

### **Task 3. Comparison of different approaches that model well stimulation in reservoir simulations**

The main objectives for Task 3 are to:

- a) Develop models where a negative skin factor is assigned.
- b) Explicitly model hydraulic fractures in reservoir models.
- c) Study and compare enhanced flow properties and the effect on injection depending on the well stimulation approach.

### **Task 4. Predict enhanced methane recovery, CO<sub>2</sub> flowback and breakthrough**

The main objectives for Task 4 are to:

- a) Develop full field scale models and incorporate all key modeling elements for coalbeds.
- b) History-match the final models and create the final baseline model.
- c) Predict enhanced methane recovery at the injectors and offset wells.
- d) Predict CO<sub>2</sub> plumes and potential breakthrough.

# THE APPLICATION OF CONSTITUTIVE LAWS TO MODEL THE DYNAMIC EVOLUTION OF PERMEABILITY IN COAL SEAMS FOR THE CASE OF CO<sub>2</sub> GEOLOGIC SEQUESTRATION AND ENHANCED COAL BED METHANE RECOVERY<sup>1</sup>

*Foteini Vasilikou, Virginia Center for Coal and Energy Research, Virginia Tech,  
Blacksburg, VA*

*Nino Ripepi, Virginia Center for Coal and Energy Research, Virginia Tech,  
Blacksburg, VA*

*Zach Agioutantis, Virginia Center for Coal and Energy Research, Virginia Tech,  
Blacksburg, VA*

*Michael Karmis, Virginia Center for Coal and Energy Research, Virginia Tech,  
Blacksburg, VA*

## **Abstract**

Injection and storage of carbon dioxide (CO<sub>2</sub>) in deep unmineable coalbeds decreases anthropogenic greenhouse gas emissions and presents a financially viable solution by enhancing recovery of coalbed methane (ECBM). Coalbeds are commonly characterized by a dual porosity system, which is comprised of a network of natural fractures (cleats) and matrix blocks of coal exhibiting highly heterogeneous porosity. The gas transport through the cleat system is governed by Darcy's Law. This study reviews and critically evaluates available models for describing coalbed permeability that can be applied to calculate gas flow in such systems. In addition, the

---

<sup>1</sup> The Application of Constitutive Laws to Model the Dynamic Evolution of Permeability in Coal Seams for the Case of CO<sub>2</sub> Geologic Sequestration and Enhanced Coal Bed Methane Recovery. F. Vasilikou, N. Ripepi, Z. Agioutantis, M. Karmis.

This paper has been published already in the proceeding of the 29th Pittsburgh Annual Coal Conference in 2012.

Foteini Vasilikou researched and prepared this manuscript, with Nino Ripepi, Zach Agioutantis and Michael Karmis providing technical and editorial input.

potential of using geomechanical models to better account for the physical processes that occur during coalbed methane production and CO<sub>2</sub> injection and storage is also investigated. The results of this review can be used for evaluating modeling approaches when employing reservoir simulators to simulate injection and storage in ECBM cases.

## **Introduction**

Historically, recovery of natural gas or coalbed methane (CBM) is described as early as 1858. By 1953 degasification of the Pittsburgh seam was underway for safety reasons. By 1980, companies began profiting from deep coal seams where natural gas was of interest as a clean and domestic energy source, whether the coal was mineable or not (Bodden and Ehrlich, 1998; Ayers, 2002; Zarrouk, 2008; Liu, 2011). Coal seams are termed as unmineable where mining is considered to be infeasible given foreseeable technology, costs, sales prices, inadequate seam thickness, poor areal continuity, adverse geology (steeply dipping, rolls, faults), poor coal quality, excessive depths and other reasons. Typical depths for unmineable coal seams are 300-900 m (Siriwardane, 2008). The most methane that could be recovered by the pressure depletion method is not anticipated to be larger than 50% of gas-in-place, even after several decades of production (Puri and Yee, 1990). Hence, in the 90's enhanced coalbed methane (ECBM) production via injection of CO<sub>2</sub> in the unmineable coal seams was suggested as a more efficient way of extracting a larger fraction of methane in place without having to overly reduce reservoir pressure. In 2005 under the Kyoto Protocol, an international agreement linked to the United Nations framework convention on climate change, a cap on reduction of greenhouse gas emissions 5% below the 1990 greenhouse levels, further increased the interest in sequestering CO<sub>2</sub> in coalbeds. Thus, enhanced coalbed methane has the twofold benefit of enhanced production and redeeming greenhouse gases pollution. In Australia, Canada, China, Poland and the USA, a number of ECBM projects are ongoing (Hamelinck et al., 2003; Law et al., 2002; Damen et al., 2005; Zarrouk, 2008).

Large 'natural gas' or methane reserves are existent all over the world such as in Canada, Russia, China, the United States and Australia.

There exist a number of physical processes which occur during production of coalbed methane and injection and storage of CO<sub>2</sub> in coal seams. Coalbeds are characterized by a dual porosity system, which is comprised of a network of natural fractures (cleats) and matrix blocks

of coal exhibiting highly heterogeneous porosity. The gas transport through the coal matrix micropores (primary porosity), driven by the concentration gradient, is controlled by Fickian diffusion. The flow of gas and water through the cleat system (secondary porosity) is governed by Darcy's Law. Methane is initially stored in the adsorbed state, within the porous structure of the coal matrix blocks, which is usually described by a Langmuir-type isotherm. During coalbed methane production, reservoir pressure is decreased through dewatering, allowing methane molecules to desorb from the internal coal matrix (Fickian diffusion) and travel through the cleat structure (Darcy Flow). The opposite process occurs during CO<sub>2</sub> injection. This results in an inverse diffusion process, where CH<sub>4</sub> molecules are desorbed from the coal matrix and replaced by CO<sub>2</sub> molecules. The combination of reservoir dewatering and its associated depressurization, CH<sub>4</sub> desorption and CO<sub>2</sub> adsorption causes alterations in the stress regime acting on the coal matrix. Gains or losses in water and gas-relative permeability can be noted, but vary greatly in accordance with the geological characteristics of the coal.

### **Coalbed Characteristics**

Coal is a highly heterogeneous porous medium that contains micropores (<2 nm), mesopores (between 2 and 50 nm), macropores (>50 nm) and natural fractures formed during coalification. (Wang 2009; Shi and Durucan, 2005). In the literature, coalbeds or coal seams are characterized by a dual-continuum system comprised by the porous coal matrix and cleats (fractures) (Liu and Rutqvist, 2009). Cleats are considered to be a system of densely spaced, orthogonal fractures; cleats are comprised of face and butt cleats. Face cleats are long, well-developed, almost planar fractures that extend parallel to each other. Butt cleats, run at an angle of roughly 90 degrees to the face cleats and usually terminate at them (Figure 1). Face and butt cleats are approximately perpendicular to the bedding planes (Liu 2011; Gu 2009).

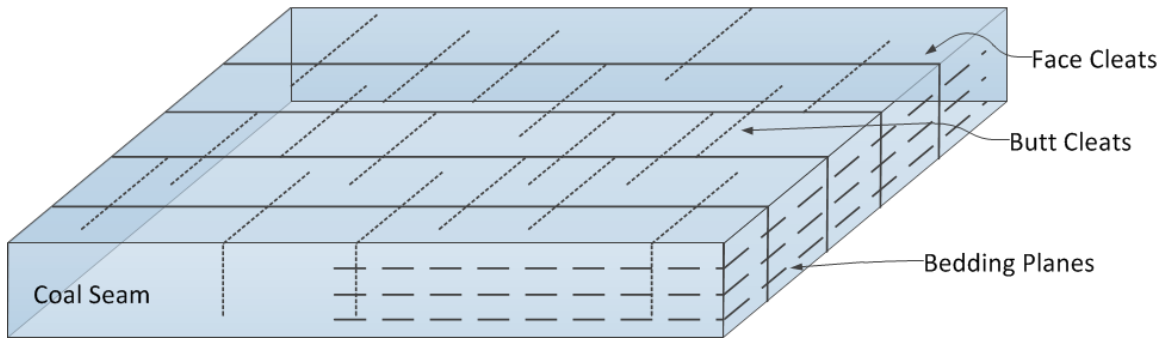


**Figure 1 - Face and Butt Cleats**

Face and butt cleats in conjunction with larger scale fractures, joints and faults constitute effective flow paths for gas in the coalbeds. As it has been postulated and confirmed by many experimental results, the anisotropic pore structure of coal results in higher permeability values along the face cleats compared to butt cleats and significantly higher than in the direction normal to the bedding plane. Indicative permeability values reported by Gash et al. (1992) are 0.6~1.7 mD for face cleats, 0.3~1 mD for butt cleats and only 0.007 mD for the direction normal to the bedding plane (Gu, 2009). The porous coal matrix permeability, is reported to be substantially less than that for the cleats system, normally eight times smaller; thus many researchers disregard coal matrix permeability and accredit the coalbed permeability to its cleats and larger scale discontinuities (Robertson, 2005; Liu and Rutqvist, 2009).

Porous coal matrix is the primary medium for gas storage in coalbeds and accounts for up to 95-98% storage, (Gray, 1987). Storage in the coal matrix is performed via two primary mechanisms. More specifically, gas can either be physically adsorbed on the very large (20-200 m<sup>2</sup>/g) (Patching, 1970) internal surface of the porous coal matrix, or it can be adsorbed within the molecular structure of the coal matrix. The remaining gas resides as either a free gas or dissolved in water within the cleats and larger fractures (Marsh, 1987; Shi and Durucan, 2005). Typically a Langmuir-type adsorption isotherm is employed to describe the adsorption phenomenon in coals (Shi and Durucan 2005).

In accordance with their basic characteristics, coalbeds can be regarded as dual porosity and single permeability systems (Harpalani and Schraufnagel, 1990; Lu and Connell, 2007; Warren and Root, 1963; Liu, 2011).

With natural gas production (CBM) and CO<sub>2</sub> storage in unmineable coalbeds (ECBM), complex interactions with varying stress state and sorption phenomena are triggered that affect

the transport and sorptive properties of coal and consequently affect production and/or injectivity rates. Therefore, understanding the mechanisms of the dynamic evolution of sorption, flow, coal deformation, porosity and permeability is of fundamental importance to CBM/ECBM recovery (Liu 2011).

## **Coalbed Methane and Enhanced Coalbed Methane Production Mechanisms**

Extraction of methane from undersaturated coalbeds activates a sequence of interactions among the porous coal matrix, fractures and adsorbed and free gas. In primary gas production, methane is extracted from the coalbed via decreasing reservoir pressure. More specifically, by dewatering the targeted seams, the pressure of the gas in the reservoir decreases which results in an increase of the effective stress and consequently closure of fracture apertures and lower permeability. Furthermore, when the gas pressure falls below the desorption point, methane is liberated from the matrix into the cleats system and the matrix shrinks. Based on the zero volume change condition, matrix shrinkage effectively causes the aperture of fractures to increase and thus fracture permeability to increase. Hence, an initial decrease in fracture permeability attributed to an increase in effective stress is counteracted by a gradual increase in permeability attributed to matrix shrinkage. The net permeability depends on the net impact of these two competing effects (Chen et al., 2008; Connell, 2009; Liu et al., 2010b, c, d; Shi and Durucan, 2004; Gu, 2009; Liu, 2011).

Coalbed methane extraction for saturated coal seams follows the same mechanisms as in the case for undersaturated coals without the dewatering phase. When pressure starts dropping there is immediate release of methane from the coal matrix to the fracture system. Finally for oversaturated coal seams, reduction of reservoir pressures results in concurrent flow of mobile water and free gas towards the production wells. As soon as the coalbed seam attains a state of saturation the production mechanism is similar to that for saturated coal seams (Gu 2009).

Carbon dioxide has been shown to have greater affinity to the porous coal matrix in contrast to methane and thus it is preferentially adsorbed onto the coal when present. According to laboratory measurements it is indicated that depending on coal rank, the matrix can adsorb almost twice the amount of carbon dioxide by volume as methane and in some cases of lower coal rank this ratio may even be as high as 10 to 1 under conditions of normal reservoir pressure (Stanton et al., 2001; Shi and Durucan, 2005). In ECBM, when carbon dioxide is competitively

adsorbed onto the coal matrix and methane is displaced the coal matrix swells. Coal matrix swelling combined with the zero volume change condition results in reduced fracture apertures and decreased fracture permeability (Mavor et al, 2002; Gu, 2009).

## **Permeability Models**

As discussed, permeability is a key parameter in both coalbed and enhanced coalbed methane production. US experience suggests that an absolute permeability of 1 mD is generally required to achieve commercial production rates. For these reasons, the complexity of the physical interactions affecting permeability has been extensively discussed in the literature and a variety of models have been proposed attempting to simulate the dynamic evolution of this phenomenon. Many of these models have also been incorporated in numerical simulators in order to quantify coal-gas interactions (Liu 2011). All of these models are based on numerous assumptions regarding flow characteristics and boundary conditions as well as the geomechanical component that may interact with the above parameters. In the following section the most important models representing the key parameters in multiphase flow problems are presented and critically evaluated. Also, in order to achieve a better understanding of the different mechanisms involved as well as the interaction of the various parameters of the model, formal definitions of the important variables are briefly outlined below.

A porous medium having a bulk volume ( $V$ ), comprised of solid volume ( $V_s$ ) and pore volume ( $V_p$ ), where  $V=V_s+V_p$ , has porosity ( $\phi$ ) which is defined as the ratio of the volume of the pores to the bulk volume of the medium,  $\phi=V_p/V$ . The permeability ( $k$ ) of the porous medium is the measure of its ability to allow fluids to pass through it and is expressed in units of area. Compressibility of a solid medium is described as the measure of relative volume change as a response to a pressure or a mean stress change. Furthermore, volumetric strain of a deformed body is defined as the ratio of the change in volume of the body to the deformation of its original volume. Effective stresses (and or strains) can be calculated from total quantities by subtracting the fraction attributed to pore pressure.

Physical processes are complex phenomena and their formal descriptions, which are also known as constitutive laws, are usually very complicated. In cases simplifying assumptions are used to facilitate analyses with a first order approximation. In the following, it will be demonstrated that researchers may apply different constitutive equations to describe the same

physical process with a varying number of (simplifying) assumptions. The basic principle of each formulation will be presented along with the underlying assumptions. On many occasions the governing equations of these physical processes are termed analytical models in contrast to the numerical models, which include the methodology for achieving a numerical solution to the analytical equation.

Liu 2011 stipulated that the total effective volumetric strain responsible for changes in coal porosity and permeability during production of CBM/ECBM as described by a thermo-poro-elastic constitutive equation is given by:

$$\Delta\varepsilon_e = \Delta\varepsilon_v + \frac{\Delta p}{K_s} - \Delta\varepsilon_s - \alpha_T \Delta T \quad (1)$$

It should be noted that the basic assumptions for this formulation are (i) that thermal contraction of a non-isothermal body is analogous to coalbed matrix shrinkage/swelling (Palmer and Mansoori, 1996), and (ii) that the coal seam is treated as a non-isothermal medium. According to Eq. (1) the total effective volumetric strain is comprised of the total volumetric strain, the coal compressive strain, the gas sorption-induced volumetric strain and the thermal strain.

This model is considered to include all major terms affecting fluid flow in single and dual porosity situations affected by the strain regime of the medium.

Porosity and permeability of the coalbed can be both described as a function of the total effective volumetric strain ( $\Delta\varepsilon_e$ ) through the following general functions:

$$\phi = \phi(\Delta\varepsilon_e) \quad (2)$$

$$k = k(\Delta\varepsilon_e) \quad (3)$$

Also, formulations relating porosity and permeability have been reported in the literature for different conceptual permeability models for coalbeds. Chilingar (1964) regarded coal as a continuum porous medium and proposed an equation relating permeability to the porosity and the effective diameter of its grains, Eq. (4).

$$k = \frac{d_e^2 \phi^3}{72 (1 - \phi)^2} \quad (4)$$

By applying Eq. (4) for initial  $(\phi_0, k_0)$  and current  $(\phi, k)$  permeability and porosity values, Eq. (5) can be derived. When the porosity is much smaller than 1 the second term of the right-hand side is close to unity and the term is dropped. Hence, the relationship between permeability and porosity for the coal matrix is as follows:

$$\frac{k}{k_0} = \left(\frac{\phi}{\phi_0}\right)^3 \left(\frac{1 - \phi_0}{1 - \phi}\right)^2 \quad \text{and for } \phi \ll 1 \text{ it follows that } \frac{k}{k_0} = \left(\frac{\phi}{\phi_0}\right)^3 \quad (5)$$

Reiss (1980) idealized coal as a collection of matchsticks (Figure 2) and considered permeability to be related to its porosity and cleat system spacing, Eq. (6).

$$k = \frac{\phi_f^3 a^3}{48} \quad (6)$$

By applying Eq. (6) for initial  $(k_0)$  and current  $(k)$  permeability values, Eq. (7) can be derived.

$$\frac{k}{k_0} = \left(\frac{\phi}{\phi_0}\right)^3 \quad (7)$$

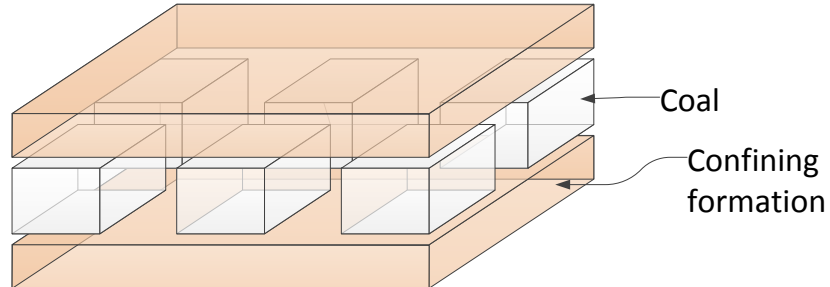


**Figure 2 - The Matchstick Model**

In Eq. (7) which is the same as the simplified version of Eq. (5), the value of the exponent is related to the flow regime, cleat size and roughness and is normally equal to 2 for laminar flow, 3 for transition flow and 4 for turbulence flow. According to the literature, flow through naturally fractured coalbed reservoirs is in the transition flow regime, and thus the exponent is taken to be 3 (Reiss, 1980; Seidle, 1992; Avraam and Payatakes, 1995; Wang, 2009).

By applying Eq. (7) which relates permeability to porosity (and thus to elemental volume conditions), permeability-change formulations are acquired which in many cases may include coal properties as well as related physical quantities. Extended research has been conducted and

many models have been proposed in the past 30 years in order to combine the flow regime to the geomechanical characteristics of the medium and examine the dynamic evolution of permeability. Different classifications have been proposed for these models according to their respective assumptions, encompassed parameters and employed solving techniques.

More specifically, Palmer (2007) grouped permeability models into analytical permeability-change models and permeability models that couple different processes through a set of flow and geomechanical equations and solve the system using numerical simulators. Gu and Chalaturnyk (2005) and Palmer (2007), further divided analytical permeability-change models into either stress or strain based models, with or without a geomechanical framework. Strain-based, permeability-change models were defined as the ones where in the case of CBM production desorption of methane changes the volumetric strain that causes the porosity to change and finally affects the permeability. In the case of the stress-based models for CBM production, desorption of methane changes the volumetric strain, which consequently changes the horizontal stress and ultimately alters the permeability.

Settari and Walters (2001), Rutqvist et al (2002) and Liu (2011) divided permeability-change models that couple fluid flow and solid deformation into decoupled simulation, sequential coupled simulations and fully coupled simulations. In fully coupled simulations, both reservoir flow variables and geomechanical variables are concurrently determined by solving a system of equations. In sequential coupled simulation, parameters pertinent to flow, such as pressure and temperatures, and geomechanical variables, such as stresses and displacements, are solved sequentially first from a reservoir simulator and then from a geomechanical simulator and coupling parameters, such as permeability and porosity are iterated between the two simulators (Figure 3). In decoupled or uncoupled simulation the changes of fluid pressures cause the changes of stresses and strains, but the changes of stresses and strains are assumed not to affect fluid pressures (Wang, 2000).

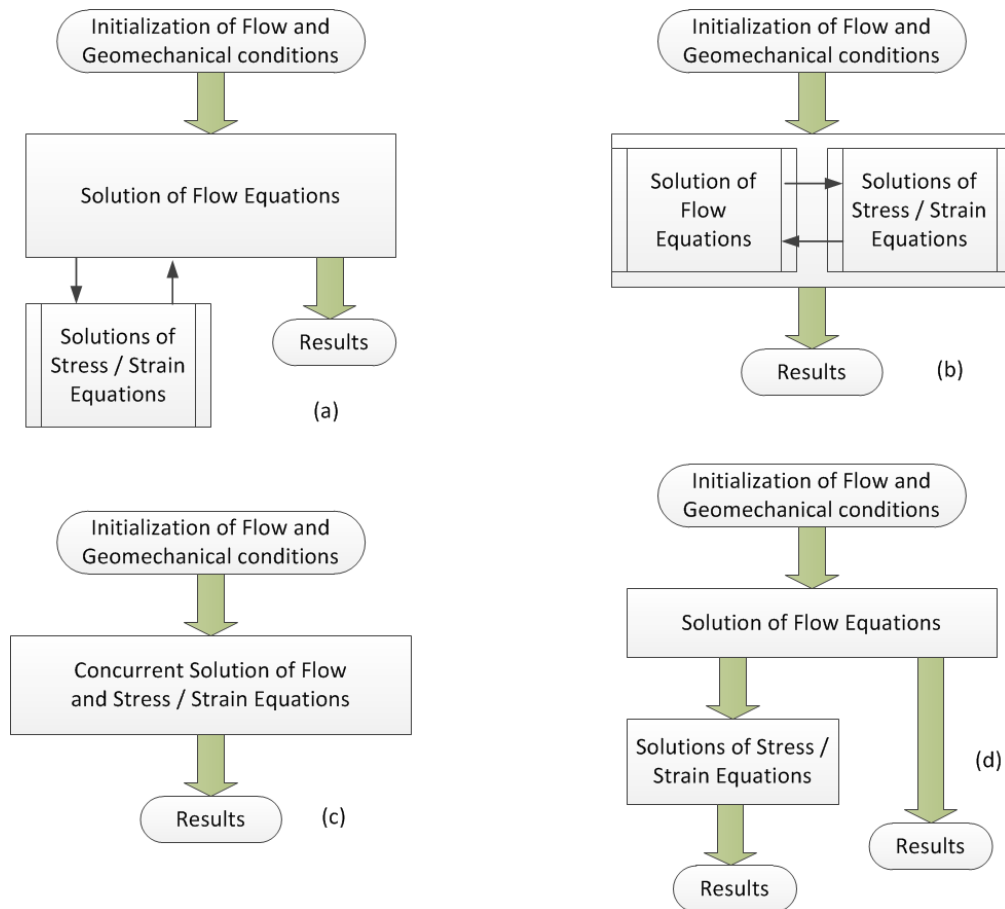


**Figure 3 - Different Modes of Coupled Simulation (a, b, c) and Uncoupled Simulation (d)**

Liu (2011), classified permeability-change models according to their reasoning of coalbed configuration and assumptions postulated. More specifically, Liu considered a class of permeability models that represents each coalbed as either a stack of matchsticks or as cubes under uniaxial strain conditions (Figure 4) and constant overburden stress exerted by the overlying geology. Liu (2011) also discussed another group of permeability models, where the coalbed is represented by a stack of separated coal matrix matchsticks that are connected through solid rock bridges of coal under reservoir conditions of variable stress state. Finally, several other classifications can be postulated among models that account for isotropic or anisotropic permeability changes within the coalbed.

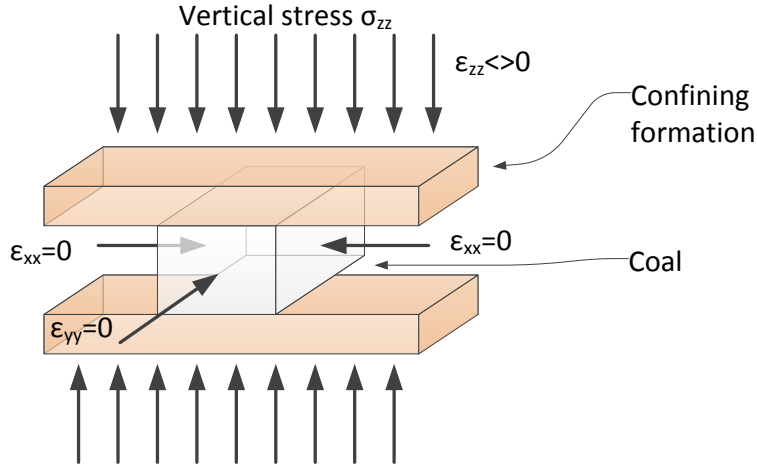


**Figure 4 - Uniaxial Strain Model**

Finally, Liu (2011) proposed upper and lower boundaries for the permeability-change models. More specifically, the minimum permeability change is given under conditions of free swelling and shrinkage as shown in Eq. (8) where the fracture aperture does not change with the volumetric strain experienced by the coal matrix blocks since the boundary is free to move with strain changes. In this case there is an increase in cleat spacing but the fracture aperture remains constant. In comparison, the maximum permeability change is expected to occur as shown in Eq. (9), under the constant volumetric model assumption where the fracture opening compensates the volume changes in the coal matrix block (Figure 5).

$$\frac{k}{k_0} = \left[ 1 + \frac{a}{\phi_0} \left( \frac{\Delta p}{K} \right) \right]^3 \rightarrow \text{Free Shrinking - Swelling Model} \quad (8)$$

$$\frac{k}{k_0} = \left[ 1 + \frac{a}{\phi_0} (\Delta \epsilon_s) \right]^3 \rightarrow \text{Constant Volumetric Model} \quad (9)$$

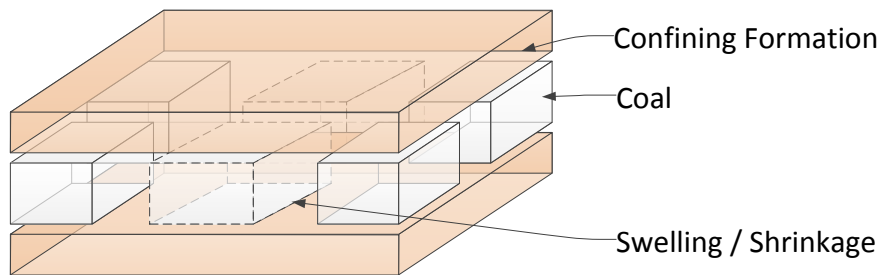


**Figure 5 - Fracture Aperture Changes with Swelling/Shrinkage**

Representative permeability-change models are shown below.

Seidle et al., (1992), Pan et al., (2010), proposed a stress based model for permeability changes, as shown in Eq. (10). In accordance with experimental results, an exponential function was used for the permeability-stress relationship (Durucan and Edwards, 1986; Gray 1987; Wang 2009). Further assumptions applied for this model, were the postulation of a matchstick geometry for the coal matrix, isotropic permeability, uniaxial strain and constant overburden stress.

$$\frac{k}{k_0} = \exp[-3 c_f(\sigma_h - \sigma_{h0})] \quad (10)$$

where  $c_f$  is the fracture cleat compressibility defined as follows

$$c_f = \frac{1}{\phi_f} \frac{\partial \phi_f}{\partial p} \quad (11)$$

This model accounts for grain compaction and the cleats volume change contribution to the permeability alteration however it does not incorporate volumetric strain due to gas adsorption or desorption.

Gilman and Beckie (2000) suggested a stress-based relationship for isotropic permeability under uniaxial strain and constant overburden stress conditions for saturated coals, as shown by Eq. (12). An exponential function was employed to relate permeability to the other parameters in the framework of poro-elasticity. A relative regular cleat system was assumed and it was also considered that each fracture reacts as an elastic body with respect to change in the normal stress component. In addition, an extremely slow mechanism of methane release from the coal matrix to the cleats was postulated.

$$\frac{k}{k_0} = \exp\left(-\frac{3 \Delta \sigma_e^h}{E_f}\right) = \exp\left[-\frac{3}{E_f} \left(-\frac{\nu}{1-\nu} \Delta p + \frac{E}{1-\nu} \gamma \Delta S\right)\right] \quad (12)$$

Seidle and Huitt (1995) described a strain based permeability change model for isotropic permeability of saturated coals in the framework of poro-elasticity under uniaxial strain and constant overburden stress reservoir conditions, as shown in Eq. (13). A cubic function was employed in this case to correlate the pertinent parameters to permeability. It was assumed that

the coal sorption-induced strain is proportional to the amount of gas sorbed and that the sorbed gas is related to pressure by Langmuir's equation (Liu, 2011).

$$\frac{k}{k_0} = \left[ 1 + \frac{\varepsilon_L}{3} \left( 1 + \frac{2}{\phi_0} \right) \left( \frac{p_0}{P_L + p_0} - \frac{p}{P_L + p} \right) \right]^3 \quad (13)$$

Shi and Durucan (2004) presented a stress based permeability model for isotropic permeability changes in the framework of linear elasticity for saturated coals, as shown in Eq. (14). An exponential function was employed to relate permeability to cleat compression and matrix shrinkage. These two terms affect the dynamic permeability evolution in a competitive way. For this model as in previous cases, uniaxial strain and constant overburden stresses were assumed.

$$\frac{k}{k_0} = \exp \left[ -3 c_f \left( \frac{\nu}{(1-\nu)} (p - p_0) + \frac{E \varepsilon_L}{3(1-\nu)} \left( \frac{p}{P_L + p} - \frac{p_0}{P_L + p_0} \right) \right) \right] \quad (14)$$

Palmer and Mansoori (1996), proposed a strain based, fully geomechanical model for isotropic permeability under conditions of uniaxial strain and constant overburden stress in the framework of linear elasticity for small strain changes, Eq. (15).

$$\frac{k}{k_0} = \left[ 1 + \frac{C_m}{\phi_0} (p - p_0) + \frac{\varepsilon_L}{\phi_0} \left( \frac{K}{M} - 1 \right) \left( \frac{p}{P_L + p} - \frac{p_0}{P_L + p_0} \right) \right]^3 \quad (15)$$

where  $M = \frac{1 - \nu}{(1 + \nu)(1 - 2\nu)}$

In 2007, Palmer and Mansoori modified their model to account for directional (anisotropic) permeability and modulus changes with depletion. The Palmer and Mansoori (2007) permeability change model is also applicable to both saturated and undersaturated coals. The Computer Modelling Group (CMG) implemented this model in their commercial reservoir simulator, GEM.

Peekot and Reeves (2002), suggested a permeability model in which matrix strain changes are extracted from a Langmuir curve of strain versus reservoir pressure which is assumed to be proportional to the adsorbed gas concentration curve (Palmer, 2007; Liu, 2011). This model is not developed within a geomechanical framework. The matrix shrinkage is proportional to the adsorbed gas concentration change multiplied by shrinkage compressibility ( $C_m$ ) that is a free

parameter. This model is incorporated in the commercial reservoir simulator package, COMET3 by ARI (Comet, 2003). It has been shown that for saturated coals the latter model and the Palmer and Mansoori (1996) model are essentially equivalent (Palmer, 2007; Liu 2011).

Cui and Bustin (2005), described a stress dependent permeability model for isotropic permeability in the poro-elasticity framework under uniaxial strain and constant overburden stress reservoir conditions, as described by Eq. (16). This model essentially accounts for the effects of pressure and sorption induced volumetric strain on permeability constrained by the adsorption isotherm.

$$\frac{k}{k_0} = \exp \left\{ -\frac{3}{K_p} \left[ \frac{(1+\nu)}{3(1-\nu)} (p - p_0) - \frac{2E}{9(1-\nu)} (\varepsilon_s - \varepsilon_{s0}) \right] \right\} \quad (16)$$

Gu and Chalaturnyk in 2010 proposed an anisotropic permeability-change model. As shown in Eq. (17), they determined a directional effective strain, comprised of the directional mechanical deformation due to stress change, the directional mechanical deformation due to pressure change, the directional matrix shrinkage/swelling due to desorption/sorption and the directional thermal contract/expansion due to temperature changes. The directional effective strain was then related to a directional permeability, Eq. (18), with a cubic function and with assuming a stack of matchsticks configuration for the coalbed.

$$\Delta\varepsilon_{li} = \Delta\varepsilon_{lEi} + \Delta\varepsilon_{lPi} + \Delta\varepsilon_{lDi} + \Delta\varepsilon_{lTi} \quad (17)$$

$$\frac{k_i}{k_0} = \left( 1 + \frac{a}{b} \Delta\varepsilon_{li} \right)^3 \quad (18)$$

Pan and Connell (2007) and Clarkson et al. (2008), proposed an elastic strain dependent model for isotropic permeability under uniaxial strain and constant overburden stress conditions, Eq. (19). This model accounts for sorption strain, Eq. (20), for a single component adsorption.

$$\frac{k}{k_0} = \left[ 1 + \frac{C_m}{\phi_0} (p - p_0) + \frac{1}{\phi_0} \left( \frac{K}{M} - 1 \right) \Delta\varepsilon_s \right]^3 \quad \text{where } M = \frac{1-\nu}{(1+\nu)(1-2\nu)} \quad (19)$$

$$\Delta\varepsilon_s = RTL \ln(1 + Bp) \frac{\rho_s}{E_s} f(x, v_s) - \frac{p}{E_s} (1 - 2\nu_s) \quad (20)$$

Robertson and Christiansen (2006) suggested an isotropic permeability-change model assuming a cubic configuration for the coalbed under variable stress reservoir conditions and

constant overlying geology, as shown in Eq. (21). In this model, effective porosity of the coal matrix is considered to be equal to zero and thus only the porosity of the coalbed is attributed to the fracture system.

$$\frac{k}{k_0} = \exp \left\{ -3 c_f \frac{1 - \exp[\alpha_c(p - p_0)]}{\alpha_c} + \frac{9}{\phi_0} \left[ \frac{1 - 2\nu}{E} (p - p_0) - \frac{\varepsilon_L}{3} \left( \frac{p}{P_L + p} \right) \ln \frac{p_0}{P_L + p_0} \right] \right\} \quad (21)$$

Zhang et al. (2008) presented a permeability change model under variable stress conditions in the poro-elasticity framework, Eq. (22).

$$\frac{k_m}{k_{m0}} = \left( \frac{1}{1 + S} [(1 + S_0)\phi_0 + a(S - S_0)] \right)^3 \quad (22)$$

where  $S$  and  $S_0$

$$S = \varepsilon_v + \frac{p}{K_s} - \varepsilon_s \quad (23)$$

$$S_0 = \varepsilon_v + \frac{p_0}{K_s} - \varepsilon_{s0} \quad (24)$$

Connell et al. (2010), Liu et al. (2010) and Liu and Rutqvist (2010), reported that when the coalbed is represented by a stack of coal matrix matchsticks separated by the cleat system, under conditions of constant confining stress (as is usually applied in laboratory experiments), then the effects of coal matrix swelling will not alter the coal permeability. This statement argues that since for a given pressure, the coal matrix blocks are fully separated by the fractures and no fixed boundaries are enforced, the swelling will translate in an increase in fracture spacing and not in a reduction of fracture aperture. Nevertheless, this conclusion does not tie in with laboratory observations, where matrix swelling causes significant changes in coal permeability under conditions of constant confining stress. As discussed by Liu (2010a), in order to account for this interaction many researchers postulated a zero lateral strain condition in the horizontal plane so that matrix swelling will result in permeability changes. (e.g., Harpalani and Chen, 1995; Robertson and Christiansen, 2006; Harpalani and Chen, 1997; Pan et al., 2010; Pini et al., 2009).

Liu et al. (2010) suggested a different approach in order to correctly reproduce the aforementioned laboratory observations, which accounts for interactions among coal matrix and

fractures. More specifically, the cleat system in this model is not considered to be completely separate neighboring matrix blocks, but assumes that there are solid bridges connecting the adjacent coal matrix blocks (Figure 6). For this coalbed configuration, coal matrix-swelling affects permeability in two opposing ways. When the bridging contacts swell, the coal matrix blocks are driven apart and thus fracture aperture increases and consequently permeability. At the same time, swelling of the matrix blocks results in reduction of fracture aperture and thus permeability.

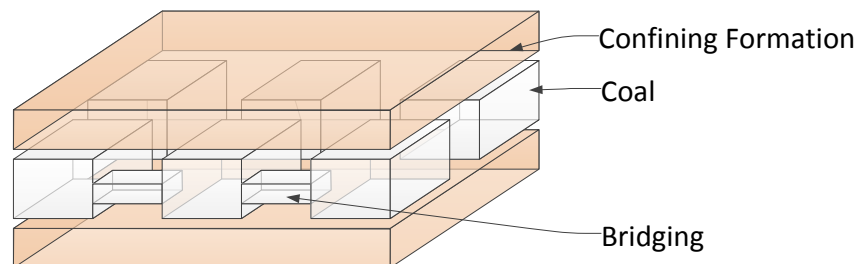


**Figure 6 - Matchstick Model with Bridging Between Coal Blocks**

Connell and Detournay (2009) suggested a sequential coupled simulation model to describe dynamic evolution of permeability in an isotropic linear elasticity framework. Their formulation was based on Shi and Durucan (2004) isotropic permeability-change stress based model. However, they discussed a modified version in which directional permeability, triaxial strain and varying overburden stress conditions were accounted for. Permeability changes for both CBM and ECBM productions cases were examined by employing the SIMED reservoir simulator (Spencer et al., 1987; Stevenson and Pinczewski, 1995) and the FLAC3D finite difference geomechanical code. It was shown that especially for the ECBM production cases, simplifying assumptions such as uniaxial strain and constant overburden stress can lead to large errors.

Gu and Chalaturnyk, 2010 proposed a sequential coupling permeability change model, where the discontinuous coal masses were considered as an equivalent elastic continuum. Their explicit-sequential coupled simulation examined pressure depleting CBM reservoirs. GEM (CMG, 2003) a multidimensional, multiphase, isothermal and compositional reservoir simulator and the geomechanical code FLAC3D (Itasca, 2002) designed for rock and soil mechanics analyses were employed to model fluid flow and calculate coalbed deformation respectively. The simulation process was as follows: (i) Calculate pore pressures, adsorbed gas volumes, water saturation and well production rates of gas and water with GEM at an arbitrary time step, then

(ii) insert pore pressures and adsorbed gas volumes in FLAC3D and calculate stresses and linear strains and finally (iii) calculate cleat permeability based on Eq. (25).

$$\frac{k}{k_0} = \frac{\left(1 + \frac{\Delta b_m}{b_m}\right)^3}{1 + \frac{\Delta a}{a}} \quad (25)$$

## **Discussion on Implementation of Permeability Models for Reservoir**

### **Simulation**

Most commercially and in-house developed software for simulating reservoir behavior for CBM/ECBM production has implemented one or more of the aforementioned analytical approaches. In order to apply these relationships to specific geological strata sequences with varying initial and boundary conditions, a numerical approach should be implemented. This implementation requires discretization of the domain in two or three dimensions (Figure 7) and the solution of the governing differential equations in space and time. Commonly finite difference schemes are used to solve the flow problem. In the more advanced, complicated approaches where the geomechanical component should also be taken into account a coupled approach should be used. This can be accomplished either using external coupling (i.e. coupling to software not directly interfaced with the flow package) or internal coupling where flow equations can be modified directly by the stress strain regime of the reservoir as prescribed by the analytical model (see also Figure 3).

The analysis provided in this study will be applied for the simulation of CBM and ECBM production for a small-scale carbon capture, utilization and storage (CCUS) project in southwest Virginia. More specifically, the injection and storage potential of unmineable coal seams will be tested by injecting 20,000 tonnes of carbon dioxide into three wells, in Buchanan County, Virginia, in the central Appalachian basin, over a period of one year (Figure 8).

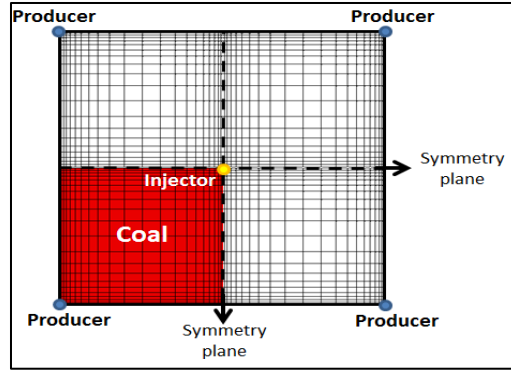


**Figure 7 - Domain Discretization**

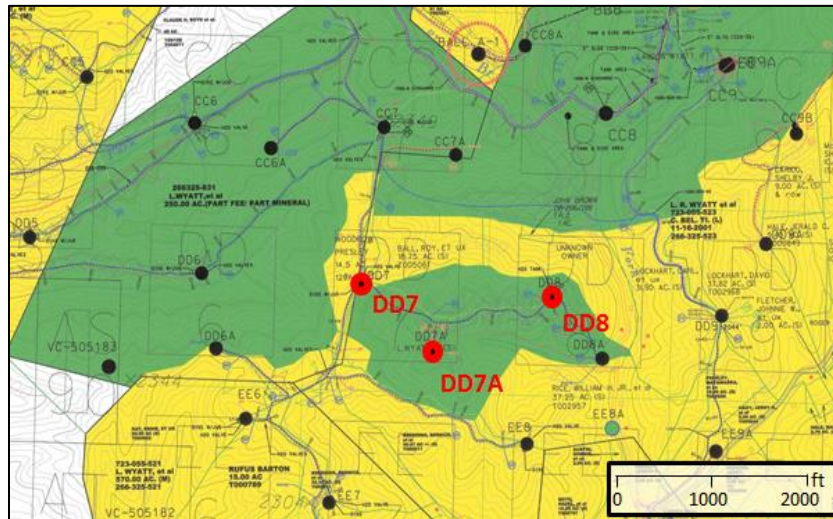


**Figure 8 - Case Study Area Showing Injection Wells**

To successfully model reservoir response to simultaneous CO<sub>2</sub> injection and CH<sub>4</sub> production several options are currently being examined. These courses of action include the following: a) to use a commercially available package with a built in geomechanics component such as GEM/CMG, b) to develop specific solutions for stresses and strains using an external package such as FLAC3D, coupled to a commercially available flow simulator (Figure 9) and c) to use other existing simulators developed by other research institutions with external or internal coupling to geomechanics.

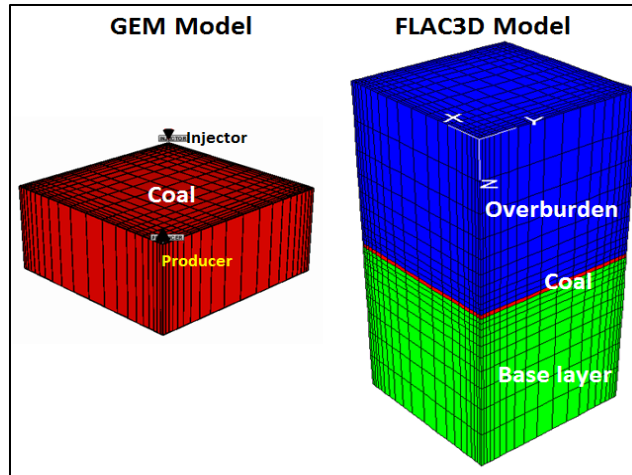


**Figure 9 - Initial Attempts for Coupled Simulation Using an External Geomechanics Package (Vasilikou et al., 2012)**

## Conclusions

Coal permeability and permeability change models are probably the most important considerations when evaluating the potential of a coal bed methane reservoir for enhanced coal bed methane production. Different analytical models may be applied depending on the available knowledge and properties of a reservoir. In the simplest considerations, the flow model will be solved without input from the changing geomechanics regime in the area. However, as complexity increases, other conditions should be taken into account (e.g., pore pressure changes, shrinkage, swelling, etc.) and thus porosity and permeability fluctuations need to be incorporated as dictated by changes in the stress and strain situation. Furthermore, in ECBM reservoirs additional complications arise due to the presence of two gases in two-phase flow conditions.

In every step of conducting a reservoir simulation, the user should be aware of the net contribution of each factor in the final result. Components with minimal contribution may be safely eliminated after consideration. Also, the underlying assumptions as well as application conditions should be evident for every analytical model, especially when performing history matching. As already discussed in the literature, improper model hypothesis and model selection will lead to large discrepancies between predicted and measured data.

The analytical model evaluation presented in this study will be utilized in reservoir simulations for ECBM production for a small-scale carbon capture, utilization and storage (CCUS) project in the central Appalachian basin.

## Acknowledgements

Financial assistance for this work was provided the U.S. Department of Energy through the National Energy Technology Laboratory's Program under Contract No. DE-FE0006827.

## Nomenclature

a	the width of the coal matrix block	$\Delta b$	fracture aperture change
B	Langmuir pressure constant ( $\text{Pa}^{-1}$ )	$\Delta p$	the change in pore pressure
b	fracture aperture	$\Delta p_s$	equivalent sorption pressure
$b_m$	the mechanical aperture of a fracture	$\Delta S$	the change of the adsorbate mass
$c_f$	coal cleat compressibility	$\Delta T$	the change in reservoir temperature
$C_m$	shrinkage compressibility	$\Delta \varepsilon_e$	the change of total effective volumetric strain
$d_e$	the effective diameter of grains	$\Delta \varepsilon_e^h$	the change of the effective horizontal strain
E	Young's modulus of coal	$\Delta \varepsilon_{IDi}$	matrix shrinkage/swelling due to desorption/sorption
$E_f$	Young's modulus for the fracture	$\Delta \varepsilon_{IEi}$	the mechanical deformation due to stress change
$E_s$	Young's modulus of the solid phase	$\Delta \varepsilon_{li}$	the directional effective strain
k	coal permeability	$\Delta \varepsilon_{IPi}$	the mechanical deformation due to pressure change
K	the bulk modulus of coal	$\Delta \varepsilon_{ITi}$	thermal contract/expansion due to temperatures changes
$k_i$	current permeability in i direction	$\Delta \varepsilon_s$	the change in sorption strain
$k_m$	coal matrix permeability	$\Delta \varepsilon_v$	the change of volumetric strain of coal
$k_{m0}$	initial coal matrix permeability	$\varepsilon_e$	the total effective volumetric strain
$K_p$	the bulk modulus of coal pore system	$\varepsilon_L$	the maximum volumetric strain
$K_s$	the bulk modulus of coal grains	$\varepsilon_s$	the sorption strain for coal
L	Langmuir sorption constant (mol/kg)	$\varepsilon_{s0}$	the initial sorption strain of coal

$p$	the gas pressure within the pores	$\varepsilon_v$	the volumetric strain of coal
$p_0$	the initial gas pressure within the pores	$\nu$	Poisson's ratio of coal
$P_L$	Langmuir pressure constant	$\nu_s$	Poisson's ratio for solid phase
$R$	the gas constant (8.314 J mol <sup>-1</sup> K <sup>-1</sup> )	$\rho_s$	the density for the solid phase
$s$	cleat spacing	$\sigma_h$	the horizontal stress
$T$	reservoir temperature	$\sigma_{h0}$	the initial horizontal stress
$\alpha_c$	change rate in fracture compressibility	$\phi$	coal porosity
$\alpha_T$	the coefficient of volumetric thermal expansion	$\phi_0$	initial coal porosity
$\gamma$	the volumetric swelling/shrinkage coefficient	$\phi_f$	the cleat porosity

## References

- Advanced Resources International, I. (2003). COMET3.
- Avraam, D. G., & Payatakes, A. C. (1995). Flow regimes and relative permeabilities during steady-state two-phase flow in porous media. *Journal of Fluid Mechanics Digital Archive*, 293, 207-236.
- Ayers, W. B. (2002). Coalbed gas systems, resources, and production and a review of contrasting cases from the San Juan and Powder River basins. *AAPG Bulletin*, 86, 1853–1890.
- Bodden, W. P., & Ehrlich, R. (1998). Permeability of coals and characteristics of desorption tests: implications for coalbed methane production. *International Journal of Coal Geology*, 35, 333–347.
- Chen, Z., Liu, J., Connell, L., Pan, Z., & Zhou, L. (2008). Impact of Effective Stress and CH<sub>4</sub>–CO<sub>2</sub> Counter-Diffusion on CO<sub>2</sub> Enhanced Coalbed Methane Recovery. Paper presented at the SPE Asia Pacific Oil and Gas Conference and Exhibition, Perth, Australia.
- Chilingar, G. V. (1964). Relationship between porosity, permeability, and grain-size distribution of sands and sandstones. Paper presented at the 6th International Sedimentological Congress.

- Clarkson, C. R., Pan, Z., Palmer, I. D., & Harpalani, S. (2008). Predicting Sorption-Induced Strain and Permeability Increase With Depletion for CBM Reservoirs. Paper presented at the SPE Annual Technical Conference and Exhibition, Denver, Colorado, USA.
- Computer Modelling Group Ltd (CMG), C. (2003). GEM. Calgary, Canada.
- Connell, L. D., Lu, M., Pan, Z. (2010). An analytical coal permeability model for tri-axial strain and stress conditions. *International Journal of Coal Geology*, 84(2), 103-114.
- Connell, L. D., & Detournay, C. (2009). Coupled flow and geomechanical processes during enhanced coal seam methane recovery through CO<sub>2</sub> sequestration. *International Journal of Coal Geology*, 77(1-2), 222-233. doi: 10.1016/j.coal.2008.09.013
- Cui, X., & Bustin, R. M. (2005). Volumetric strain associated with methane desorption and its impact on coalbed gas production from deep coal seams. *AAPG Bulletin*, 89(9), 1181-1202.
- Damen, K., Faaij, A., Van Bergen, F., Gale, J., & Lysen, E. (2005). Identification of early opportunities for CO<sub>2</sub> sequestration — worldwide screening for CO<sub>2</sub>-EOR and CO<sub>2</sub>- ECBM projects. *Energy*, 30(10), 1931-1952.
- Durucan, S., & Edwards, J. S. (1986). The effects of stress and fracturing on permeability of coal. *Mining Science & Technology*, 3, 205-216.
- Gash, B. W., Richard, F. V., Potter, G., & Corgan, J. M. (1992). The Effects of Cleat Orientation and Confining Pressure on Cleat Porosity, Permeability and Relative Permeability in Coal. Paper presented at the SPWLA/SCA Symposium, Oklahoma City.
- Gilman, A., & Beckie, R. (2000). Flow of coal-bed methane to a gallery. *Transport in Porous Media*, 41(1), 1-16.
- Gray, I. (1987). Reservoir engineering in coal seams: part 1—the physical process of gas storage and movement in coal seams. *SPE Reservoir Engineering*, 2(1), 28-34.
- Gu, F. (2009). Reservoir and Geomechanical Coupled Simulation of CO<sub>2</sub> Sequestration and Enhanced Coalbed Methane Recovery. Doctor of Philosophy, University of Alberta, Edmonton, Alberta.
- Gu, F., & Chalaturnyk, J. J. (2005). Analysis of coalbed methane production by reservoir and geomechanical coupling simulation. *Journal of Canadian Petroleum Technology*, 44(10).
- Gu, F., & Chalaturnyk, R. (2010). Permeability and porosity models considering anisotropy and discontinuity of coalbeds and application in coupled simulation. *Journal of Petroleum Science and Engineering* 74(3-4), 113-131.

- Hamelinck, C. N., Faaij, A. P. C., Turkenburg, W. C., Van Bergen, H. J. M., Pagnier, Barzandji, O. H. M., Wolf, K.-H., A., A., & Ruijg, G. J. (2002). CO<sub>2</sub> enhanced coalbed methane production in the Netherlands. *Energy*, 27, 647-674.
- Harpalani, S., & Chen, G. (1997). Influence of gas production induced volumetric strain on permeability of coal. *Geotechnical and Geological Engineering*, 15(4), 303-325.
- Harpalani, S., & Chen, G. (1995). Estimation of changes in fracture porosity of coal with gas emission. *Fuel*, 74(10), 1491-1498.
- Harpalani, S., & Schraufnagel, R. A. (1990). Shrinkage of coal matrix with release of gas and its impact on permeability of coal. *Fuel*, 69(5).
- Itasca. (2005). *FLAC3D: Fast Lagrangian analysis of continua in 3 dimensions. Theory and background*. Minnesota, USA.
- Law, D. H. S., Meer, v. d., L.G.H., & Gunter, W. D. (2002). Numerical simulation comparison study for enhanced coalbed methane recovery processes. Paper presented at the Gas Technology Symposium Calgary.
- Liu, F., Lu, P., Zhu, C., & Xiao, Y. (2010a). Coupled reactive flow and transport modeling of CO<sub>2</sub> sequestration in the Mt. Simon sandstone formation, Midwest U.S.A. *International Journal of Greenhouse Gas Control*. doi: doi:10.1016/j.ijggc.2010.08.008
- Liu, H.-H., & Rutqvist, J. (2009). A New Coal-Permeability Model: Internal Swelling Stress and Fracture–Matrix Interaction. *Transport in Porous Media*, 82(1), 157-171. doi: 10.1007/s11242-009-9442-x
- Liu, J., Chen, Z., Elsworth, D., Miao, X., & Mao, X. (2010b). Evaluation of stress-controlled coal swelling processes. *International Journal of Coal Geology*, 83(4), 446-455.
- Liu, J., Chen, Z., Elsworth, D., Miao, X., & Mao, X. (2010c). Linking gas-sorption induced changes in coal permeability to directional strains through a modulus reduction ratio. *International Journal of Coal Geology*, 83(1), 21-30.
- Liu, J., Chen, Z., Elsworth, D., Qu, H., & Chen, D. (2011). Interactions of multiple processes during CBM extraction: A critical review. *International Journal of Coal Geology*, 87(3-4), 175-189. doi: 10.1016/j.coal.2011.06.004
- Liu, J., Chen, Z., & Qu, H. (2010d). Multiphysics of coal–gas interactions: the scientific foundation for CBM extraction. Paper presented at the SPE Asia Pacific Oil and Gas Conference and Exhibition, Queensland, Australia.

- Lu, M., & Connell, L. D. (2007). A model for the flow of gas mixtures in adsorption dominated dual porosity reservoirs incorporating multi-component matrix diffusion: Part I. Theoretical development. *Journal of Petroleum Science and Engineering*, 59(1-2), 17-26.
- Marsh, H. (1987). Adsorption methods to study microporosity in coals and carbons—a critique. *Carbon*, 25(49-58).
- Mavor, M. J., Gunter, W. D., Robinson, J. R., Law, D. H. S., & Gale, J. (2002). Testing for CO<sub>2</sub> Sequestration and Enhanced Methane Production From Coal. Paper presented at the SPE Gas Technology Symposium, Richardson, Texas, USA.
- Palmer, I. D., Mavor, M., Gunter, B. (2007). Permeability changes in coal seams during production and injection. Paper presented at the International Coalbed Methane Symposium., Tuscaloosa, Alabama.
- Palmer, I. D., & Mansoori, J. (1996). How permeability depends on stress and pore pressure in coalbeds: a new model. Paper presented at the SPE Annual Technical Conference and Exhibition, Denver, Colorado.
- Pan, Z., & Connell, L. D. (2007). A theoretical model for gas adsorption-induced coal swelling. *International Journal of Coal Geology*, 69(4), 243-252.
- Pan, Z., Connell, L. D., & Camilleri, M. (2010). Laboratory characterisation of coal reservoir permeability for primary and enhanced coalbed methane recovery. *International Journal of Coal Geology*, 82(3-4), 257-267.
- Patching, T. H. (1970). Retention and release of gas in coal — a review. *Canadian Mining and Metallurgical Bulletin*, 63(703), 1302-1308.
- Peekot, L. J., & Reeves, S. R. (2002). Modeling the Effects of Matrix Shrinkage and Differential Swelling on Coalbed Methane Recovery and Carbon Sequestration: U.S. Department of Energy.
- Pini, R., Ottiger, S., Burlini, L., Storti, G., & Mazzotti, M. (2009). Role of adsorption and swelling on the dynamics of gas injection in coal. *Journal of Geophysical Research*, 114(B4), B04203.
- Puri, R., & Yee, D. (1990). Enhanced Coalbed Methane Recovery. Paper presented at the SPE Annual Technical Conference and Exhibition, New Orleans, Louisiana.
- Reiss, L. H. (1980). *The Reservoir Engineering Aspects of Fractured Formations*, Houston.

- Robertson, E. P. (2005). Modeling permeability in coal using sorption-induced strain data. Paper presented at the SPE Annual Technical Conference and Exhibition, Dallas, Texas.
- Robertson, E. P., Christiansen. (2006). A permeability model for coal and other fractured, sorptive-elastic media. Paper presented at the SPE Eastern Regional Meeting, Canton, Ohio, USA.
- Rutqvist, J., Wu, Y.-S., Tsang, C.-F., & Bodvarsson, G. (2002). A modeling approach for analysis of coupled multiphase fluid flow, heat transfer, and deformation in fractured porous rock. *Int. J. Rock Mech. Min. Sci.*, 39, 429-442.
- Seidle, J. P., Jeansonne, M. W., & Erickson, D. J. (1992). Application of matchstick geometry to stress dependent permeability in coals. Paper presented at the SPE Rocky Mountain Regional Meeting, Wyoming.
- Seidle, J. R., & Huitt, L. G. (1995). Experimental measurement of coal matrix shrinkage due to gas desorption and implications for cleat permeability increases. Paper presented at the International Meeting on Petroleum Engineering, Beijing, China.
- Settari, A., Walters, D. A., & Duke Engineering and Services Inc, D. E. a. S. (2001). Advances in Coupled Geomechanical and Reservoir Modeling With Applications to Reservoir Compaction. *SPE Journal*, 6(3), 334-342.
- Shi, J. Q., & Durucan, S. (2004). Drawdown induced changes in permeability of coalbeds: a new interpretation of the reservoir response to primary recovery. *Transport in Porous Media* 56(1), 1-16.
- Shi, J. Q., & Durucan, S. (2005). CO<sub>2</sub> Storage in Deep Unminable Coal Seams. *Oil & Gas Science and Technology – Rev. IFP*, 60(3).
- Siriwardane, H., Haljasmaa, I., McLendon, R., Irdi, G., Soong, Y., & Bromhal, G. (2009). Influence of carbon dioxide on coal permeability determined by pressure transient methods. *International Journal of Coal Geology*, 77(1-2), 109-118. doi: 10.1016/j.coal.2008.08.006
- Spencer, S. J., Somers, M.L., Pinczewski, W.V., Doig, I.D. (1987). Numerical simulation of gas drainage from coal seams. Paper presented at the 62nd SPE Annual Technical Conference and Exhibition, Houston.
- Stanton, R., Flores, R., Warwick, P. D., Gluskoter, H., & G.D., S. (2001). Coalbed Sequestration of Carbon Dioxide. Paper presented at the 1st National Conference on Carbon Sequestration, Washington, USA.

- Stevenson, M., & Pinczewski, V. (1995). SIMED II — Multi-component Coalbed Gas Simulator. User's Manual Version 1.21: Centre for Petroleum Engineering, University of New South Wales.
- Vasilikou, F., Keles, C., Ripepi, N., & Gilliland, E. (2012). Coupling Reservoir and Geomechanical Models to Assess Enhanced Coalbed Methane Recovery in Central Appalachian Coal. Pittsburgh: US DOE/NETL.
- Wang, G. X., Massarotto, P., & Rudolph, V. (2009). An improved permeability model of coal for coalbed methane recovery and CO<sub>2</sub> geosequestration. *International Journal of Coal Geology*, 77(1-2), 127-136. doi: 10.1016/j.coal.2008.10.007.
- Wang, H. F. (2000). *Theory of Linear Poroelasticity with Application to Geomechanics and Hydrogeology*. USA: Princeton University Press.
- Warren, J. E., Root, P. J., & CO., G. R. A. D. (1963). The Behavior of Naturally Fractured Reservoirs. *SPE Journal*, 3(3), 245 - 255.
- Zarrouk, S. J., & Moore, T. A. (2009). Preliminary reservoir model of enhanced coalbed methane (ECBM) in a subbituminous coal seam, Huntly Coalfield, New Zealand. *International Journal of Coal Geology*, 77(1-2), 153-161. doi: 10.1016/j.coal.2008.08.007.
- Zhang, H., Liu, J., & Elsworth, D. (2008). How sorption-induced matrix deformation affects gas flow in coal seams: a new FE model. *International Journal of Rock Mechanics and Mining Sciences*, 45(8), 1226-1236.

# EXPERIENCES IN RESERVOIR MODEL CALIBRATION FOR COAL BED METHANE PRODUCTION IN DEEP COAL SEAMS IN RUSSELL COUNTY, VIRGINIA<sup>2</sup>

*Foteini Vasilikou, Virginia Center for Coal and Energy Research, Virginia Tech,  
Blacksburg, VA*

*Cigdem Keles, Virginia Center for Coal and Energy Research, Virginia Tech,  
Blacksburg, VA*

*Zach Agioutantis, Virginia Center for Coal and Energy Research, Virginia Tech,  
Blacksburg, VA*

*Nino Ripepi, Virginia Center for Coal and Energy Research, Virginia Tech,  
Blacksburg, VA*

*Michael Karmis, Virginia Center for Coal and Energy Research, Virginia Tech,  
Blacksburg, VA*

## **Abstract**

Injection and storage of carbon dioxide (CO<sub>2</sub>) on the coal seam matrix has two benefits: mitigation of greenhouse gas emissions and enhanced recovery of coalbed methane (ECBM). The theory of ECBM is based on the natural affinity for the porous coal matrix to preferentially adsorb CO<sub>2</sub> over methane. According to laboratory measurements on bituminous Appalachian coals, the coal matrix can adsorb almost twice the amount of CO<sub>2</sub> by volume as methane at

---

<sup>2</sup> Experiences in Reservoir Model Calibration for Coal Bed Methane Production in Deep Coal Seams in Russell County, Virginia.

F. Vasilikou, C. Keles, Z. Agioutantis, N. Ripepi, M. Karmis. 2013 Symposium on Environmental Considerations in Energy Production, SME, April 14-18, Charleston, West Virginia.

Reprinted with permission of SME.

Foteini Vasilikou researched and prepared this manuscript, with Cigdem Keles, Zach Agioutantis, Nino Ripepi and Michael Karmis providing technical and editorial input.

typical reservoir pressures. Based on the fact that coalbed methane (CBM) is currently economically produced in many areas in the world, presents the likelihood that CO<sub>2</sub> injected under the appropriate conditions could sequester the CO<sub>2</sub> while displacing and producing CBM.

The Coal Seam Group of the Southeast Regional Carbon Sequestration Partnership (SECARB) has recently completed the injection of 1,000 tons of carbon dioxide into multiple deep unminable coal seams as part of a field validation test at their Russell County, VA site in Central Appalachia and is planning the injection of 20,000 tons of CO<sub>2</sub> in a nearby field in Buchanan County, VA. This paper presents the reservoir modeling procedure and the parameters developed in order to obtain an accurate history match for both gas and water production for a group of eight mature CBM wells that were utilized in the Russell County field test. Optimal parameters were determined both for the single well models as well as for the combined eight-well model. This model will form the base model for simulating CO<sub>2</sub> injection and subsequently predicting post-injection behavior for the upcoming injection test at the Buchanan county site.

## **Introduction**

The Coal Seam Group of the Southeast Regional Carbon Sequestration Partnership (SECARB) has recently completed the injection of 1,000 tons of carbon dioxide into multiple deep unminable coal seams as part of a field validation test at their Russell County, VA site in Central Appalachia (Ripepi et al, 2009).

Figure 10 shows an aerial view of the general area, while Figure 11 shows an aerial view of the injection well (BD114), two monitoring wells (black dots) and the closest offset producing CBM wells.

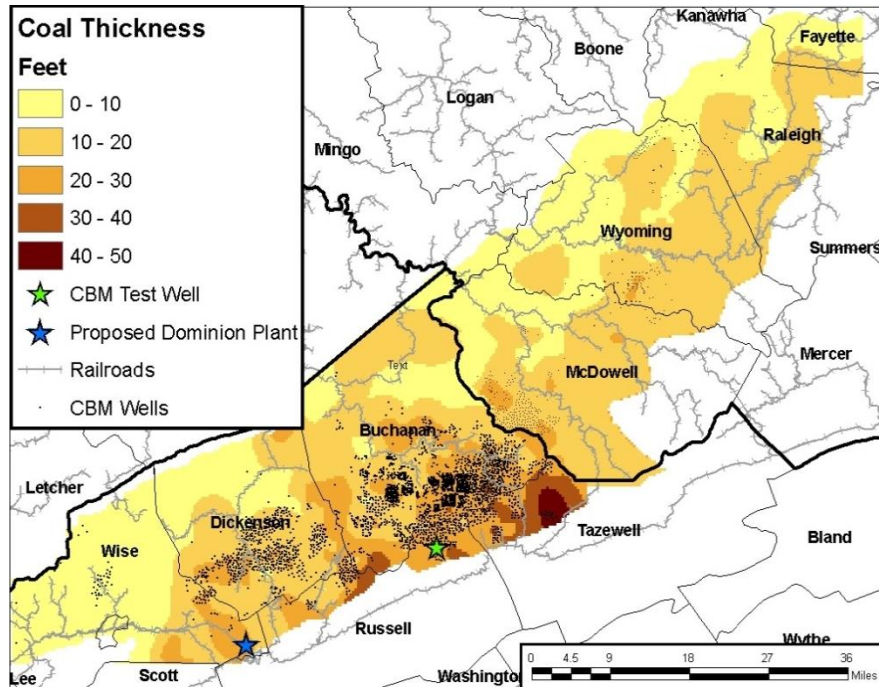


**Figure 10 - Location of Field Test Site (Ripepi et al, 2009)**

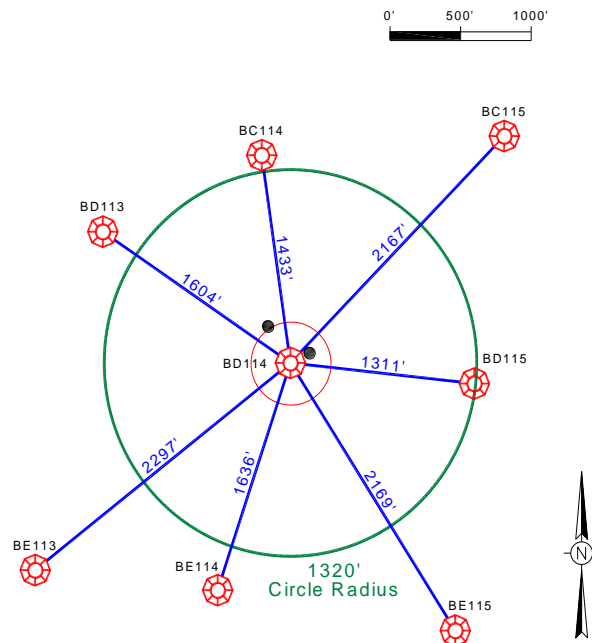


**Figure 11 - Layout of Injection and Offset Wells (Karmis et al., 2008)**

Prior to conducting the injection test a reservoir simulator was built which predicted the extent of the CO<sub>2</sub> plume based on history matching of CH<sub>4</sub> and water production data (VCCER, 2011). In this paper the original reservoir simulation is extended by using new knowledge

regarding seam geometry, coal properties (gas content, adsorption isotherms, anisotropy in permeability), butt and face cleat orientation and by considering well interference.

## **Geology**

A carbon dioxide injection site was selected in Russell County, Virginia, where an existing CBM well was donated by CNX Gas Corporation, a subsidiary of CONSOL Energy Inc. The injection well may be found referenced by its company well name, BD114, or by the State of Virginia designation, RU-0084. BD114 is located at an elevation of 2,523 feet in the Honaker District of Russell County, Virginia.

The Central Appalachian Basin is a northeast-to-southwest trending basin encompassing approximately 10,000 square miles in southwestern Virginia, southern West Virginia and eastern Kentucky (Conrad et al., 2006). Production of CBM began in 1988 with the development of the Nora Field in Dickenson County, Virginia followed by CONSOL Energy developing the Oakwood Field in Buchanan County, Virginia. Since that time, over 5,600 CBM wells have been drilled and brought on-line as producing gas wells in southwest Virginia through 2012 (VaDMME, 2013). The coals in the region near the injection site include those of the Pocahontas Formation and Lee Formation which directly overlies the late Mississippian Bluestone Formation. Coal seams of the Pocahontas and Lee Formation are medium to low-volatile bituminous, high rank and high gas content coals that include the Pocahontas No. 1 through Pocahontas No. 9 seams (Pocahontas Formation and the Upper Seaboard, Greasy Creek, Middle and Lower Seaboard, Upper and Middle Horsepen, War Creek, and Lower Horsepen coals (Lee Formation).

The Upper Horsepen (UH) 2&3 coal seams are the thickest single completion at 3.7 feet of net coal at a depth of 1,374 feet, with a 0.2 feet parting between the seams. The Pocahontas No. 3 coal seam is 2,208 feet deep and 2.4 feet thick at the test site and well outside of current deep mining activities.

The primary confining units include multiple layers of low permeability shale and siltstone beds that range in thickness from five to 55 feet in the vicinity of the injection well. Permeability for the shale and siltstone units is expected to range from 0.001 to 0.1 md, with low porosity. Even the sandstone units are considered to provide confining beds due to the well cemented nature of these rocks. The Lee and Pocahontas Formation sandstones are known to have low

permeability and porosity values, and do not produce natural gas in this area. The tight sandstone units range in thickness from five to 60 feet at the injection site. The sandstone units are expected to have porosity values that range from 1.0 to 3.0 percent and permeability values ranging from 0.1 to 1.0 md based on core testing. All lithologies will encounter some natural fractures; however, these fractures are likely to be cemented with quartz and calcite and are not expected to provide permeability pathways based on core analysis, well logging and field testing (Karmis et al., 2008).

Face and butt cleat planes were measured at two coal seam outcrop locations near the site and they corresponded to within 7 degrees of the known face and butt cleat directions of N18W and N167E respectively, for the deep mined Pocahontas No. 3 coal seam in Buchanan County. A Rose Diagram (Figure 12) was developed to graphically display the cleat directions from the injection well (VCCER, 2011).

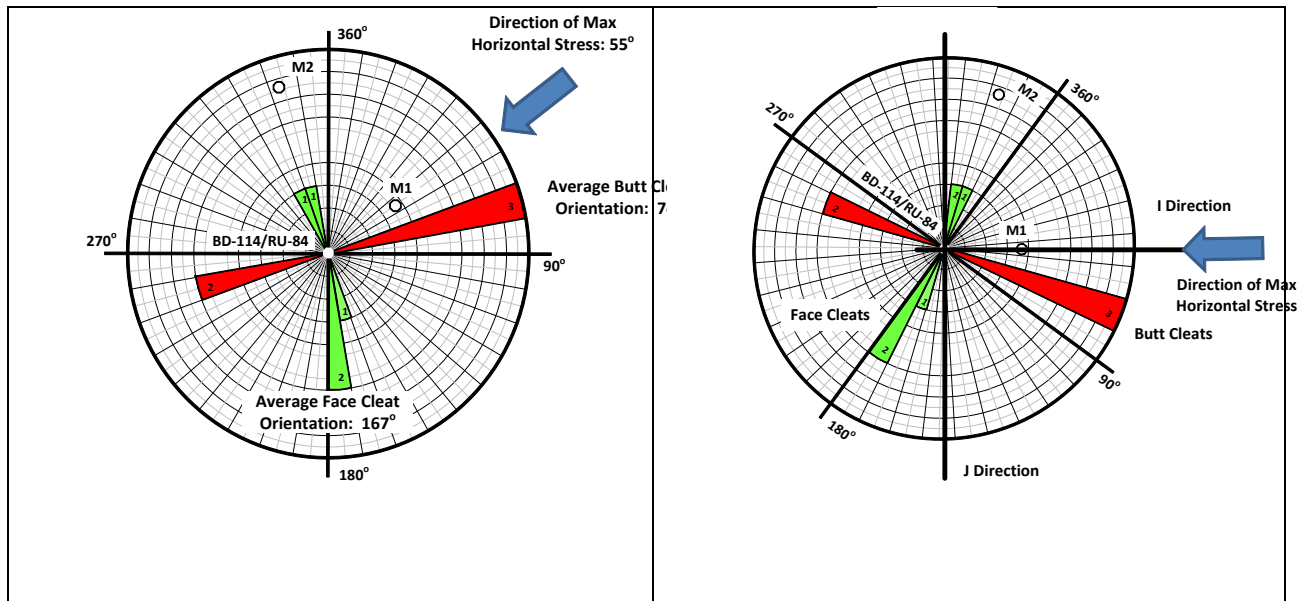


**Figure 12 - (A) Rose Diagram Showing Face and Butt Cleat Orientation (B) Rotation by 35° Clockwise**

## Well Stimulation

Twenty-four separate coal seams, totaling 36.3 feet, between the depths of 1,044 and 2,259 feet were perforated through the casing (Table 1) for well stimulation. The coal seams perforated for the four stage well stimulation average 1.5 feet thick.

BD114 was stimulated over perforations ranging in depth from 1,044.5 to 2,258 feet (318.36 to 688.24 m), using a four-stage nitrogen foam hydraulic fracturing treatment (VaDMME, 2002). These four stages included 24 separate coal seams with a combined coal thickness of 36.3 feet (11.1 m), which were completed (i.e. perforated and fracked) (Table 1). The first stage of the injection well was not considered completed and was abandoned due to loss of energy and “sanding off.” Therefore, a packer was set at 1,400 feet in the casing of BD114 and a string of 2 7/8-inch (7.2 cm) tubing was run back to the surface to isolate the injection zone. Thus, the interval for injection comprised only the first three stages of the stimulation program.

**Table 1 - BD114 Stimulated Coal Seams (VaDMME, 2002)**

Hydraulic Fracture Stage	Coal Seam	Depth to Coal		Coal Thickness		Cumulative Completed Coal Thickness		Zone Thickness	
		(ft)	(m)	(ft)	(m)	(ft)	(m)	(ft)	(m)
<b>Stage 4</b>	Greasy Creek 1	1,045	318.4	1.2	0.4	1.2	0.4	9.6	3.0
	Seaboard 2	1,191	362.9	0.5	0.2	1.7	0.6		
	LowerSeaboard 1&2	1,251	381.3	2.0	0.6	3.7	1.2		
	Lower Seaboard 3	1,313	400.3	2.2	0.7	5.9	1.9		
	UpperHorsepen 2&3	1,374	418.9	3.7	1.1	9.6	3.0		
<b>Stage 3</b>	Middle Horsepen 1	1,421	433.0	2.2	0.7	11.8	3.7	9.8	3.0
	Middle Horsepen 2	1,497	456.4	0.7	0.2	12.5	3.9		
	Pocahontas 11	1,547	471.5	1.9	0.6	14.4	4.5		
	Pocahontas 10	1,573	479.5	1.0	0.3	15.4	4.8		
	Lower Horsepen 1	1,622	494.4	2.1	0.6	17.5	5.4		
	Lower Horsepen 2	1,627	495.9	1.9	0.6	19.4	6.0		
<b>Stage 2</b>	Pocahontas 9	1,664	507.0	1.8	0.5	21.2	6.5	9.3	2.8
	Pocahontas 8-1	1,710	521.2	2.0	0.6	23.2	7.1		
	Pocahontas 8-2	1,725	525.8	1.3	0.4	24.5	7.5		
	Pocahontas 7-1A	1,758	535.9	0.8	0.2	25.3	7.7		
	Pocahontas 7-1B	1,765	538.0	0.9	0.3	26.2	8.0		
	Pocahontas 7-2	1,850	563.9	1.6	0.5	27.8	8.5		
	Pocahontas 7-3	1,875	571.5	0.9	0.3	28.7	8.8		
<b>Stage 1</b>	Pocahontas 6	1,984	604.8	0.5	0.2	29.2	9.0	7.6	2.3
	Pocahontas 5	2,033	619.7	0.7	0.2	29.9	9.2		
	Pocahontas 4-1	2,125	647.7	1.9	0.6	31.8	9.8		
	Pocahontas 4-2	2,148	654.7	1.1	0.3	32.9	10.1		
	Pocahontas 3-1	2,208	673.0	2.4	0.7	35.3	10.8		
	Pocahontas 3-4	2,258	688.3	1.0	0.3	36.3	11.1		
<b>Total</b>	24 Coal Seams			36.3	11.1	36.3	11.1	36.3	11.1

## Production History

BD114 was brought on-line as a CBM producing well in 2002. Water is produced through a 2 7/8-inch string of tubing set below the Pocahontas No. 3 coal seam, and gas is produced between the casing and the tubing (annulus). Up until injection commenced in 2009, BD114 has averaged production of 1.19 thousand cubic meters (Mm<sup>3</sup>) (42 thousand cubic feet (Mcf)) of natural gas per day and 2.2 barrels of water per day (Figure 13). BD114 produced 2.89 MMm<sup>3</sup> (102 MMcf), and 5,360 barrels of water prior to being taken off-line for conversion to an injection well. Gas production to date is nearly 10 percent of the estimated gas in place (VCCER, 2011). BD114 is a below average gas producer for this gas field. The average production of the seven offset wells is 1.87 Mm<sup>3</sup> (66 Mcf) per day of natural gas and 2.5 barrels per day of water. Figure 13 presents the gas production history for the injection well and the nearby offset wells (VCCER, 2011).

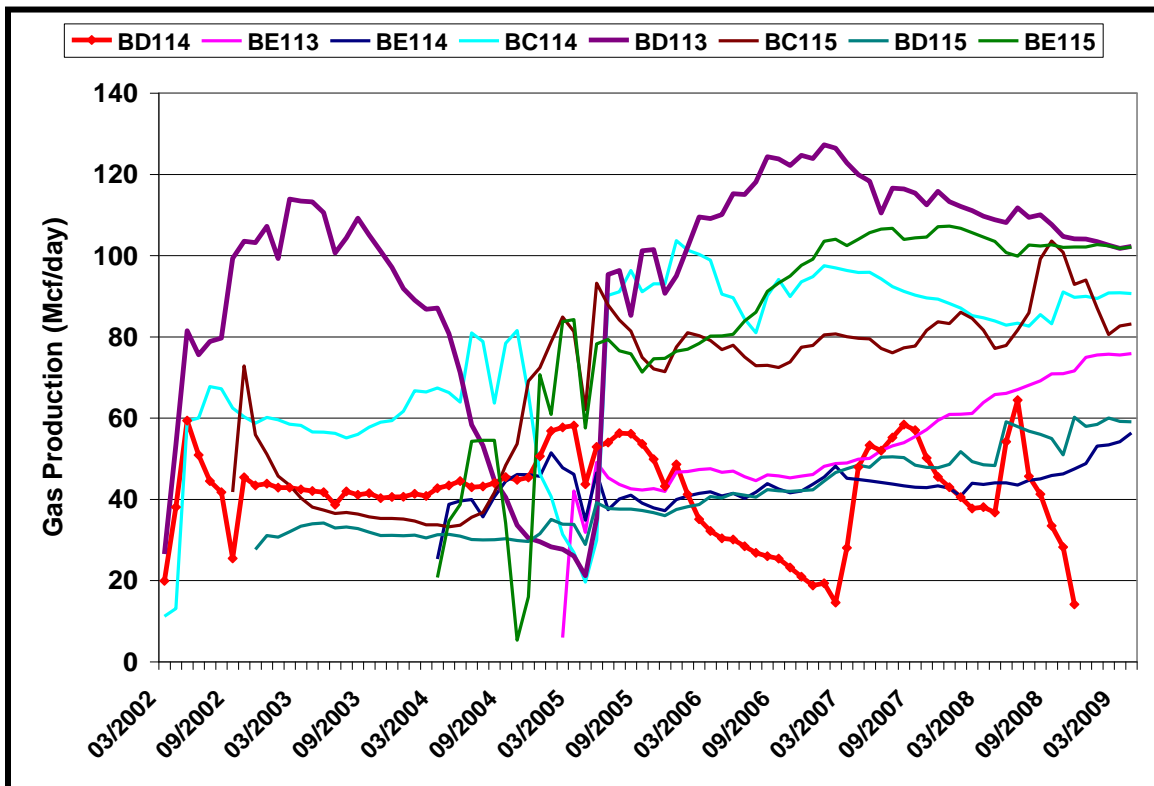


Figure 13 - Gas Production History at the Injection and the Offset Wells

## **Modeling**

### **Description of Production Model**

Preliminary reservoir modeling prior to the actual field test where CO<sub>2</sub> was injected into the coal seams was conducted utilizing Advanced Resources' COMET3 reservoir simulator for CBM. The ultimate goal of this preliminary modeling was to estimate the size of the CO<sub>2</sub> plume as well as the expected CO<sub>2</sub> injection rate that could be achieved during injection operations. As additional laboratory analysis, field data and results from the CO<sub>2</sub> injection field test became available the need to revise the original reservoir model became apparent. At the same time, Computer Modeling Group Ltd.'s GEM software, a compositional and unconventional reservoir simulator, was utilized since it could simulate the effect of fractures. This paper discusses the setup and parameters for production modeling of the Russell county field test using CMG's reservoir simulator. The ultimate goal of the current study will be to obtain a good history match that will help modeling of Enhanced Coal Bed Methane production after the injection well comes back on line. The latter work is detailed in Vasilikou et al. (2013).

A dual porosity, single permeability model was setup, since coal matrix permeability is considered extremely low. As mentioned before, there were four fracture stages including a total of 24 coal seams. Gas and water rates were available per well and therefore, only aggregate production was available for all seams. Since coal seams have different characteristics it was decided to model four equivalent coal seams at the highest elevation of each fracture stage. The thickness of these modeled coal seams corresponds to the sum of the thicknesses of each seam within the fracture stage. A grid was generated that covers all wells with nearly the same distance from the boundaries for all wells.

The orientation of the hydraulic fractures was critical in determining grid generation. As the model can only allow for hydraulic fractures along either the I (x) or J (y) direction, and hydraulic fractures were developed along the maximum horizontal stress in the area (Figure 12), the grid was rotated by 35 degrees clockwise (-35°) to orient the maximum horizontal stress in the I direction. In addition, it was assumed that the permeability in the I direction is equal to butt cleat permeability and that in the J direction equal to face cleat permeability.

Furthermore, it was assumed that the modeled group of eight wells can be considered independent of other wells surrounding this grid. The resulting grid for all layers including the eight wells is shown in 3D view in Figure 14.

Although, actual fracture modeling was not accomplished within the scope of this study, nevertheless, the foundation was set and results will be presented in the upcoming paper by Vasilikou et al. (2013).

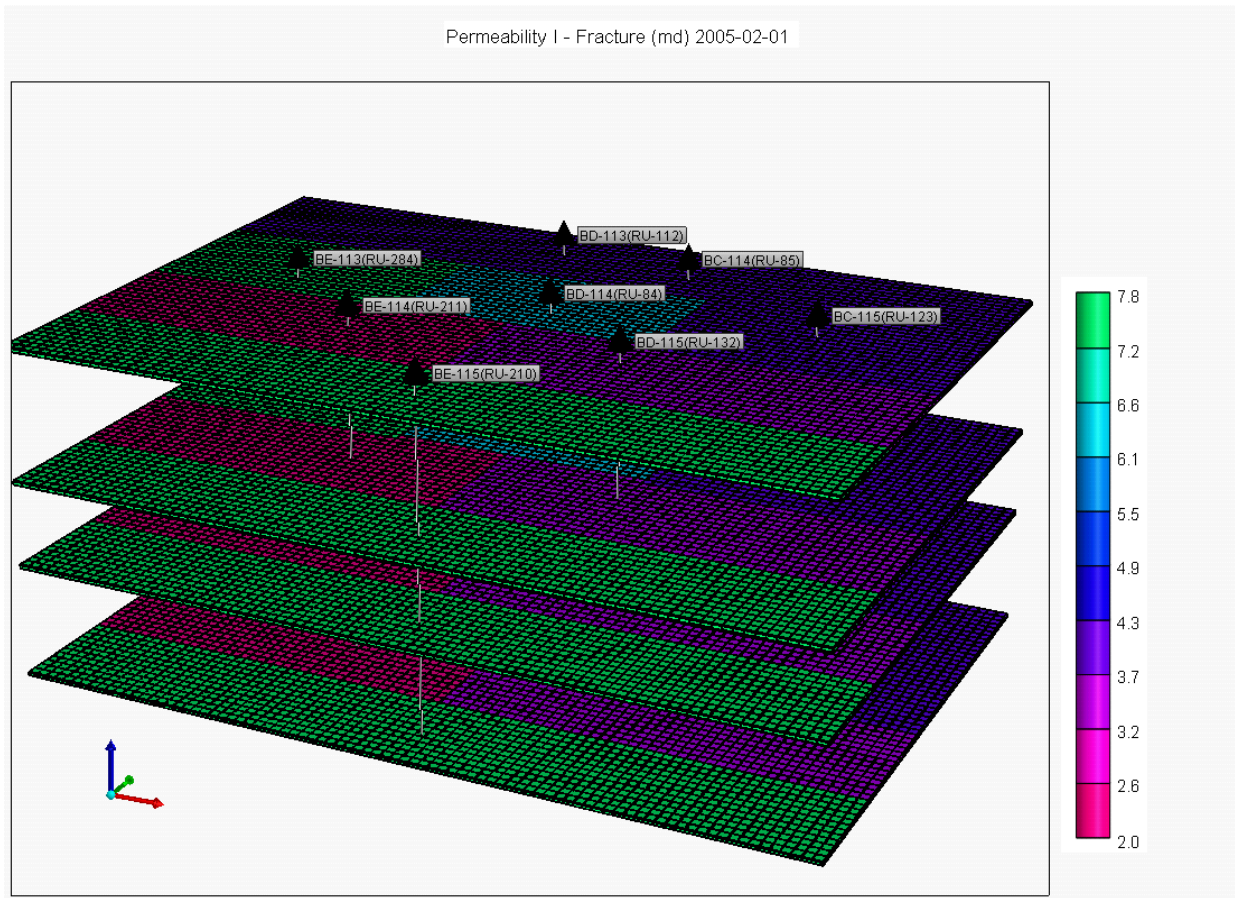


**Figure 14 - 3D View of Model Grid and Wells**

The parameters and material properties shown in Table 2 were assembled utilizing data from (a) collected from monitoring well BD114-M2 (Figure 12), (b) coal sample analysis (Harpalani, 2012).

In addition it should be noted that historical production data for gas and water were aggregated on a monthly basis.

**Table 2 - Parameters and Material Properties Used in the Reservoir Model**

Number of Grid Blocks per Direction (combined model)	I= 84, J= 56
Number of Grid Blocks per Direction (single-well models)	Variable (typical I=25,J=14)
Grid Block Sizes per Direction (combined model), m	DI=25, DJ=25
Coal Layers and Thicknesses, m	4 Layers;(i) 2.93, (ii) 2.98, (iii) 2.83, (iv) 2.31
Coal Layers Depths- Grid Tops, m	318.4, 433, 507, 604.8
Coal (Matrix) Porosity, %	6.5%, dual porosity model
Cleat (Fracture) Porosity, %	Variable, 1-3%, dual porosity model
Matrix Permeability, mD	Not in use, single permeability model
Cleat Permeability, mD	Variable (domain divided into 6 regions), 2-18.97 mD, face to butt cleats ratio:1-5
Fracture Spacing per Direction, m	I: 0.00508, J: 0.00508, K: 0.00508
Well Radius, m	0.088
Formation Compressibility (Matrix & Fracture), 1/kPa	2.90075E-07 (at reference pressure 4136.8 kPa) (Harpalani, 2012)
Reservoir Temperature, °C	27.2
Water Density, kg/m <sup>3</sup>	1000.8 at reference pressure 101.3 kPa
Relative Permeability Curves Gas-Water	Gash et al. 1993, Mavor et al. 1953 (see Figure 15)
Adsorption Isotherms for Methane according to Langmuir. Langmuir Constants VL, gmole/kg; PL, 1/kPa	Layer 1: Pocahontas 11, VL= 0.8201299, PL= 0.0005224 Layer 2: Pocahontas 11, VL= 0.8559385, PL= 0.0005224 Layer 3: Pocahontas 7, VL= 0.8201299, PL= 0.00047818 Layer 4: Pocahontas 3, VL= 0.7700043, PL= 0.00034816 (VCCER, 2011)
Coal Density, kg/m <sup>3</sup>	1323.9 (VCCER, 2011)
Methane Desorption Time, days	50
Pore Pressure Gradient, kPa/m	7

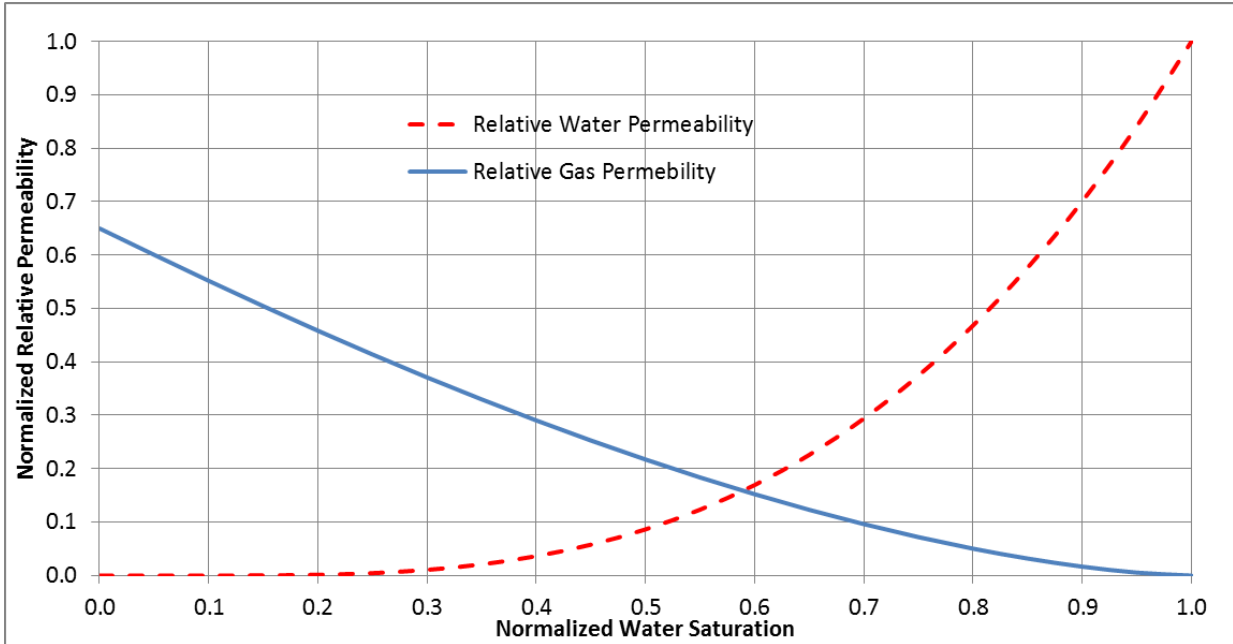


**Figure 15 - Relative Permeability Curves Used in the Single Well Runs (Gash et al. 1993, Mavor et al. 1953) (SWT: Water Relative Permeability or Water Saturation Fraction; SLT: Gas Relative Permeability or Gas Saturation Fraction) (see Table 2)**

Previous work (VCCER, 2011) had shown that cleat permeability may be different around each producing well. Under this assumption eight single-well models were setup which comprised 25 to 50 cells in the X direction, approximately 20 cells in the Y direction and 1 cell in the Z direction for each of the four modeled seams. Single-well models used the cleat permeability regions shown in Figure 16 and Figure 17.

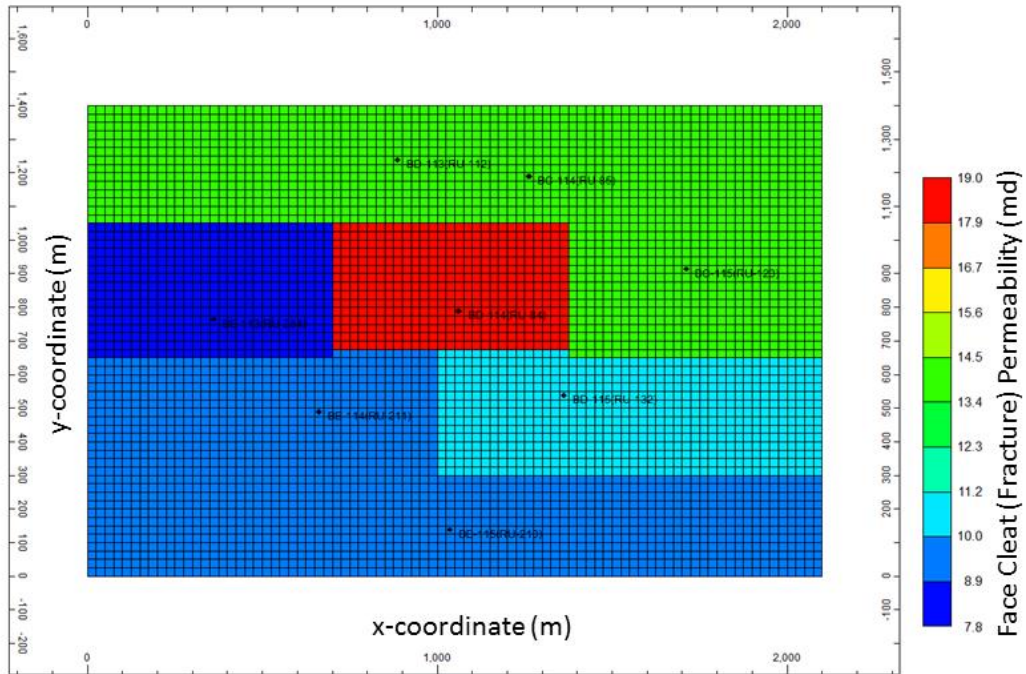


Figure 16 - Face Cleat Permeability Regions for Single-Well Models and Combined Model

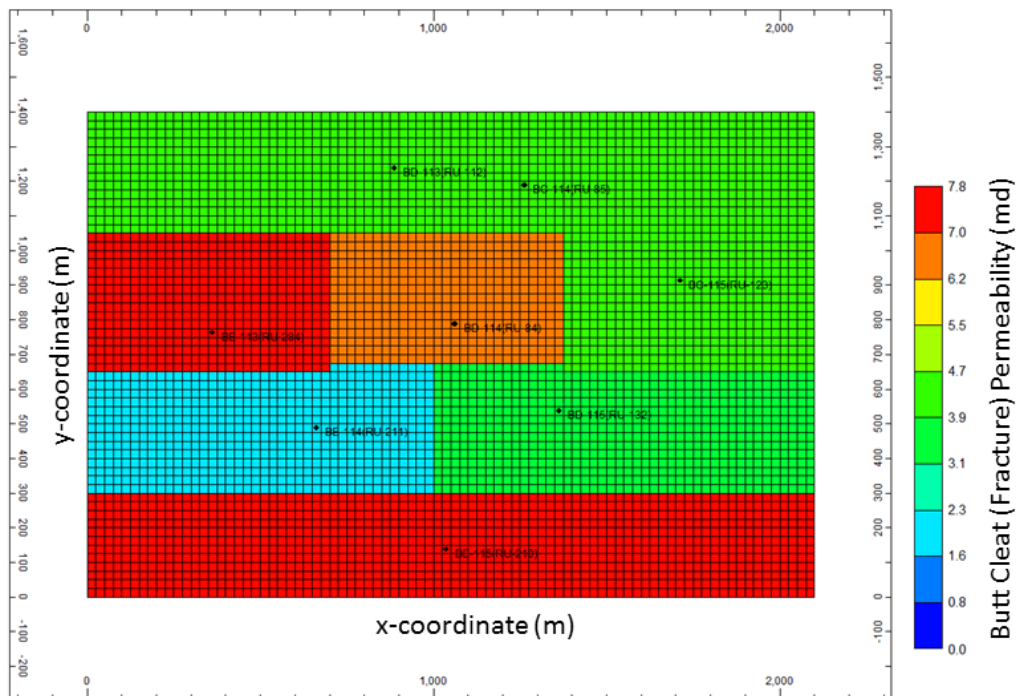


Figure 17 - Butt Cleat Permeability Regions for Single-Well Models and Combined Model

## Results and Discussion

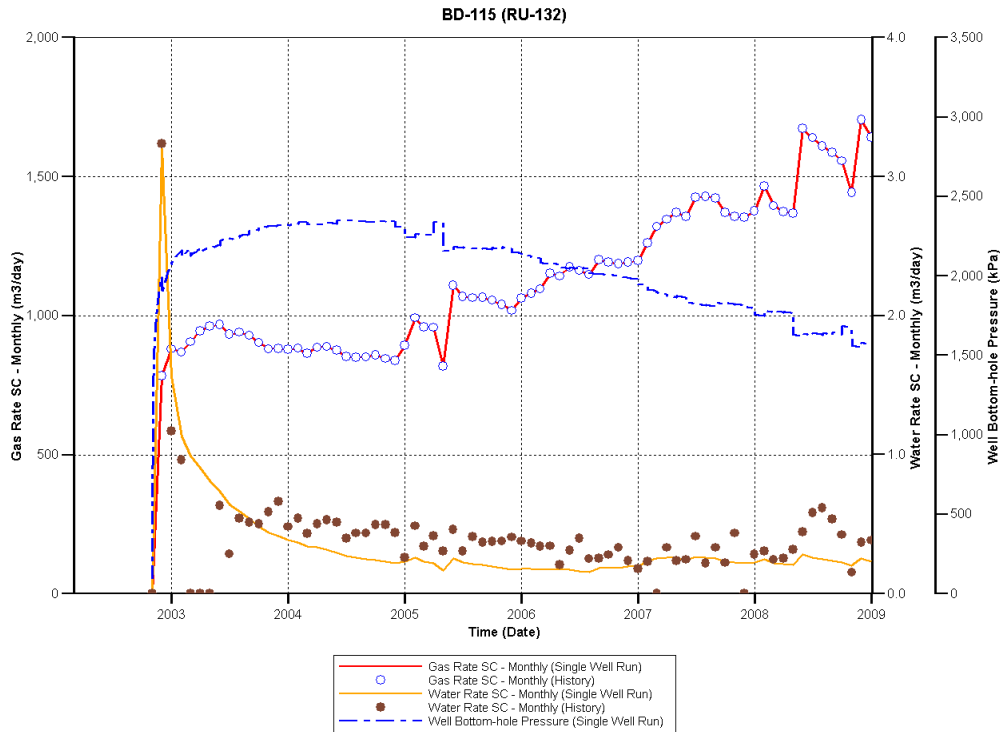
Table 3 shows the optimal parameters determined for the single-well runs. The bottom hole pressure (assumed to be equal to the reservoir pore pressure during production) also follows an expected trend, i.e. increased for higher water production, and with a decreasing trend as gas rate values increase. Note that these models do not include modeling of hydraulic fractures. Models with hydraulic fractures are discussed in Vasilikou et al. (2013).

**Table 3 - Optimal Parameters Determined for the Dingle-Well Runs**

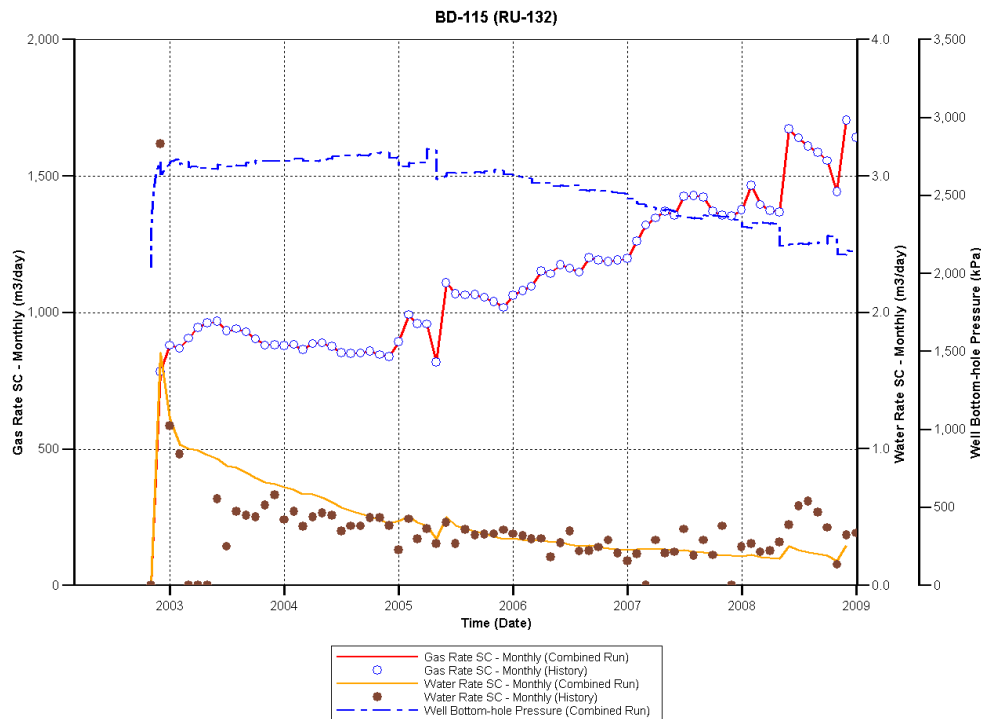
Well	Fracture Porosity	Face Cleat Permeability (mD)	Butt Cleat Permeability (mD)	Face to Butt Cleat Permeability Ratio	Bottom Hole Pressure (kPa)	Water Saturation in the Cleats
RU-84	0.0013	18.97	6.32	3	200	1
RU-85	0.001	14.42	4.12	3.5	700	1
RU-112	0.0013	14.42	4.12	3.5	1200	0.9
RU-123	0.001	14.42	4.12	3.5	200	0.8
RU-132	0.001	10.42	3.47	3	200	0.9
RU-210	0.001	10	7.8	1.28	1300	1
RU-211	0.001	10	2	5	1400	1
RU-284	0.001	7.8	7.8	1	1250	1

Figure 18 presents the reservoir simulation history-match results for BD-115 (RU-132) for a single well run. Gas rate predictions match exactly the measured data, while water rate predictions are adequate based on the quality of measured water data. The data for water production by well are estimated by dividing the total water production of a group of wells by the time the water pump on each well operated, unlike gas production which is measured at each well. The bottom hole pressure (assumed to be equal to the reservoir pore pressure during production) also follows an expected trend, i.e. increased for higher water production, and with a decreasing trend as gas rate values increase.

Figure 19 presents the reservoir simulation history-match results for BD-115 (RU-132) for a combined run where the single run optimum parameters were utilized as inputs for each well. In both cases the gas rate match is perfect as the primary simulation constraint comprises matching the gas rate.



**Figure 18 - History Match on Gas and Water Rates for Well BD-115 (RU-132) Under a Single Well Run. The Bottom Hole Pressure is Also Shown**



**Figure 19 - History Match of Gas and Water Rates for Well BD-115 (RU-132) for the Combined Run. The Bottom Hole Pressure is Also Shown**

The optimal parameters for the combined model were then determined using the optimization algorithm (CMOST) built into the CMG/GEM package. The initial range for each optimized parameter was determined using data ranges that were based on the data in Table 3 for the single-well runs. The actual data ranges entered into the optimizer are shown in Table 4. The optimization algorithm was instructed to find optimum parameter combinations in these ranges. The objective function was set to minimize the error on cumulative water while the operating constraint was to match the gas produced. The face to butt cleat permeability ratio was kept at 3 for all runs because preliminary runs showed that approximate ratio to be valid for all wells. Although the algorithm should examine all possible combinations, some parameter combinations are evidently not tested due to some internal optimization. In total 835 runs were completed using CMOST. Table 5 shows the results obtained for all wells.

**Table 4 - Parameter Range Used as Input in the CMOST Model Runs**

Fracture Porosity	Butt Cleat Permeability (mD)	Bottom Hole Pressure (kPa)	Water Saturation in the Cleats
0.0010	1	200	0.900
0.0015	2	500	0.925
0.0020	3	800	0.950
0.0025	4	1100	0.975
0.0030	5	1400	1.000
	6	1700	
		2000	

In addition the optimum relative permeability curves were determined by the CMOST algorithm. Two of these diagrams are shown in Figure 20. The fact that different optimum curves are calculated for each well indicates that the relative permeability curves have a significant impact on the gas and water rate calculations, may differ considerably between wells.

**Table 5 - Optimal Parameters After CMOST Runs and Manual Adjustments for the Multi-Well Runs**

Well	Fracture Porosity	Face Cleat Permeability (mD)	Butt Cleat Permeability (mD)	Face to Butt Cleat Permeability Ratio	Bottom Hole Pressure (kPa)	Water Saturation in the Cleats
RU-84	0.0020	12.0	4.0	3	200	0.950
RU-85	0.0011	10.5	3.5	3	200	0.975
RU-112	0.0010	9.0	3.0	3	800	0.950
RU-123	0.0010	18.0	6.0	3	500	0.800
RU-132	0.0026	16.8	5.6	3	1100	0.975
RU-210	0.0015	9.0	3.0	3	1500	0.950
RU-211	0.0025	9.0	3.0	3	1700	0.950
RU-284	0.0010	9.0	3.0	3	800	0.900

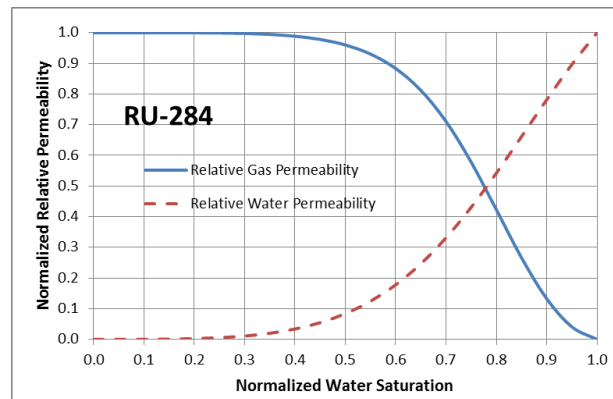
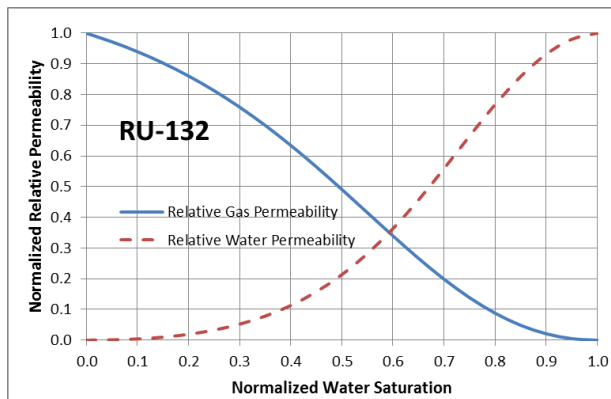


**Figure 20 - Relative Permeability Curves as Determined by the Optimization Algorithm for Two of the Eight Production Wells (SWT: Water Relative Permeability or Water Saturation Fraction; SLT: Gas Relative Permeability or Gas Saturation Fraction)**

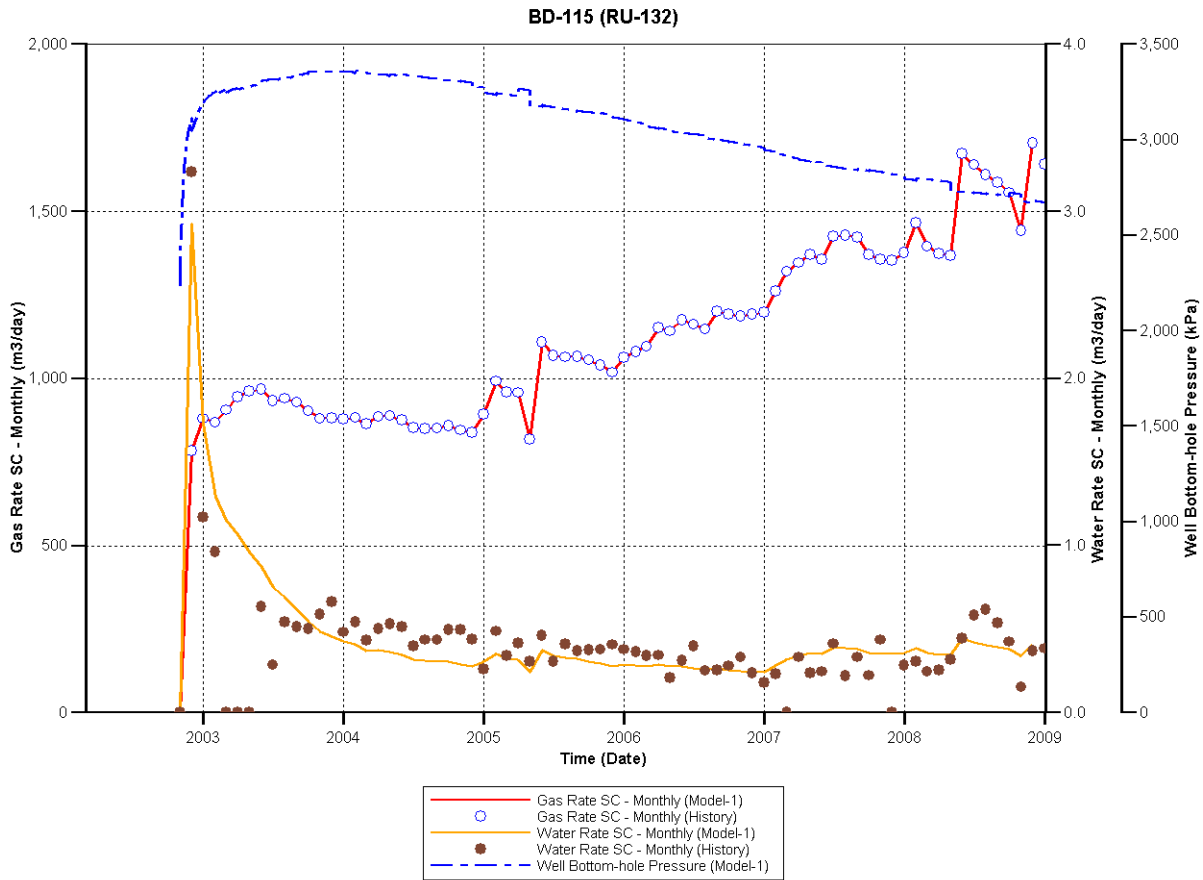


**Figure 21 - History Match on Gas and Water Rates for Well BD-115 (RU-132) for the Combined Run with Optimized Input Parameters. The Bottom Hole Pressure is Also Shown**

Figure 21 presents the reservoir simulation history-match results for BD-115 (RU-132) for a combined run where the optimal parameters from the combined well optimization were used. It is clear that the calculated water rate production matches the measured data better than in the case of the previous two models (single or combined run). At the same time the maximum pore pressure calculated for this production history match is higher than in previous runs, reaching almost 3500 kPa at its maximum.

## Conclusions

In this paper, the modeling procedure for coal bed methane production of selected wells in Russell County, VA is discussed in detail. Through parametric analysis and optimization, the best parameters for this reservoir are identified. Utilizing these parameters, the model can

accurately predict the gas production rate for all wells through history matching, while the total water produced from the reservoir matches reasonably well the measured values.

In addition, the model identifies the most sensitive parameters in the simulation and how these interact in closely spaced wells. The development of this model along with the optimal parameters that were calculated will be subsequently used for modeling of CO<sub>2</sub> injection and the corresponding enhanced gas recovery potential in the same group of seams.

## **Acknowledgments**

Financial assistance for this work was provided by the U.S. Department of Energy through the National Energy Technology Laboratory's Program under Contract No. DE-FC26-04NT42590 and DE-FE0006827.

## **References**

- Gash, B.W., Volz, R.F., Potter, G., and Corgan, J. M. 1993. The effects of cleat orientation and confining pressure on cleat porosity, permeability and relative permeability in coal. Paper 9321 in Proceedings of the 1993 International CoalBed Methane Symposium. Tuscaloosa: University of Alabama.
- Mavor, M.J. and Robinson, J.R., 1993, "Analysis of Coal Gas Reservoir Interference and Cavity Well," Paper SPE, 25860, presented at the Joint Rocky Mountain Regional and Low Permeability Reservoirs Symposium, Denver, CO, April 26-28.
- Computer Modelling Group Ltd (CMG), C. (2003). GEM. Calgary, Canada.
- Ripepi, N., Karmis, M., Miskovic, I., Shea C., and J.M. Conrad. 2009. Results from the Central Appalachian Basin Field Verification Test in Coal Seams. 26th Annual International Pittsburgh Coal Conference, Pittsburgh, PA, USA, 2009. CD-ROM of Proceedings, Paper # 33-4.
- Karmis, M., Ripepi, N., Miskovic, I., Conrad, M., Miller, M., and C. Shea. 2008. CO<sub>2</sub> Sequestration in Unminable Coal Seams: Characterization, Modeling, Assessment and Testing of Sinks in Central Appalachia. Twenty-Fifth Annual International Pittsburgh Coal Conference, Pittsburgh, PA, USA, 2008. CD-ROM of Proceedings, Paper # 29-3.

- Conrad, J. M., Miller, M. J., Phillips, J., Ripepi, N. 2006. Characterization of Central Appalachian Basin CBM Development: Potential for Carbon Sequestration and Enhanced CBM Recovery, 2006 International Coalbed Methane Symposium, Preprint 0625, Tuscaloosa, AL.
- Virginia Department of Mines, Minerals and Energy (VaDMME). 2013. <http://www.dmme.virginia.gov/DGO/Production/2010-County.pdf>, accessed: February 2013.
- Conrad, J. M. , Miller, M. J., Ripepi N. 2007. Potential for Carbon Sequestration in the Central Appalachian Basin. Air and Waste Management Association Conference, 2007, Paper # 187.
- Vasilikou, F. C. Keles, Z. Agioutantis, N. Ripepi and M. Karmis, 2013. Model Verification of Carbon Dioxide Sequestration in Unminable Coal Seams with Enhanced Coal Bed Methane Recovery, to be published in 23rd World Mining Congress, August 11-15, Montreal, Canada.
- Virginia Center for Coal and Energy Research (VCCER). 2011. Final Technical Report: Characterization and Field Validation of the Carbon Sequestration Potential of Coal Seams in the Central Appalachian Basin, 2011: Blacksburg, VA.
- Virginia Department of Mines, Minerals and Energy (VaDMME). 2002. “CBM-PGP-BD114 Completion Report”, Form DGO-GO-15, 105 p.
- Harpalani, S, personal communication, December 14, 2012.

# **MODEL VERIFICATION OF CARBON DIOXIDE SEQUESTRATION IN UNMINEABLE COAL SEAMS WITH ENHANCED COALBED METHANE RECOVERY<sup>3</sup>**

*Foteini Vasilikou, Virginia Center for Coal and Energy Research, Virginia Tech,  
Blacksburg, VA*

*Cigdem Keles, Virginia Center for Coal and Energy Research, Virginia Tech,  
Blacksburg, VA*

*Zach Agioutantis, Department of Mineral Resources Engineering,  
Technical University of Crete*

*Nino Ripepi, Virginia Center for Coal and Energy Research, Virginia Tech,  
Blacksburg, VA*

*Michael Karmis, Virginia Center for Coal and Energy Research, Virginia Tech,  
Blacksburg, VA*

## **Abstract**

Commercial deployment of Carbon Capture Utilization and Storage (CCUS) requires field testing of a scale that can stress the geologic reservoirs. One such reservoir of interest consists of unminable coal seams that exhibit favorable characteristics and depositional environments and lower pressure and temperature than other, deeper, reservoirs. Such conditions can reduce compression costs while utilizing the action of adsorption that offers a more effective carbon dioxide (CO<sub>2</sub>) bonding than free storage or solution. To ensure the success of such tests, a

---

<sup>3</sup> Model Verification of Carbon Dioxide Sequestration in Unmineable Coal Seams with Enhanced Coalbed Methane Recovery.

F. Vasilikou, C. Keles, Z. Agioutantis, N. Ripepi, M. Karmis 2013 23<sup>rd</sup> World Mining Congress, Montreal, Canada.

Used with permission of the Canadian Institute of Mining, Metallurgy and Petroleum.

Foteini Vasilikou researched and prepared this manuscript, with Cigdem Keles, Zach Agioutantis, Nino Ripepi and Michael Karmis providing technical and editorial input.

number of parameters should be accurately determined, such as the seam geometry and stratigraphy, coal porosity and permeability parameters as well as optimum injection conditions. In essence the CO<sub>2</sub> injection model should be calibrated for the reservoir characteristics using all available data. History matching calibrations are based on gas and water production from existing wells prior to injection. This paper will present reservoir models that were developed for a pilot--scale 907 tonnes (1000 tons) CO<sub>2</sub> injection test that was performed in 2009 through one legacy coalbed methane production well in Russell County, Virginia, USA. The model incorporates a number of individual coal seams about 0.3 m (1ft) in thickness located at depths ranging from 300 to 700 m (1,000 to 2,200 feet). Model calibration was performed through history matching to prior production data, and subsequently the model was utilized to develop different injection scenarios. The developed model was used after injection to calculate CO<sub>2</sub> plume distribution patterns that were monitored at the injection test. The paper will present model data and assumptions with a special emphasis on the effect of hydraulic fractures and the skin factor to the coalbed methane (CBM) production model.

## **Introduction**

The mitigation of greenhouse gas emissions and enhanced recovery of coalbed methane are benefits to sequestering CO<sub>2</sub> in coal seams. This is possible because of the affinity of coal to preferentially adsorb CO<sub>2</sub> over methane (Shi and Durucan, 2005). Coalbed methane (CBM) is the most significant natural gas reserve in the Virginia portion of the Central Appalachian Basin, USA and currently is economically produced in many fields in the Basin from vertical CBM wells. The recovery factor for vertical CBM well development is estimated that 55% of the gas in place would be recovered by primary recovery techniques, 20% of the gas in place is unrecoverable residual gas, and the remaining 25% can be recovered by implementing CO<sub>2</sub>-sequestration operations. Since coal has a greater affinity for CO<sub>2</sub> than for methane gas, the injected CO<sub>2</sub> should preferentially be adsorbed on the surface of the coal, thereby releasing methane gas that would be recovered at offset producing CBM wells. A field verification test successfully injected 907 tonnes of CO<sub>2</sub> into a mature CBM production well at the Russell County, Virginia test site hosted by CNX Gas. The injection commenced on January 9, 2009 and was completed on February 10, 2009. The maximum daily injection rate was over 50 tonnes of CO<sub>2</sub> per day, with an average injection rate above 36 tonnes per day.

## Field Description

The Central Appalachian Basin is a northeast-to-southwest trending basin encompassing approximately 25,900 km<sup>2</sup> in southwestern Virginia, southern West Virginia and eastern Kentucky (Conrad, 2006). Production of CBM began in 1988 with the development of the Nora Field in Dickenson County, Virginia followed by CONSOL Energy / CNX Gas developing the Oakwood Field in Buchanan County, Virginia. Since that time, over 5,600 CBM wells have been drilled and brought on-line as producing gas wells in southwest Virginia through 2012 (VaDMME, 2013). As of year-end 2010, the coal seams in the Central Appalachian Basin had produced over 28 km<sup>3</sup> of CBM (VaDMME, 2013). Virginia is the primary producer of CBM in the basin accounting for over 90% of the production. In 2010, Virginia produced a record 3.4 km<sup>3</sup> of CBM which accounted for nearly 80% of the natural gas produced in the Commonwealth (VaDMME, 2013). The U.S. Department of Energy (2013) stated that Virginia accounted for 5.1% of the CBM production in the U.S. in 2010 and accounts for 10% of the CBM reserves, nearly 57 km<sup>3</sup>. The majority of CBM development is in areas where gas contents range between 12.5 – 18.7 cubic meters of gas per tonne of coal (Conrad, 2006), making these seams some of the gassiest in the country. The CBM productivity of the basin indicates that coal permeability should allow for carbon dioxide injection and storage (Karmis, 2008).

The coals in the region include those of the Lee Formation and Pocahontas Formation and are medium to low-volatile bituminous, high rank and high gas content coals. In the area of the injection, there are multiple thin unmineable coal seams (up to 24 separate coals) with net coal thickness of up to 11 m. The coals average less than 0.6 m in thickness and are deposited over a large range in depth, 250 to 700 m.

Based on geologic characterization and production studies, wells in the South Oakwood CBM Field were deemed appropriate for the injection test. These CBM wells were developed on 242,800 m<sup>2</sup> grid spacing from 2002 to 2005. Stimulation occurs through perforations in the well casing into coals greater than 0.15 m thick with a multiple-stage nitrogen foam hydraulic fracturing treatment (VaDMME, 2002). The purpose of hydraulic fracturing is to breakdown the coal and create fractures that allow gas to flow through the coal matrix to the fractures and then to the wellbore. In order to keep these fractures open for gas to flow to the well bore, a proppant

of coarse sand was injected with the high pressure nitrogen foam. Water is produced through a 73.025 mm string of tubing set below the deepest coal seam, and gas is produced between the casing and the tubing (annulus). The water is removed from the formation to decrease the pressure of the bed and to allow for the methane to be desorbed and be produced through the well (Holman, 1996).

CNX Gas donated an existing CBM well in the South Oakwood Field in Russell County, Virginia for the carbon dioxide injection field test. The injection well is referenced by its well name, BD114, or by its designation assigned by the State of Virginia, RU-84. Prior to injection, BD114 averaged production of 1189 m<sup>3</sup> of natural gas per day and 0.26 m<sup>3</sup> of water per day since 2002 and is a slightly below average gas producer for this gas field.

### **Field Site Layout**

A coal field cleat examination was completed to verify the cleat direction of coals at the injection site verses known face and butt cleat directions of N18W and N67E respectively, for the deep mined Pocahontas No. 3 coal seam in Buchanan County. Face and butt cleat planes were measured at two coal seam outcrop locations near the site and they corresponded to within 7 degrees of the known values. A Rose Diagram (Figure 22) was developed to graphically display the cleat directions from the injection well (VCCER, 2011).

Prior to injecting carbon dioxide, two monitor wells were drilled in close proximity to the injection well (BD-114), one 41.2 m away (M1) and the other 87.5 m away (M2). The two monitor wells were drilled at roughly 90 degree offsets from the injection well through the deepest coal seam that had been perforated in the injection well and exposed each coal seam being injected into using a packer and tubing. These monitor wells were used to monitor the pressure of plume, as well as composition of gas at each well. This study affirms that the monitoring wells for the test site are arranged in both the hydraulic fracture (M1) and face cleat (M2) directions (Figure 22).

### **CO<sub>2</sub> Injection**

The field test successfully injected 907 tonnes of CO<sub>2</sub> at the Russell County, Virginia test site hosted by CNX Gas. The injection commenced on January 9, 2009 and was completed on February 10, 2009. The data was gathered on a minute basis throughout the one-month injection

and then averaged on an hourly basis to smooth out the curves. Throughout the injection, the temperature of CO<sub>2</sub> injection was maintained close to 100 degrees Fahrenheit, the pressure was held below 6895 kPa (1,000 psia) and the flow rate varied according to CO<sub>2</sub> delivery availability and operating below the maximum pressure. The maximum daily injection rate was over 50 tonnes of CO<sub>2</sub> per day, with an average injection rate above 36 tonnes per day. During the last three days of injection, at close to maximum pressure, the injection rate declined to a low of 15.4 tonnes per day. The decrease in the injection rate could be attributed to either the pressure of the reservoir pushing back or swelling of the coals due to adsorption of CO<sub>2</sub> at the higher pressures. Results from the injection provided essential data for establishing the conditions under which CO<sub>2</sub> can be injected into underlying coal seams, ultimately to establish a reasonable estimate of the volume of CO<sub>2</sub> that can be sequestered in Central Appalachian coal seams through predictive reservoir modeling.

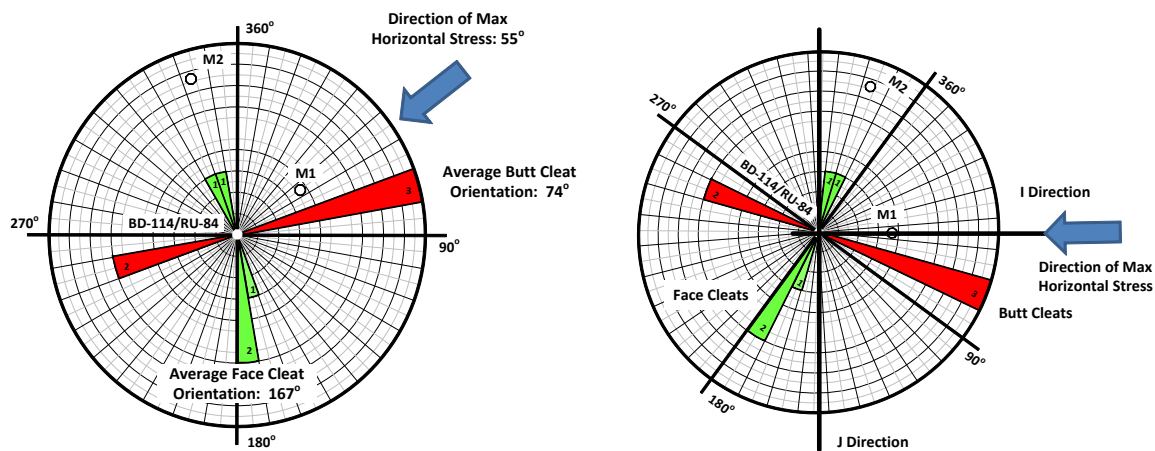


**Figure 22 - (A) Rose Diagram Showing Face and Butt Cleat Orientation (B) Rotation by 35° degrees clockwise**

### Injection Logging

While the CO<sub>2</sub> was being injected at a defined temperature, pressure, and rate, a spinner survey was run downhole to establish the quantity of CO<sub>2</sub> being injected into each coal seam. As part of the spinner survey, temperature and pressure were logged via a wireline downhole to help profile the injection operations. This survey encountered problems in that the spinner ran into liquid CO<sub>2</sub> at 506 m deep in the wellbore. The temperature log shows the sudden decrease in

temperature which happened when the CO<sub>2</sub> changed phases from gas to liquid. The results of the temperature log show significant changes in temperature occurring at each open perforation where CO<sub>2</sub> was injected into coal seams. The change in temperature was plotted and shows that the greatest change occurred at the shallowest seams that were receiving CO<sub>2</sub>. The change in temperature most likely can be correlated with flow rate (VCCER, 2012).

### **Monitoring Well Results**

As the CO<sub>2</sub> injection commenced, it was obvious that there was a direct connection through existing hydraulic fractures to the closest monitoring well, M1. Within 30 minutes of starting the injection operation, the pressure in M1 unexpectedly raised rapidly to 3,447 kPa (500 psia) and CO<sub>2</sub> content increased to greater than 95%. The profile of the pressure in M1 followed closely with the pressure at the injection well, lagging about 690 kPa (100 psia) through the one month injection. At the end of the injection, the pressure in M2 mirrored M1 and the injection well. It is unknown if the rise in pressure in M2 was as quick as M1, but the results indicate that the M2 is also interconnected in a fracture network with the injection well, BD114 as the CO<sub>2</sub> content in M2 also reached greater than 95%.

### **Reservoir Modeling**

The CBM production data between 2002 and 2009 was used to develop a reservoir model of the area. The original model was developed utilizing Advanced Resources' COMET3 reservoir simulator for CBM (Ripepi et al., 2009), but in 2013 a new model was developed using Computer Modeling Group Ltd.'s GEM software, a compositional and unconventional reservoir simulator (Vasilikou et al., 2013), so that the effect of fractures could be incorporated. The 2013 study utilized a different geometry and reservoir parameters resulting in a better history match than before, while obtaining insight regarding the specific reservoir characteristics and behavior. This paper complements existing work by introducing the effect of hydraulic fractures to the CBM production model by employing two methods: using the "Skin Factor" (SF) approach and using the "Hydraulic Fracture" (HF) approach. Subsequently the central production well is converted to an injector and CO<sub>2</sub> is injected into the reservoir for a month according to the injection history presented in the previous section.

## **Theoretical Considerations for the Skin Factor and the Hydraulic Fracture Approach**

The permeability near the wellbore is different from the permeability deeper in the formation. It is either reduced as affected by drilling activities or it is enhanced due to well stimulation. This reduced or enhanced permeability zone, termed as “skin” zone, causes an additional pressure change when compared to the pressure drop due to the original permeability of the formation. According to Hawkins (1956), the additional pressure change across this zone can be approximated by Darcy’s equation by introducing a skin factor term, defined as follows:

$$s = \left[ \frac{k}{k_{skin}} - 1 \right] \ln(r_e/r_w) \quad (26)$$

When the permeability around the wellbore is higher than the formation permeability, i.e., due to well stimulation,  $k_{skin} > k$ , the first term of eq (26) is negative. Since the  $\ln(r_e/r_w)$  term is always positive, in cases of stimulated wells the skin factor is always negative. In GEM, the skin factor is incorporated in the molar flow rate equation of a particular layer into the well. The extent of the effective radius ( $r_e$ ) for each well can be calculated using the following equation (Peaceman, 1983). For the case of the SF Model, a skin factor of -4 was used for all the wells in the modeling area.

$$r_e = 0.28 \frac{\sqrt{Dx^2K_y + Dy^2K_x}}{\sqrt{k_x + \sqrt{k_y}}} \quad (27)$$

Darcy’s equation is employed in order to simulate laminar flow of fluid through porous media. However, as it has been reported in literature, for hydraulically fractured wells, gas flow velocities near the wellbore and the pressure drop, are not proportionally increased. For this reason in order to account for both laminar and turbulent phenomena the following equation suggested by Forchheimer (1914) is used:

$$\frac{\Delta p}{\Delta L} = \frac{\mu v}{k} + \beta \rho v^2 \quad (28)$$

where  $\frac{\Delta p}{\Delta L}$  is the pressure gradient,  $\mu$  the viscosity,  $k$  the formation’s permeability,  $\rho$  the fluid’s density, and  $\beta$  the non-Darcy flow coefficient, a factor characteristic of the porous medium. The  $\beta$  factor is dependent on the gas saturation in the hydraulic fracture, the relative permeability of gas flow and the fracture porosity. Several authors have published different correlations of the  $\beta$  factor. In GEM, the following models can be applied in order to determine the  $\beta$  factor: The Geertsma, Frederick and Graves I or II or a general non-Darcy correlation model.

Another important aspect of accurately simulating a non-Darcy flow response in the hydraulic fractures is the use of a pseudo fracture. More specifically, in order to model an actual fracture width of 0.0058 meters, as in the case of the HF model, very high fracture permeability (i.e. 60,000md) is assigned to that narrow fracture. This is subsequently mapped to the modeled fracture width, i.e. 0.4m and converted to effective permeability by observing the equation  $k \times \text{width} = \text{constant}$ .

### **The Importance of Relative Permeability**

The relative permeability (RP) is defined as the ratio of the effective permeability (EP) to a given fluid at a definite saturation to the permeability at 100% saturation ( $k$ ). Since  $k$  is a constant for a given porous material, the RP varies with the fluid saturation in the same fashion as does the EP. The RP to a fluid will vary from a value of zero at some low saturation of that fluid to a value of 1.0 at 100% saturation of that fluid. In this case study, only two phase flow in the cleats needs to be considered: flow of water and flow of gas ( $\text{CH}_4$ ). In the current case study, the initial water saturation in the cleats is assumed high and numerically is assigned between 0.9 and 1.0. The RP curves are then optimized to work with the permeability of the strata to yield the appropriate water and gas rates. Figure 23 presents a typical example of the RP curves for two of the wells in the modelled area. In addition, Figure 24 compares the RP curves used in the SF and HF approaches.

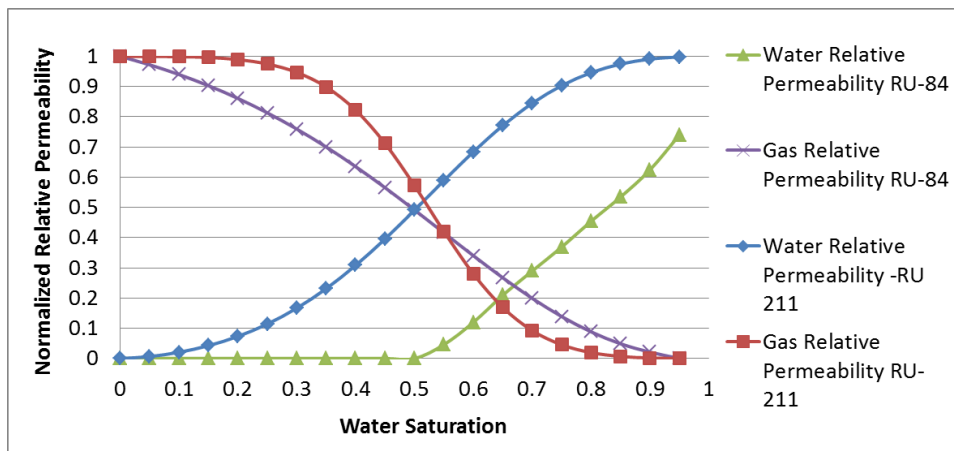


**Figure 23 - Typical Relative Permeability Curves for Two Wells**

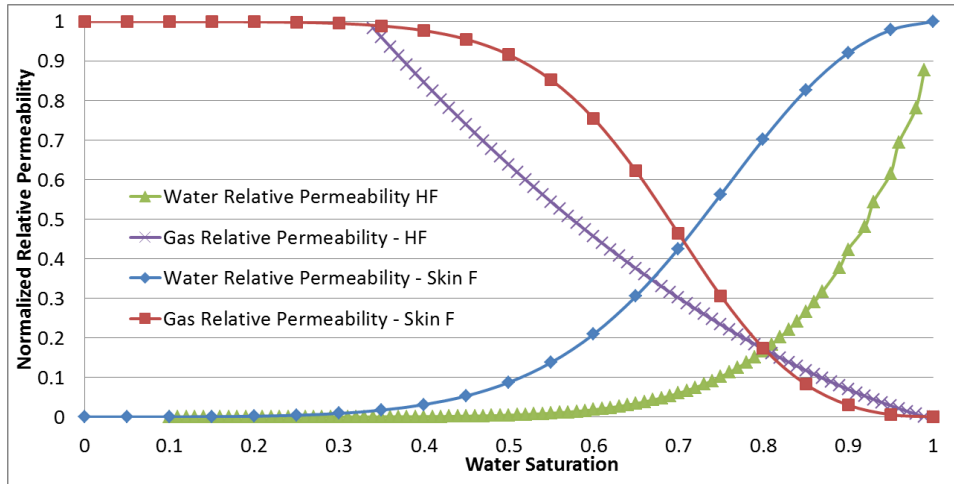


**Figure 24 - Relative Permeability Curves for the HF and SF Models**

**History Match**

A dual porosity, single permeability model was setup, since coal matrix permeability is considered extremely low. The 24 coal seams encountered at the test site were grouped in four flat zones set at the average elevation of each group (Vasilikou et al., 2013). The generated grid encompasses all production wells allowing for a distance of 150-200 m between each well and the grid boundary. The grid size was set to 25mx25m, with the grid extending to 84 blocks in the I (x) direction and 56 blocks in the J (y) direction.

The orientation of the hydraulic fractures was critical in determining grid generation. As the GEM model can only allow for hydraulic fractures along either the I (x) or J (y) direction, and hydraulic fractures were developed along the maximum horizontal stress in the area, the grid was rotated by 35 degrees clockwise to orient the maximum horizontal stress in the I direction (Vasilikou et al., 2013). In addition, it was assumed that the permeability in the I direction is equal to the butt cleat permeability and that the permeability in the J direction is equal to the face cleat permeability. Furthermore, the modeled group of eight wells was considered independent of other wells surrounding this grid. The resulting grid for all layers including the eight wells is shown in 3D view in Figure 25. The face cleat permeability distribution for all layers varies between 8 and 12 md variation. Similar results are obtained for the SF and HF models, where the face cleat permeability values are in the same range as before, but different since these reservoir models exhibit different flow characteristics.

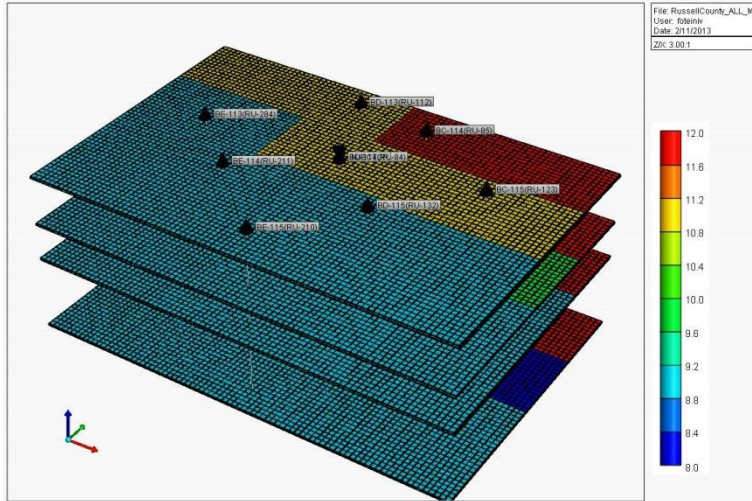


**Figure 25 - Face Cleat Permeability Variation for the Base Model**

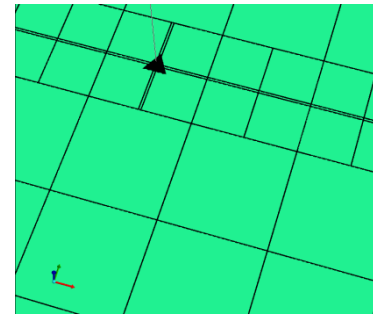


**Figure 26 - Typical HF Discretization for All Wells**

Figure 26 presents a detail of the model at the central production / injection well where the hydraulic fracture is shown as an area with finer grid discretization. The effective permeability for that area is in the order of 57,000 mD. It should be noted that these are optimum permeability values as determined by optimization of the reservoir properties. The RP curves varied per well for the base model, while they were kept constant for the SF and HF models since the later allow for higher permeability values in the near well bore areas. Adsorption isotherms for CO<sub>2</sub> and CH<sub>4</sub> were developed by a commercial laboratory, Pine Crest Technology, on three coal seams that are representative of coals developed for CBM in the South Oakwood CBM field.

In all above runs, the primary operating constraint was to meet the gas rate, while the secondary operating constraint was that the bottom hole pressure should not fall below a minimum value of 200 kPa. The objective function for the optimization was to minimize the error for the cumulative water that is recorded per well. It should be noted that the water output logged contains water introduced into the well and the formation during the hydraulic fracturing procedure.

## Results and Discussion

Figure 27 compares the cumulative water produced at well BC-115 (RU-123) over a six year period. The dots represent the measured values, while the dashed lines represent the calculated values by the three models discussed previously. In this case all models over-predict the water

produced. Although only one such diagram is presented in this paper, such charts can be composed for all wells. For other wells, the calculated cumulative water does not follow the same pattern and some models under predict while others over predict the measured values. It should be emphasized, that a complex problem like water and gas production from multiple wells may have more than one solution depending on the parameters selected. In fact, the solution space can be considered practically infinite. In addition, the HF model requires more computer resources to complete than the other models, while it is also the most sensitive of the three when input parameters vary. In all cases the models matched the historic data for the gas rate very well.

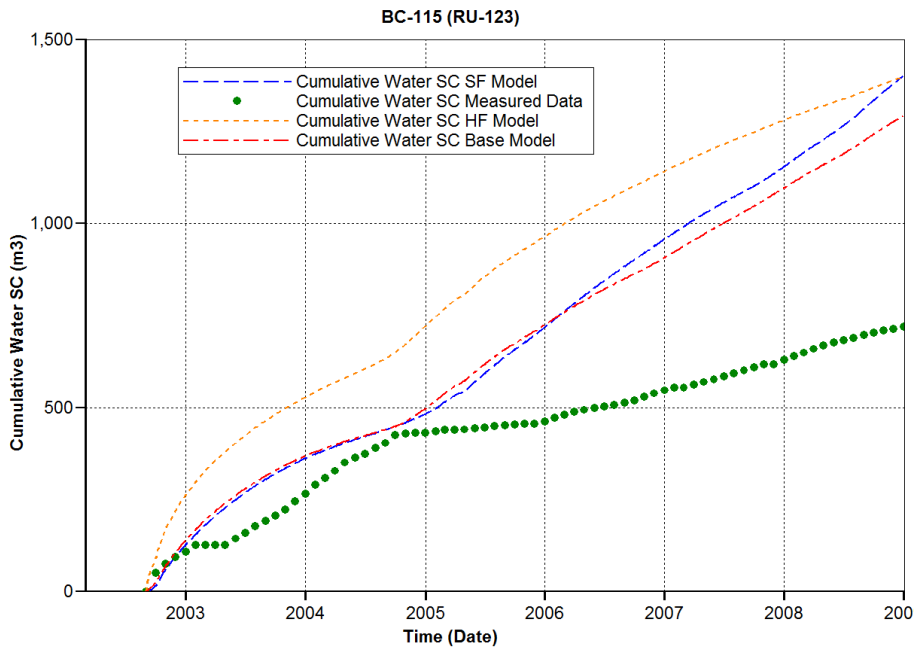


**Figure 27 - Cumulative Water Production vs. Measured Data for Well BC-115 (RU-123) for All Models**

Following the production simulation, and the respective history match, CO<sub>2</sub> was injected into well BD 114 (RU 84) for a period of about one month. The actual injection data were available on a daily basis, while the production data were available on a monthly basis. Figure 28 presents the injected gas rate (surface conditions, m<sup>3</sup>/day) and the injected cumulative gas (surface conditions, m<sup>3</sup>) for the injection period. Following injection, the injector well was shut in for a few months.

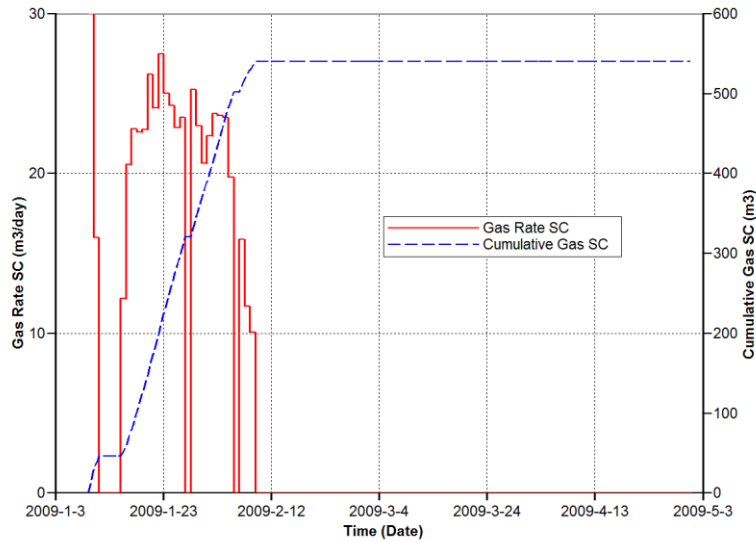


**Figure 28 - Gas Rate and Cumulative Gas during CO<sub>2</sub> Injection into Well BD 114 (RU 84)**

Figure 29 shows the spatial distribution of the CO<sub>2</sub> plume around the injector well immediately after injection has been completed for the HF model. As expected, the plume travels along the high EP zones on either side of the well. In addition the CO<sub>2</sub> plume decreases in magnitude as depth increases. Results indicate that the topmost injection zone received more CO<sub>2</sub> than the injection zone at the bottom. In addition, the simulated CO<sub>2</sub> plume reaches the location of monitoring well M1 which was drilled in the path of the hydraulic fractures (see Figure 22 B). The SF and base models show a uniformly distributed CO<sub>2</sub> around the well bore.

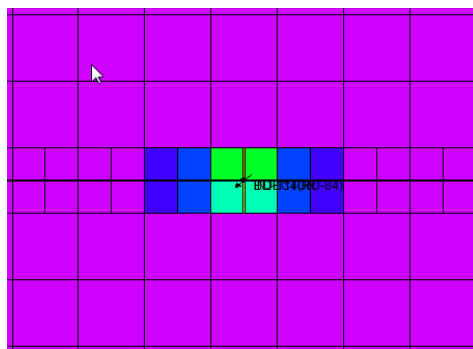


**Figure 29 - CO<sub>2</sub> Plume around Injection Well Immediately After Injection Has Been Completed In the HF Model**

## **Conclusions**

Due to the complexity, non-linearity and parameter variability of CBM reservoir modeling multiple solutions may be obtained that satisfy input parameters, boundary conditions, solution constraints and the objective function. A successful model should predict future production after being calibrated using historic data. In this work, two advanced CBM production models (the Skin Factor model and the Hydraulic Fracture model) were developed by incorporating the effects of permeability changes due to hydraulic fracturing. The models are compared to each other and also compared to a base model that does not incorporate any effective permeability changes due to fracturing.

The advantage of the SF model is that it can run in much less time than the HF model. The skin factor approach however induces a symmetric effective permeability change around each well since the skin factor is not directional. This is also evident in the plume representations for the SF models. In contrast the HF models correctly account for preferential effective permeability changes around the fractured area, but take a lot more computer resources to complete. Although all models converge and meet the specified gas rate and cumulative gas production values, none of the models provides a unique match to water production data for all wells.

These preliminary results verify that the injection process characterized by sorption and the process of flowback followed by CH<sub>4</sub> and/or CO<sub>2</sub> desorption is mainly driven by the effective permeability of the formation around each well. The skin factor approach may be applicable for large scale simulations where well interference is not an issue, while the hydraulic fracture simulation should be used when more accuracy in the formation and migration of injected and/or produced gases is needed.

## **Acknowledgments**

Financial assistance for this work was provided by the U.S. Department of Energy through the National Energy Technology Laboratory's Program under Contract No. DE-FC26-04NT42590 and DE-FE0006827.

## References

- GEM (Version 2011.12) [Computer software]. Calgary, Canada: Computer Modelling Group Ltd (CMG).
- Conrad, J.M., Miller, M.J., Phillips, J. & Ripepi, N. (2006). Characterization of Central Appalachian Basin CBM development: Potential for carbon sequestration and enhanced CBM recovery, 2006 International Coalbed Methane Symposium, Preprint 0625, Tuscaloosa, AL.
- Conrad, J.M., Miller, M.J. & Ripepi N. (2007). Potential for carbon sequestration in the Central Appalachian Basin. Air and Waste Management Association Conference, 2007, Paper # 187.
- Forchheimer, P. (1914). *Hydraulik*, Teubner, Leipzig and Berlin, 116-118.
- Hawkins, M. (1956). A note on the skin effect. *Trans. AIME*, 207, 356-357.
- Holman, T. (1996). Analysis and optimization of coalbed methane gas well, production (master's thesis). Retrieved from Virginia Polytechnic Institute and State University, Blacksburg, VA.
- Karmis, M., Ripepi, N., Miskovic, I., Conrad, J.M., Miller, M.J., & Shea, C. (2008). CO<sub>2</sub> Sequestration in unminable coal seams: Characterization, modeling, assessment and testing of sinks in Central Appalachia. Twenty-Fifth Annual International Pittsburgh Coal Conference, Pittsburgh, PA, USA, 2008. CD-ROM of Proceedings, Paper # 29-3.
- Peaceman, D.W., (1983). Interpretation of well-block pressures in numerical reservoir simulation with non-square grid blocks and anisotropic permeability. *Society of Petroleum Engineers Journal*, 23, 531-543.
- Ripepi, N., Karmis, M., Miskovic, I., Shea C., & Conrad, J.M. (2009). Results from the Central Appalachian Basin field verification test in coal seams. 26th Annual International Pittsburgh Coal Conference, Pittsburgh, PA, USA, 2009. CD-ROM of Proceedings, Paper # 33-4.
- Shi, J.Q. & Durucan, S. (2005). CO<sub>2</sub> Storage in deep unminable coal seams. *Oil & Gas Science and Technology, IFP*, 60(3), 547-558.
- United States Department of Energy (2013). Coalbed methane proved reserves and production, Energy Information Administration, accessed February 14: Retrieved from U.S. Energy Information Administration website:  
[http://www.eia.gov/dnav/ng/NG\\_ENR\\_COALBED\\_DCU\\_NUS\\_A.htm](http://www.eia.gov/dnav/ng/NG_ENR_COALBED_DCU_NUS_A.htm)

Vasilikou, F. Keles, C., Agioutantis, Z., Ripepi N. and Karmis, M. (2013). Experiences in reservoir model calibration for coalbed methane production in deep coal seams in Russell County, Virginia, Proceedings, Symposium on Environmental Considerations in Energy Production, April 14-18, 2013, Charleston, West Virginia (in press).

Virginia Center for Coal and Energy Research (VCCER) (2011). Final technical report: Characterization and Field Validation of the Carbon Sequestration Potential of Coal Seams in the Central Appalachian Basin, 2011: Blacksburg, VA.

Virginia Department of Mines, Minerals and Energy (VaDMME) (2002). CBM-PGP-BD114 Completion Report, Form DGO-GO-15, 105 p.

Virginia Department of Mines, Minerals and Energy (VaDMME) (2013), accessed February 2013: Retrieved from Virginia Department of Mines, Minerals and Energy website: <http://www.dmme.virginia.gov/DGO/Production/2010-County.pdf>

**RESERVOIR SIMULATIONS FOR COAL BED METHANE (CH<sub>4</sub>)  
PRODUCTION AND CARBON DIOXIDE (CO<sub>2</sub>) INJECTION IN DEEP  
COAL SEAMS IN BUCHANAN COUNTY, VIRGINIA<sup>4</sup>**

*Foteini Vasilikou, Virginia Center for Coal and Energy Research, Virginia Tech,  
Blacksburg, VA*

*Zach Agioutantis, Department of Mineral Resources Engineering,  
Technical University of Crete*

*Nino Ripepi, Virginia Center for Coal and Energy Research, Virginia Tech,  
Blacksburg, VA*

*Michael Karmis, Virginia Center for Coal and Energy Research, Virginia Tech,  
Blacksburg, VA*

***Reservoir Model Calibration for Coal Bed Methane Production from Deep Coal  
Seams in Buchanan County, Virginia***

**Abstract**

The potential of commercial deployment of CO<sub>2</sub> sequestration in unmineable coal seams, as a measure to mitigate the greenhouse gas effect, is being tested through a series of small- to medium-scale injection projects in the Appalachian Basin. Indispensable tools for these projects are reservoir simulations in which the involved processes, both prior to and post injection field tests are modeled to enhance understanding and to be used as a decision tool. Due to the large number of modeling input parameters and the high uncertainty in their values determination, for development of representative models initial model sensitivity analysis of the key input parameters is required. In this paper, preliminary single-well reservoir parametric simulations are conducted to identify how the variation of selected reservoir parameters and properties affect model results. More specifically, this sensitivity analysis focused on three areas: a) the effect of

---

<sup>4</sup> This paper is intended for publication.

Foteini Vasilikou collected the data, researched, and wrote this manuscript with technical input from Zach Agioutantis, Nino Ripepi and Michael Karmis.

selected initial conditions (pressure gradient, adsorption isotherm, and porosity), b) the influence of the production mechanism (permeability, relative permeability, and compressibility), and c) the contribution of the well characteristics (hydraulically stimulated well, skin factor). This modeling work forms the base for calibration of reservoir models for simulating CO<sub>2</sub> injection and subsequent prediction of post-injection behavior for an upcoming injection test in Buchanan County, VA.

## **Introduction**

The Coal Seam Group, led by researchers at the Virginia Center for Coal and Energy Research (VCCER), part of the Southeast Regional Carbon Sequestration Partnership (SECARB), completed a small-scale validation field test in Russell County, Virginia, during 2009, where 1,000 tons of CO<sub>2</sub> were injected into one vertical coalbed methane well over a period of one month (Ripepi et al., 2009). Prior to conducting the injection test, preliminary reservoir simulation models were developed to predict the extent of the CO<sub>2</sub> plumes and estimate injection pressures (VCCER, 2011). After the injection test was completed the original reservoir models were updated to account for post injection data and were refined based on the knowledge gained (Vasilikou et al., 2013).

In 2014, the VCCER will be performing a larger scale validation test in Buchanan County, Virginia, approximately seven miles to the north west of the Russell County site. Twenty thousand (20,000) tons of CO<sub>2</sub> will be injected into three vertical coalbed methane wells over a period of one year. The enhanced understanding of the production and injection mechanisms into stacked geologic systems gained from the small injection test in Russell County, along with updated reservoir software capabilities, will be used to develop improved simulation predictions for the CO<sub>2</sub> injection test in Buchanan County.

## **Geology**

CNX Gas Corporation, a subsidiary of CONSOL Energy Inc., has donated three vertical coalbed methane production (CBM) wells in Buchanan County, Virginia within the Central Appalachian Basin region. These three production wells will be shut in and converted into injection wells a month prior to the field injection test start date. As recorded by the State of Virginia the candidate injection wells, BU 1923, BU 3337, BU 1998 or alternatively as

referenced by their company name, DD7, DD7A, DD8, are at an elevation of 2286.6 feet, 1932.2 feet, and 1876.2 feet, respectively (DMME, 2011).

The Central Appalachian Basin is a northeast-to-southwest trending basin encompassing approximately 10,000 square miles in southwestern Virginia, southern West Virginia and eastern Kentucky (Conrad et al., 2006). Production of CBM began in 1988 with the development of the Nora Field in Dickenson County, Virginia, followed by CONSOL Energy developing the Oakwood Field in Buchanan County, Virginia. The coals in the region near the injection site include those of the Pocahontas Formation and Lee Formation, which directly overlie the late Mississippian Bluestone Formation. Coal seams of the Pocahontas and Lee Formation are medium to low-volatile bituminous, high rank and high gas content coals that include the Pocahontas No. 1 through Pocahontas No. 11 seams (Pocahontas Formation and the Greasy Creek, Middle and Lower Seaboard and Upper Horsepen coals) (Vasilikou et al, 2013).

Cardno MM&A, a research partner on this project, created a database for the coal seams in the study area by integrating data from donated sources with geophysical well log data from the Virginia Division of Gas and Oil and the West Virginia Geological and Economic Survey (VCCER, 2014). This database was used to create elevation structure maps and net thickness isopachs for both the Lee and Pocahontas Formation coals in southwestern Virginia and southern West Virginia, encompassing the Central Appalachian Basin. This assessment accounts for the coal seams that were stimulated for coalbed methane development.

Natural occurring fracture networks in coalbeds and the face and butt cleat planes were measured at two coal seam outcrop locations near the site and they corresponded to within 7 degrees of the published face and butt cleat directions of N18W and N167E respectively, for the deep mined Pocahontas No. 3 coal seam in Buchanan County (McCulloch, 1974).

The primary confining units in the study area include multiple layers of low permeability shale and siltstone beds. Permeability for the shale and siltstone units is expected to range from 0.001 to 0.1 mD, with low porosity (Grimm, 2010). The Lee and Pocahontas Formation sandstones are known to have low permeability and porosity values, and do not produce natural gas in this area (VCCER, 2011). Based on well log interpretations, the sandstone units are expected to have porosity values that range from 1.0 to 3.0 percent and permeability values ranging from 0.1 to 1.0 mD. All lithologies will encounter some natural fractures; however, these fractures are likely to be cemented with quartz and calcite and are not expected to provide

permeability pathways based on core analysis, well logging and field testing (Karmis et al., 2008).

## **Well Stimulation**

All wells within the study area have been perforated and hydraulically fractured using a nitrogen foam hydraulic fracturing treatment. The wells selected for injection, DD7 (BU 1923), DD7A (BU 3337), DD8 (BU 1998) were stimulated in November 2000, March 2007 and May 2001, respectively. DD7 was completed in four zones ranging in depth over 1216-1385 feet, 1531-1570 feet, 1674-1866 feet and 1997-2133 feet. DD7A was stimulated in three stages at 856-975.5 feet, 1203-1420 feet and 1599-1803.5 feet. DD8 was completed in three zones ranging in depth over 871-1205 feet, 1311-1677.5 feet and 1710.5-1802 feet (DMME, 2011).

In each well, the main hydraulic fractures at each perforation are oriented at approximately N57E (VCCER, 2011). Although in some cases fracturing may extend up to 700-800 feet away from the borehole, in this analysis a more conservative approach was used where the fracture half-length is assumed to be 350 feet. In addition, after personal communication with the operator of the wells, it was suggested that only 40 percent of the coal seams per stage were successfully completed (CNX, 2013).

## **Production History**

The three injectors, DD7, DD7A, and DD8, were brought on-line as coalbed methane production wells in 2000, 2007 and 2001, respectively. To date, DD7, DD7A, and DD8 have averaged a production of 82.52 Mcf, 41.25 Mcf and 47.88 Mcf of natural gas per day and 1.42 barrels, 1.11 barrels and 1.74 barrels of water per day (DMME, 2013). The cumulative gas production of these three wells to date is estimated to account for 58 percent, 56 percent and 33 percent, respectively, of their expected ultimate gas recovery (VCCER, 2014).

The gas production data are measured at each well, whereas the water production data are estimated by dividing the total production of a group of wells by the total time the water pump on each well was operating. For this reason, there is a higher degree of confidence in the accuracy of the gas production data versus the reported water production of the wells.

Figure 30 shows historic gas production rates for the three selected injection wells, DD7, DD7A and DD8. Daily water production for the three injectors is shown in Figure 31.

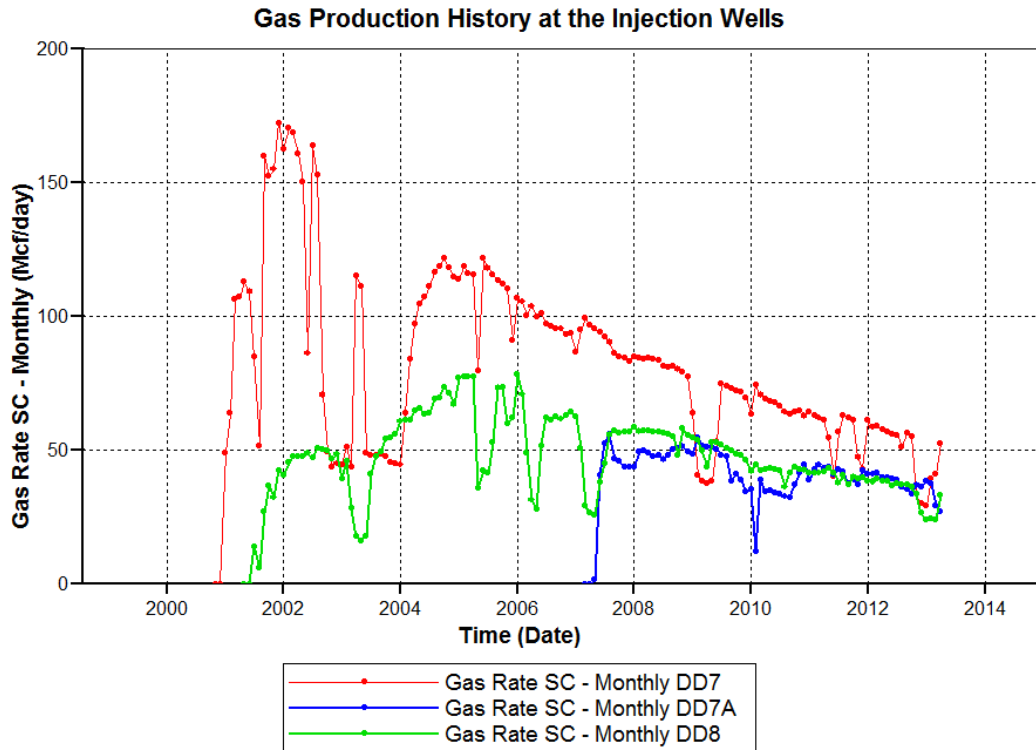


**Figure 30 - Daily Gas Production Rate of the Injection Wells**

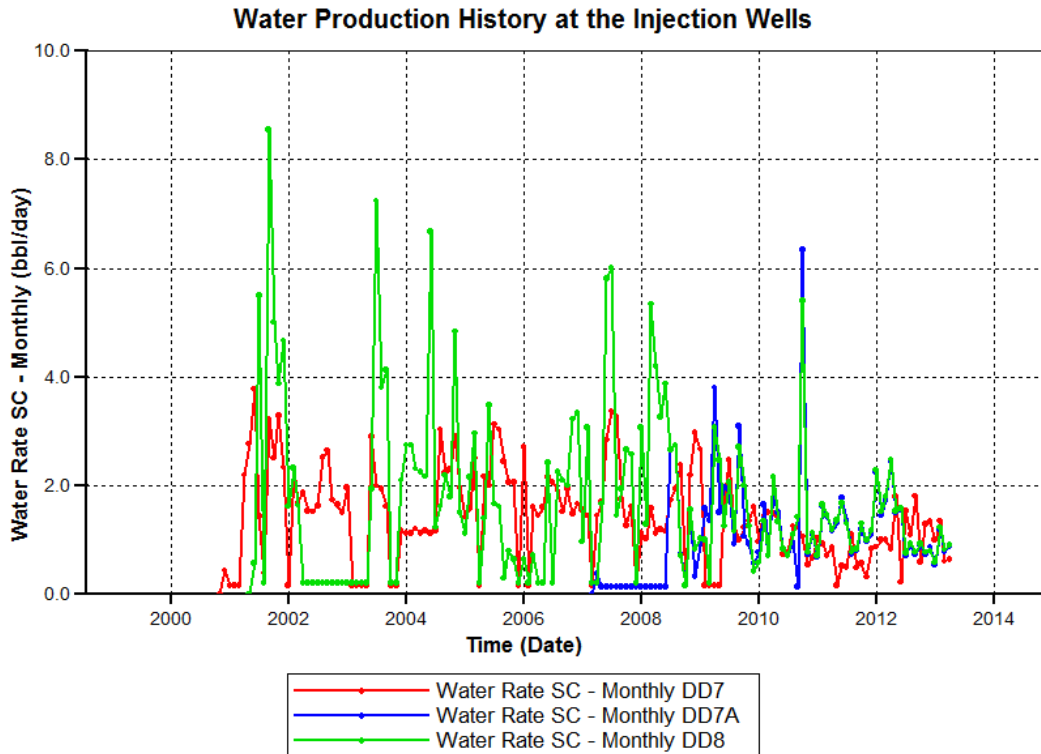


**Figure 31 - Daily Water Production Rate of the Injection Wells**

## Description of Reservoir Model

Reservoir simulations prior to commencing with the CO<sub>2</sub> injection field test were performed to estimate the extent of the CO<sub>2</sub> plumes, the storage capacity of unmineable coal seams and the potential of enhanced gas recovery of the field. The reservoir simulator employed in this study is the compositional and unconventional simulator GEM by the Computer Modeling Group Ltd.

This paper focuses on studying the interaction of key properties which affect the initial gas and water volumetrics in coalbeds and the production mechanism from multiple thin coal seams. In addition, well characteristics relevant to how the well was drilled and perforated, such as the frequency of hydraulic fractures, the fracture lengths and widths, are examined with respect to ultimate well productivity. Due to the nature of the multi-seam configuration of the study area and the degree of interference between input parameters, this paper focuses on part of the study area that includes a single well, DD7, in order to investigate commingled primary production for different scenarios. Simulation results of the whole study area with CO<sub>2</sub> injection in three of the wells are detailed below.

The geologic structure employed for the single well simulations in this study is an 18-layer model (Figure 32A) proposed by Cardno MM&A (2013), a project subcontractor. Table 6 shows the top elevations and thicknesses for each simulated coal seam. Numbering of the layers starts with the shallowest seams and increases towards the deepest seams. The drainage area for the single well simulations is approximately 42 acres.

In addition, based on a slightly different interpretation of the aforementioned geologic structure proposed by Cardno MM&A, a second structure where 5 zones of coal seams are assumed is also investigated in order to examine sensitivity of model response to variation of number of layers in the model (Figure 32B).

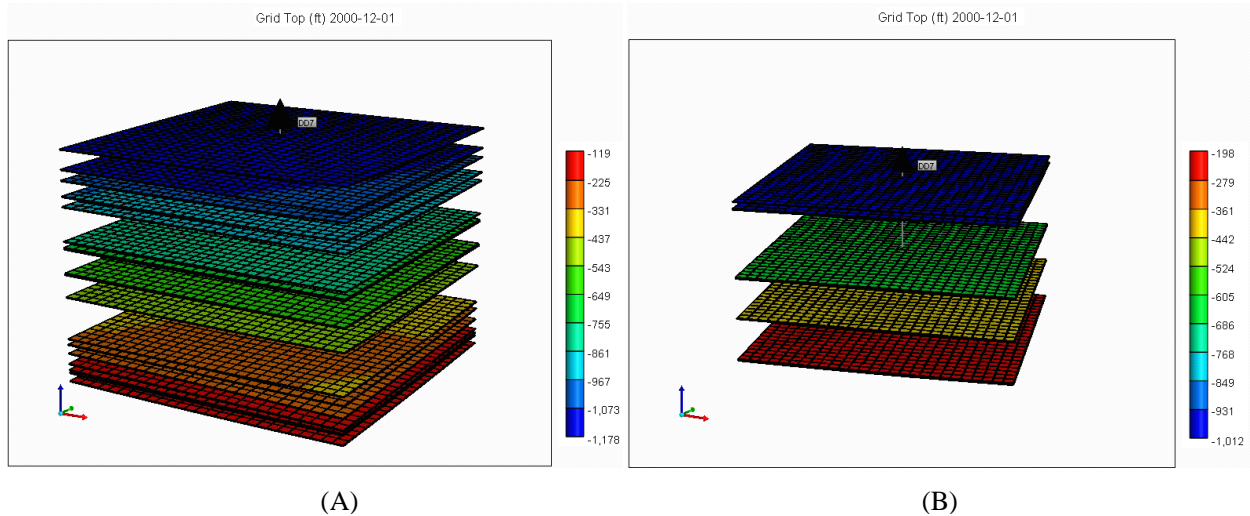


**Figure 32 - (A) 18-Layer Model, (B) 5-Zone Model**

### **18- Layer Models**

The key parameters investigated in this analysis are: (i) pore pressure gradient, (ii) coal and cleat porosity, (iii) Langmuir constants, (iv) water saturation in cleats, (v) cleat permeability, (vi) relative permeability curves to water and gas, (vii) methane desorption time from the coal matrix, (viii) skin factor and (ix) hydraulic fractures for well stimulation. The primary objective in each model was to match the historic gas and water production up to year 2013 for the selected well (Figure 33).

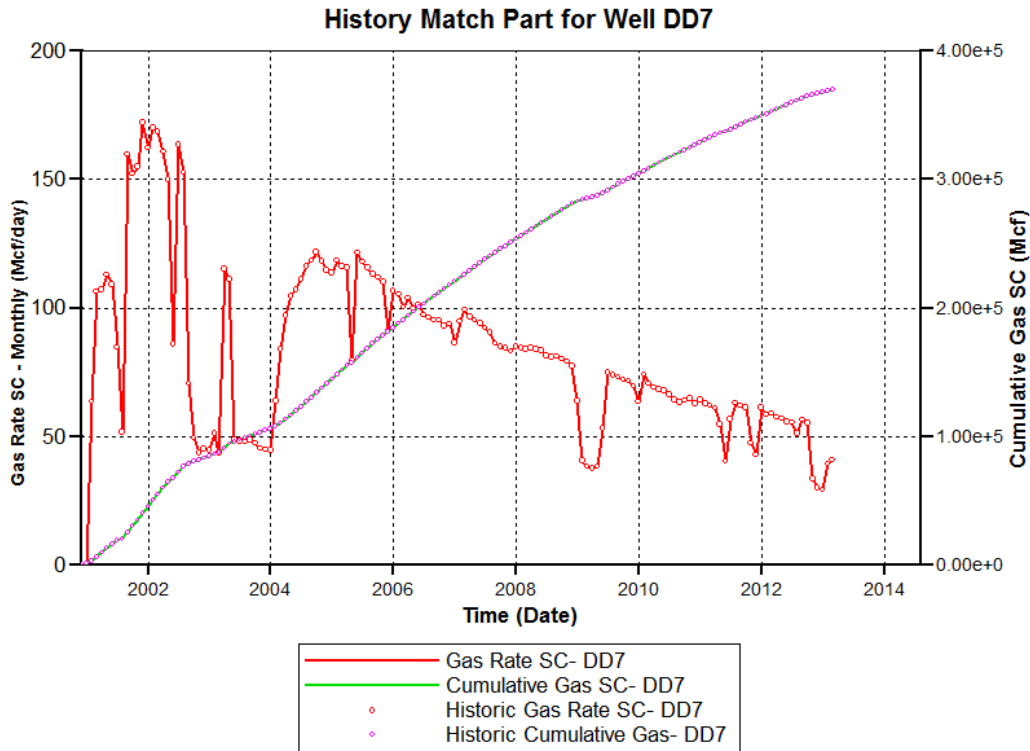


**Figure 33 - History Matching of Monthly Gas Rate and Cumulative Gas for Well DD7 Up to Year 2013**

The first set of input parameters that were varied in the simulations is as follows: pore pressure gradient, coal and cleat porosity, Langmuir volume and Langmuir pressure constants, and the initial water saturation in the cleats, shown in Table 7. The remaining parameters used in the first set of models (C) are kept constant as shown in Table 6. Cases C1 through C11 investigate the effect of the aforementioned parameters on the initial gas and water in place of the models. In cases C1, C2 and C3 the variation of the original gas and water in place is examined in relationship to the variation of the Langmuir volume constant,  $V_L$ ; in case C4, the water saturation in the cleats is reduced from 100 to 90 percent and all the other parameters are the same as in case C1; in case C5 the Langmuir pressure constant,  $P_L$ , is reduced from 0.01 to 0.003 and the rest of the assigned properties are the same as in case C3; in cases C6, C7, C8 all the parameters are kept the same as in cases C1, C2, C3 respectively, but the pore pressure gradient assigned in the fractures is increased from 0.315 psi/ft to 0.36 psi/ft; in cases C9, C10, C11 the coal and cleat porosity are reduced compared to the respective values in cases C1, C2, C3 from 1 percent (Pashin, 2014) to 0.15 percent (Liu et al., 2012) and from 0.1 to 0.015 percent. Figure 34 shows the effect of the variation of the Langmuir constants to the amount of adsorbed

gas per coal mass constrained by the minimum and maximum pore pressures at the shallower and deeper seam, respectively, depending on the pore pressure gradient employed.

**Table 6 - Parameters and Material Properties Used in the 18-Layer Reservoir Model**

Number of Grid Blocks per Direction	I=27,J=27, K=18 Layers
Grid Block Sizes per Direction, ft	DI=50, DJ=50, DK= Variable
Coal Layers and Thicknesses, ft	(L1) 0.02-1.38, (L2) 0.71-1.49, (L3) 0.52-1.10, (L4) 1.31-1.69, (L5) 1.31-1.69, (L6) 0.28-0.79, (L7) 0.53-0.80, (L8) 0.66-1, (L9) 1.93-2.49, (L10) 0.01-0.46, (L11) 0.61-1.25, (L12) 0.01-0.87, (L13) 0.71-1.40, (L14) 0.61-1.19, (L15) 1.61-2.19, (L16) 0.61-1, (L17) 0.02-1.07, (L18) 0.303-0.526
Coal Layer Elevations-Grid Tops, ft	(L1) 1,163-1,178, (L2) 1,067-1,086, (L3) 1,026-1,041, (L4) 955-972, (L5) 909-934, (L6) 759-776, (L7) 730-750, (L8) 724-743, (L9) 615-633, (L10) 612-624, (L11) 512-526, (L12) 327-343, (L13) 295-318, (L14) 243-267, (L15) 193-219, (L16) 176-195, (L17) 169-182, (L18) 119-144
Pore Pressure Gradient, psi/ft	0.315
Coal (Matrix) Porosity, %	1
Cleat (Fracture) Porosity, %	0.1
Coal (Matrix) Permeability, mD	Not in use, single permeability model (GEM, 2003)
Cleat (Fracture) Permeability, mD	I: 30, J: 30, K: 3
Relative Permeability Curves Gas-Water	Relative water permeability 1 and relative gas permeability 1 ( Figure 35)
Langmuir Adsorption Constants	Langmuir Volume Constant, $V_L= 800$ scf/ton Langmuir Pressure Constant, $P_L= 333$ psi
Fracture Spacing per Direction, ft	I: 0.01667, J: 0.01667, K: 0.01667
Well Radius, ft	0.13124
Formation Compressibility (Matrix & Fracture), 1/psi	2E-08 (at reference pressure 416.15 psi) (Harpalani, 2012)
Reservoir Temperature, °F	69.8
Water Density, lb/ft <sup>3</sup>	62.4779 (at reference pressure 416.15 psi)
Coal Density, lb/ft <sup>3</sup>	82.65(VCCER, 2011)
Desorption Time, days	20
Cleat (Fracture) Water Saturation	1
Well Stimulation	Not in use, zero skin factor, no hydraulic fractures

**Table 7 - Set of Parameters Varied in Simulations for Cases C1 to C11**

Parameters	C1	C2	C3	C4	C5	C6	C7	C8	C9	C10	C11
Pressure Gradient, psi/ft	0.315	0.315	0.315	0.315	0.315	0.36	0.36	0.36	0.315	0.315	0.315
Coal (Matrix) Porosity, %	1	1	1	1	1	1	1	1	0.15	0.15	0.15
Cleat (Fracture) Porosity, %	0.1	0.1	0.1	0.1	0.1	0.1	0.1	0.1	0.015	0.015	0.015
Langmuir Constant, $V_L$ , scf/ton	500	650	800	500	800	500	650	800	500	650	800
Langmuir Constant, $P_L$ , 1/psi	0.01	0.01	0.01	0.01	0.003	0.01	0.01	0.01	0.01	0.01	0.01
Water Saturation in Cleats, %	100	100	100	90	100	100	100	100	100	100	100

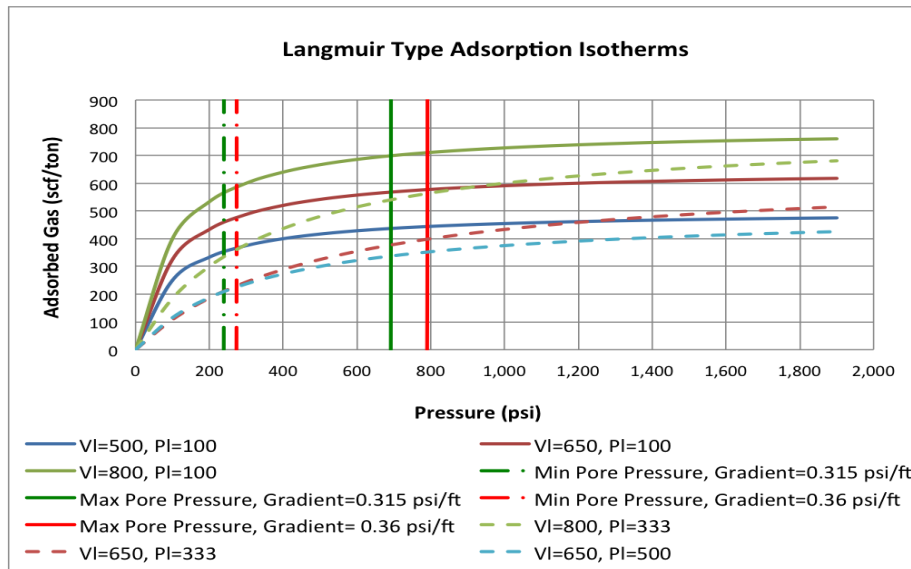


**Figure 34 - Langmuir Adsorption Isotherms for Langmuir Volume Constants 500, 650, 800 scf/ton and Langmuir Pressure Constants 100 and 333 psi; Maximum and Minimum Pore Pressures in the Reservoir for Pressure Gradients 0.315 and 0.36 psi/ft**

The second input parameter investigated was cleat permeability. The sensitivity of the 18-layer model to variation of cleat permeability was examined. Three models - P1, P2 and P3 - with an isotropic cleat permeability in space and in depth of 20 mD, 30 mD and 45 mD (same as in cases C1 through C11) were studied. The rest of the parameters were kept constant as shown in Table 6.

Two different relative permeability curves for water and two for gas were considered in this analysis as shown in Figure 35. All other input parameters for the models were as shown in Table 6.

Desorption time from the coal matrix to the cleat system was also varied. In the investigation of cases C1 to C11 desorption time was set to 20 days. Desorption times of 5 and 50 days was also examined. The rest of the parameters were kept constant as shown in Table 6.

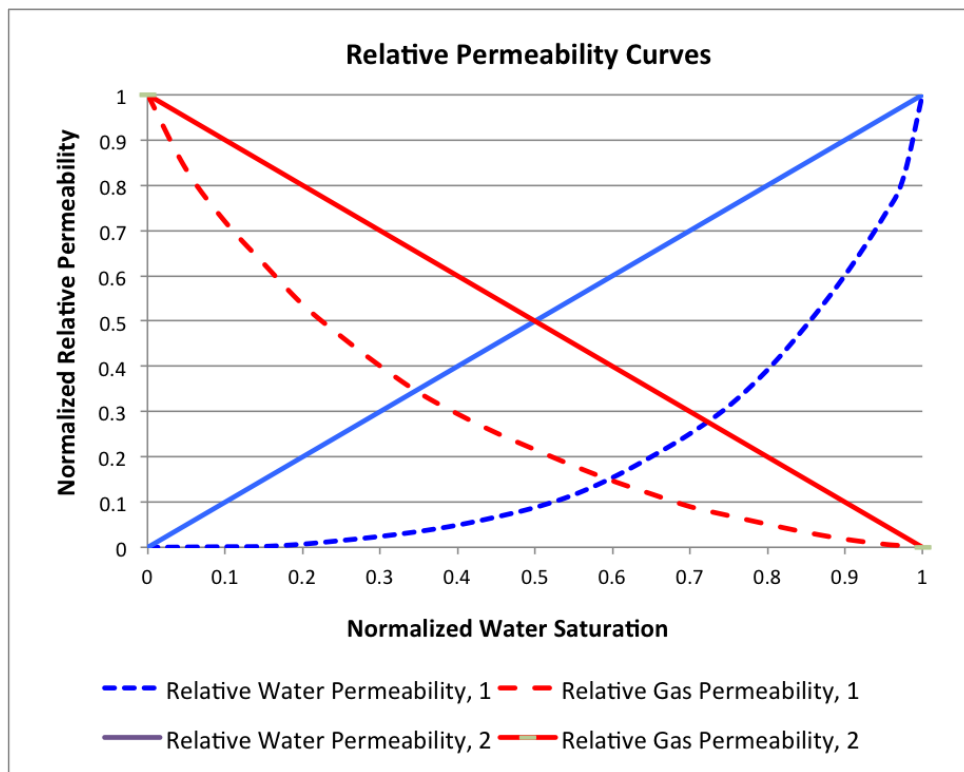


**Figure 35 - Different Scenarios for the Relative Permeability Curves to Water and Gas**

Because it was hydraulically stimulated, to account for enhanced flow properties around DD7 three scenarios were studied (S1, S2 and S3). In the first scenario (S1) a skin equal to zero was assigned; in the second (S2) a negative skin of -2 and in the third (S3) a negative skin of -4

was used. The minimum value of skin factor that could be assigned in order to maintain a positive production index for the well was -4.

Another way to account for hydraulically stimulated wells in reservoir simulations is to explicitly model hydraulic fractures. This approach is more computationally intensive compared to assigning a negative skin factor. For the purposes of this investigation four scenarios with hydraulic fractures were studied. In all four scenarios (H1, H2, H3, H4) only 40 percent of the seams per stage, as suggested by the operator of the wells, were assumed to be successfully fractured. For scenarios H1, H2 and H3 the thickest seams per stage were selected to be fractured (Pashin, 2014). In scenario H4 the seams per stage selected to be hydraulically fractured were the ones that initially had a higher amount of gas in place. The properties of the hydraulic fractures assumed in the modeling work and the layer numbers selected to be fractured per scenario are shown in Table 8.

**Table 8 - Input Parameters for Modeling Hydraulic Fractures in Scenarios H1, H2, H3, H4**

	H1	H2	H3	H4
Layer Number with HF	4, 6, 8, 12, 14, 16, 18	4, 6, 8, 12, 14, 16, 18	4, 6, 8, 12, 14, 16, 18	4, 5, 9, 13, 15, 16, 18
Primary Fracture Width (ft)	0.00833 (GEM, 2003)	0.01042 (EPA, 2004)	0.12500 (EPA, 2004)	0.00833 (GEM, 2003)
Primary Fracture Permeability (mD)	6,000 (GEM, 2003)	6,000 (GEM, 2003)	6,000 (GEM, 2003)	6,000 (GEM, 2003)
Fracture Half Length (ft)	300	300	300	300
Grid Refinement	I: 9, J: 9, K: 1	I: 9, J: 9, K: 1	I: 9, J: 9, K: 1	I: 9, J: 9, K: 1
Effective Fracture Permeability (mD)	55	61	405	55

### **5-Zone Model**

Finally, due to restricted computational capabilities with respect to model size, it is common practice in reservoir modeling when simulating complex geologic structures to aggregate

geologic layers/units into zones in order to reduce the number of elements in the simulation. In this study a 5-zone geologic structure, as previously mentioned, for the investigated area (VCCER, 2013) was compared to the 18-layer model employed in the modeling work. Table 9 shows the input parameters for the 5-zone geologic structure.

**Table 9 - Parameters and Material Properties Used in the 5-Zone Reservoir Model**

Number of Grid Blocks per Direction	I=27, J=27, K=5 Layers
Grid Block Sizes per Direction, ft	DI=50, DJ=50, DK= Variable
Coal Layers and Thicknesses, ft	(L1) 0.01-2.38, (L2) 2.6-6.3, (L3) 3.9-6.7, (L4) 0.01-1.84, (L5) 5.3-8
Coal Layers Elevations-Grid Tops, ft	(L1) 992.8-1011.9, (L2) 960-979.1, (L3) 615.9-636.7 (L4) 406.4-429.3, (L5) 198.1-218.3
Pore Pressure Gradient, psi/ft	0.315
Coal (Matrix) Porosity, %	1
Cleat (Fracture) Porosity, %	0.1
Coal (Matrix) Permeability, mD	Not in use, single permeability model (GEM, 2003)
Cleat (Fracture) Permeability, mD	I: 30, J: 30, K: 3
Relative Permeability Curves Gas-Water	Relative water permeability 1 and relative gas permeability 1 ( Figure 35)
Langmuir Adsorption Constants	Langmuir Volume Constant, $V_L= 800$ scf/ton Langmuir Pressure Constant, $P_L= 333$ psi
Fracture Spacing per Direction, ft	I: 0.01667, J: 0.01667, K: 0.01667
Well Radius, ft	0.13124
Formation Compressibility (Matrix & Fracture), 1/psi	2E-08 (at reference pressure 416.15 psi) (Harpalani, 2012)
Reservoir Temperature, °F	69.8
Water Density, lb/ft <sup>3</sup>	62.4779 (at reference pressure 416.15 psi)
Coal Density, lb/ft <sup>3</sup>	82.65(VCCER, 2011)
Desorption Time, days	20
Cleat (Fracture) Water Saturation	1
Well Stimulation	Not in use, zero skin factor, no hydraulic fractures

## Results and Discussion

### Initial Volumetrics

The results of the parametric analysis for the (C) models are shown in Figure 36 and Figure 37. For cases C1, C2 and C3, where the Langmuir volume constant was varied as shown in Table 7, the original gas in place in case C1 increased by 29.92 and 42.87 percent compared to cases C2 and C3, respectively. The original water in the system, shown in Figure 37, for cases C1, C2

and C3 was not affected by the variation of the Langmuir constant volume and it was the same for all cases.

In case C4 the initial water saturation in the cleat system was reduced from 100 to 90 percent. A negligible increase in the original gas in place was noted of approximately 0.42 percent in case C4 compared to case C1. The small increase was due to the increase of free gas in the cleat system. The original water in place was affected the most by the reduction in the initial water cleat saturation. In case C4 the original water in place reduced by 10 percent compared to case C1 (Figure 37).

In cases C5 and C3 all input parameters are the same with the exception of the Langmuir pressure constant, which in case C5 is reduced from 0.01 1/psi to 0.003 1/psi. The change in the Langmuir pressure constant had an effect on the curvature of the adsorption isotherm as shown in Figure 34 and, for the given pore pressure range in the reservoir, it resulted in a reduction of the original gas in place in the system of approximately 28.22 percent (Figure 36). As expected, the original water in place of the system was not affected by the reduction in the Langmuir pressure constant.

In cases C6, C7, C8 a higher pore pressure gradient of 0.36 psi/ft compared to 0.315 psi/ft of cases C1, C2, C3 is assigned in the models and all other input parameters are assumed to be the same. The increased pore pressure gradient used in cases C6, C7 and C8 resulted in an increase by 2.22 percent of the original gas in place compared to cases C1, C2 and C3. There was no change in the original water in place because of the increase in pore pressure.

In cases C9, C10 and C11, both the coal and cleat porosity of the models were reduced to 0.15 percent and to 0.015 percent respectively, compared to cases C1, C2, C3. Reduction of the coal porosity results in a negligible increase of the original gas in place (Figure 36). Reduction in the cleat porosity has a significant effect to the original water in place (Figure 37). It results in a decrease of 85 percent of the overall water in the system from cases C1, C2, and C3 to C9, C10 and C11.

In all cases aforementioned more than 99 percent of the original gas in place is stored in an adsorbed state on the coal matrix. Only in case C4, where an initial cleat water saturation less than 100 percent was assigned, there was more than 1 percent free gas in the cleat system. In the models it is assumed that no methane is dissolved in the water.

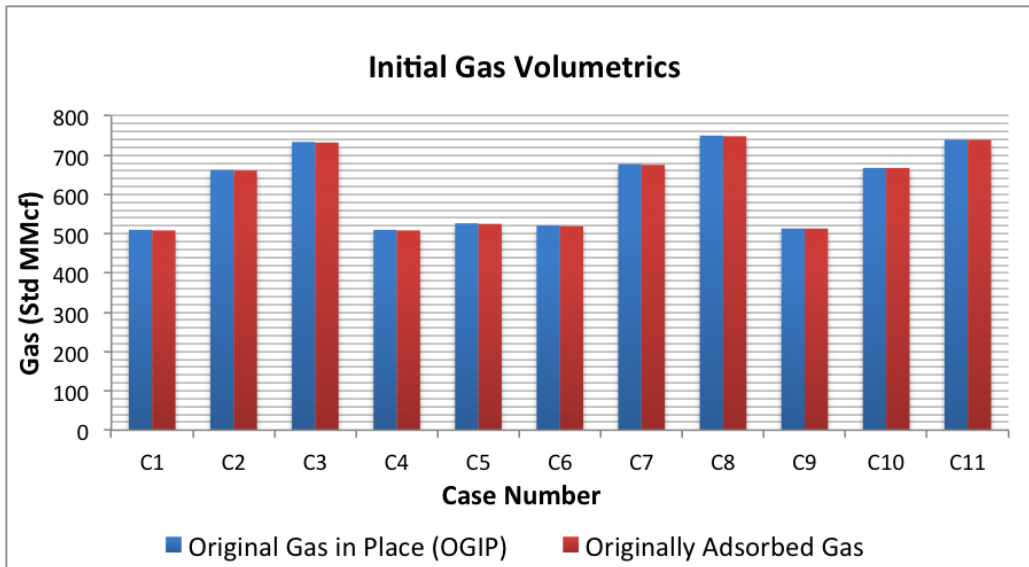


**Figure 36 - Original Gas in Place in the Model and Initially Adsorbed Gas on the Coal Matrix for All Cases (C)**

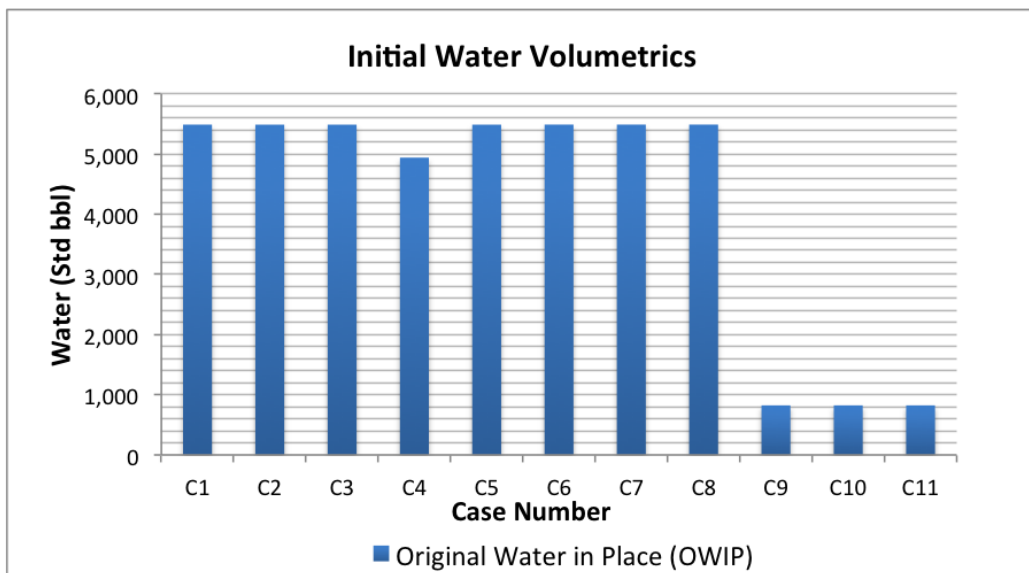


**Figure 37 - Original Water in Place for All Cases (C)**

Figure 38 presents the coal matrix volume profile development with depth at the different seams elevations for the 18- layer geologic structure for cases C3 and Case 11. Reduction in both the coal and cleat porosity in case C11 compared to case C3 results only in 0.08 percent increase of the coal (matrix) volume per seam in case C11 (Figure 38).

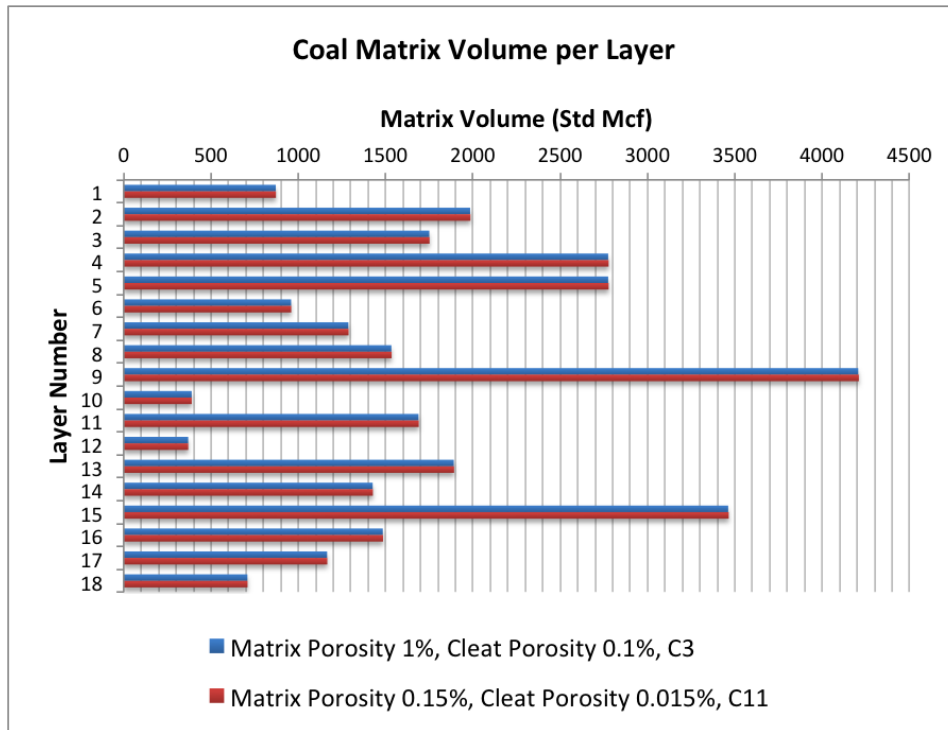


**Figure 38 - Coal Matrix Volume per Layer Starting from the Shallowest (Layer 1) to the Deepest (Layer 18) Seam for Cases C3 and C11**

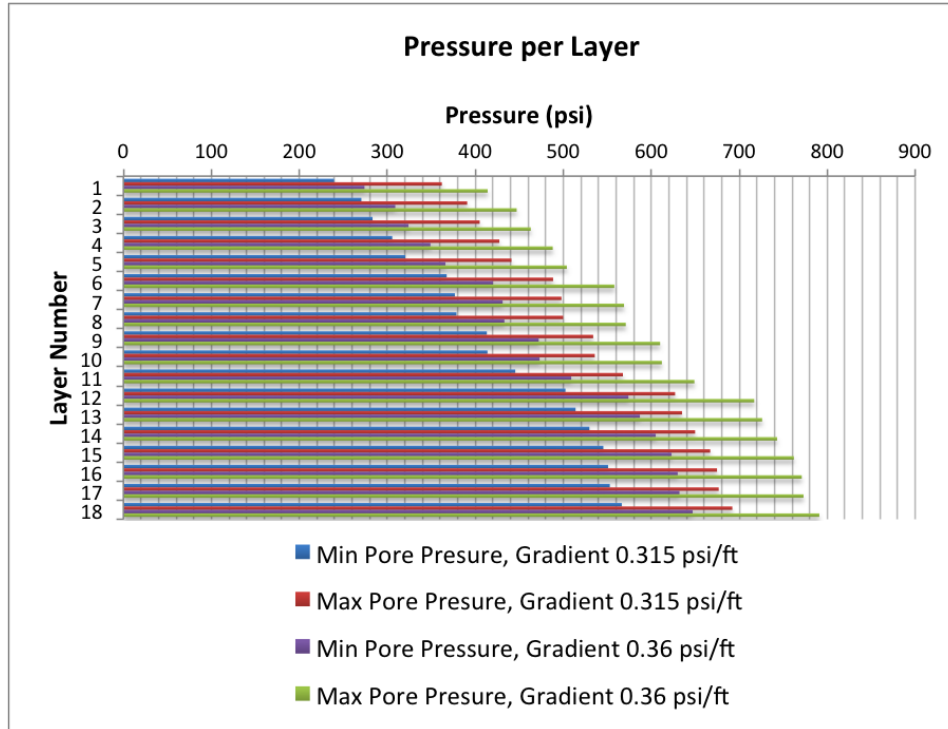


**Figure 39 - Minimum and Maximum Pore Pressures per Layer for Two Different Pressure Gradients Used In C Cases**

For the coal seams in the study area in Buchanan County, VA, the pore pressure gradient is assumed to range between 0.315 and 0.36 psi/ft (VCCER, 2013). By employing the 18-layer geologic structure proposed, the pressure profile per depth per coal seam for the two different pore pressure gradients of 0.315 psi/ft and 0.36 psi/ft is developed as shown in Figure 39. For the 0.315 psi/ft pressure gradient assumed, pore pressures in the model range between 239- 692 psi. For the 0.36 psi/ft gradient, pore pressures in the 18-layer model vary between 274-791 psi.

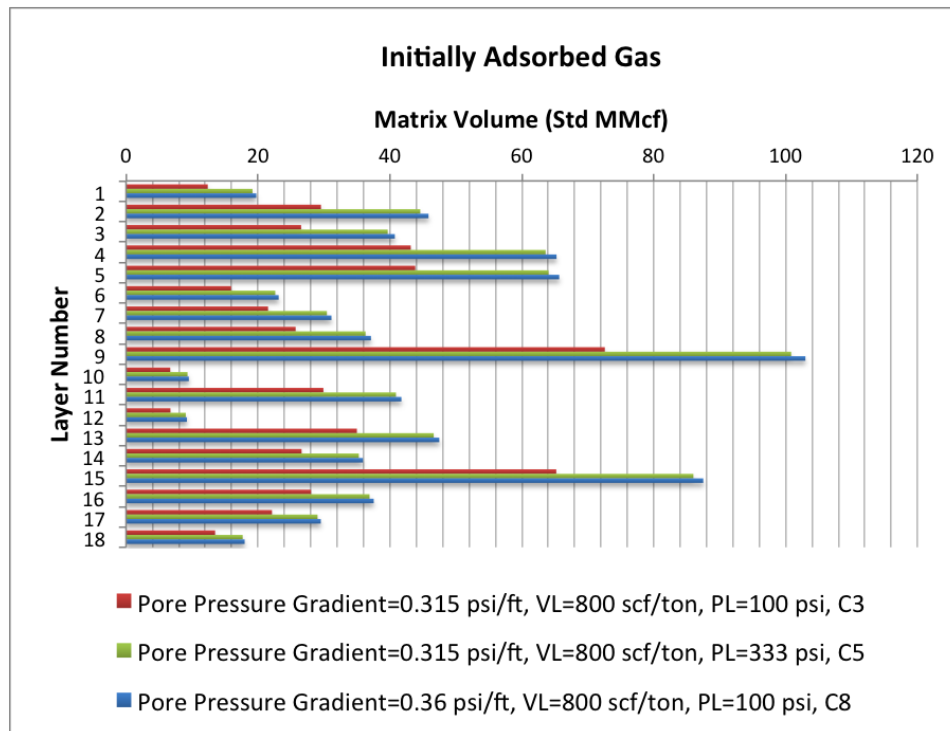


**Figure 40 - Initially Adsorbed Gas per Layer for Cases C3, C5 and C8**

The initial coal matrix volume per seam (Figure 38) with specific adsorption properties assigned and the initial pore pressures per layer (Figure 39) shape the initially adsorbed gas profile in depth for the 18-layer model. Figure 40 presents the initially adsorbed gas per coal seam for cases C3, C5 and C8. Initially adsorbed gas for case C8 is higher than in case C5 and significantly higher compared to case C3. In case C8, the lower Langmuir pressure constant used shifts the adsorption isotherm towards higher gas contents per coal mass and, with the pore pressures range shifted to the right as shown in Figure 34, overall higher originally adsorbed gas in the model compared to cases C5 and C3 (Figure 40) was expected. Layers 9 and 15 have the highest initially adsorbed gas for all cases. It must be noted that coal matrix volume is

significantly higher for layers 9 and 15 compared to the other layers. For layers 4 and 5, while coal matrix volumetrics for layer 4 is greater than layer 5, layer 5 is a deeper seam with a higher pore pressure and thus has a greater initial amount of adsorbed gas. This is also the case for layers 2 and 13 with similar coal matrix volumetrics, but due to the significant difference in pore pressures the deepest seam has higher initial adsorbed gas content.

### **Production Mechanism**

In the analysis of the (C) models, variation of the input parameters under consideration affected the initial volumetrics of the models. Parameters such as cleat permeability, relative permeability curves to water and gas, and desorption time have an effect on the production mechanism of coalbed wells.

Three different scenarios for cleat permeability were examined. In scenarios P1, P2 and P3, cleat permeability of 20, 30 and 45 mD was respectively assigned, with a primary operational constraint to meet the historic water rate and with a secondary constraint of minimum bottom hole pressure. The results showed that the percentage of gas produced over the initial gas in place for scenarios P1, P2 and P3 was 35.40, 35.40 and 39.84 percent, respectively. There is essentially no change in the recovery factor between scenarios P1 and P2, whereas an increase of 12.32 percent in gas production is noted for scenario P3. The layers in order of highest to lowest production were as follows: layer 9, 15, 5, 4, 13, 2, 11, 16, 3, 8, 17, 14, 7, 6, 18, 1, 12, and 10. As expected, the layers with the highest initial gas content are also the ones producing the most gas.

Two different curves for relative permeability to water and two curves for relative permeability to gas were studied (Figure 35). In coalbed reservoirs primary dewatering of the seams is important for gas production. Hence, the magnitude of the relative permeability to water for high water saturations is important for gas production. When water and gas start to co-exist in the cleats, the shape of the relative permeability curves has a significant effect on the production profile. In this analysis, when relative permeability to water 1 was changed to relative permeability to water 2 (Figure 35), more water was initially produced but gas production did not start until lower water saturations and ultimately gas deliverability of the system were reduced. When relative permeability curve to gas was changed from (1) to (2), as shown in Figure 35, initial water deliverability was unaffected and gas production increased.

Regarding variations in desorption time of 5, 20 and 50 days, the results show that the percentage of gas recovery over the initial gas in place are 39.94, 39.84 and 39.64 percent,

respectively. It was expected that the lower and hence faster desorption time used in the modeling work would yield higher gas production, but it is not significant.

From the investigation of the (S) models where a skin factor was used to account for enhanced flow around the well, it was shown that recovery factors of the original gas in place for scenarios S1 (zero skin), S2 (negative 2) and S3 (negative 4) were 38.82, 41.59 and 45.77, respectively. The recovery factors in the (S) models were higher compared to the ones of the (H) models where hydraulic fractures were explicitly simulated. For the H models, recovery factors for scenarios H1, H2, H3 and H4 were 38.00, 38.68, 40.50 and 38.38 percent, respectively. It must be noted that even scenario S1, where a zero skin factor is used, has a higher recovery factor than most of the H models. This is most likely due to the different flow properties assumed for the H models versus the S models. For the H models, it must be noted that increase in the primary fracture width (Table 8) yields an increased effective permeability and ultimately a higher recovery factor. Also, in scenario H4 where hydraulic fractures per stage were selected based on higher initial gas content, the recovery factor was slightly higher compared to the recovery of scenario H1 where stimulated seams were selected based on the thickest seams per stage criterion.

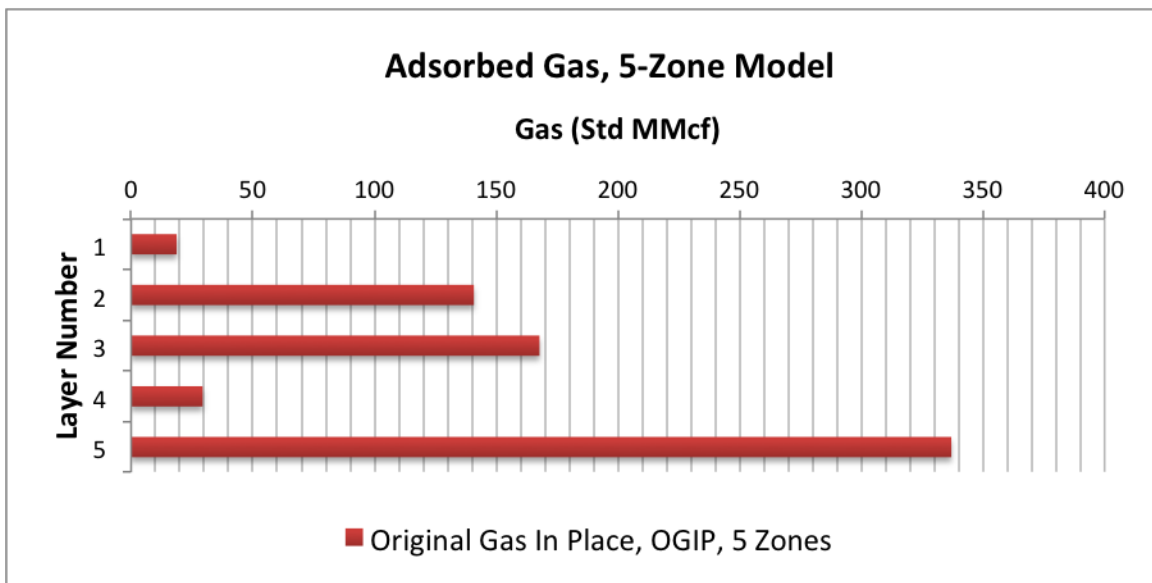
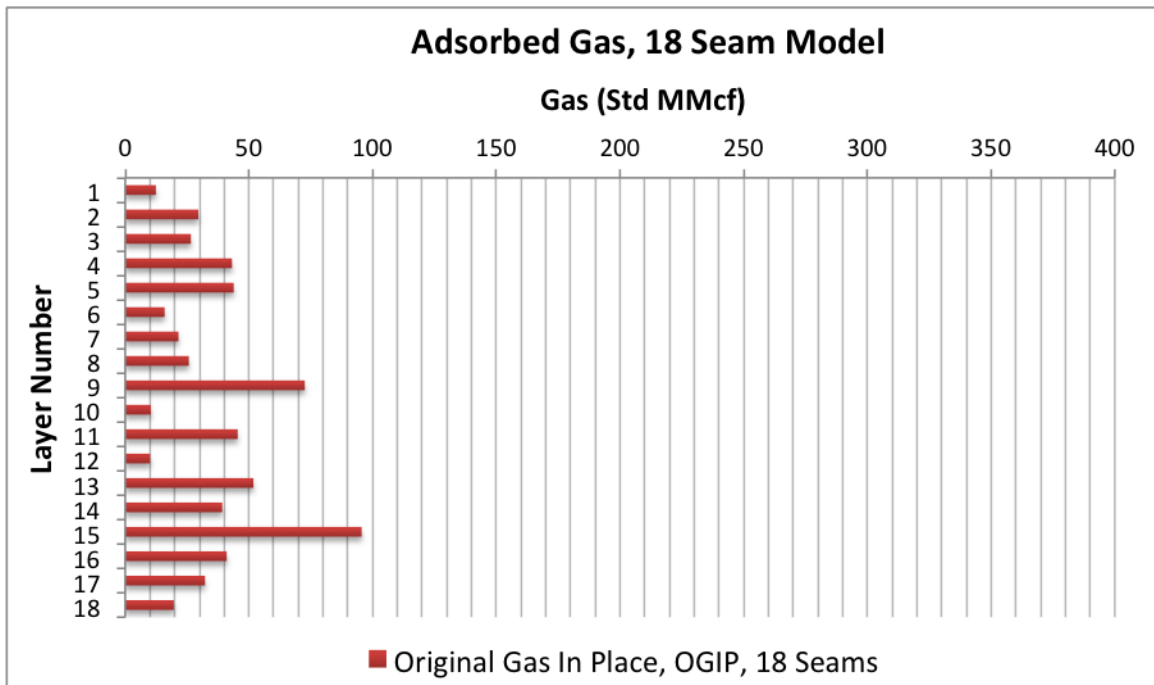


Figure 41 - Originally Adsorbed Gas per Layer for the 5-Zone Model



**Figure 42 - Originally Adsorbed Gas per Layer for the 18-Layer Model**

The results regarding the two different geologic structures considered, the 5-zone model and the 18-layer model, showed that the original gas in place was  $6.95 \times 10^5$  and  $6.38 \times 10^5$  Mcf, respectively. The gas recovery factor for the 5-zone model was higher compared to the 18-layer model, which was expected since the original gas in place was also higher.

## Conclusions

This paper discusses in detail a sensitivity analysis with respect to key input modeling parameters for the injection site in Buchanan County, VA. Through parametric analysis, the effect of several input parameters is determined. Identifying the contribution of each parameter is important in deciding the optimal modeling configuration and approach for the full field scale simulation of the CO<sub>2</sub> injection in unmineable coals seams for the Buchanan County site.

## ***CO<sub>2</sub> Injection Model for Enhanced Coalbed Methane Recovery in Deep Coal Seams in Buchanan County, VA***

### **Abstract**

This paper presents preliminary reservoir simulations which were conducted to predict the amount of carbon dioxide that can be stored in multiple thin coal seams following injection, the extent of CO<sub>2</sub> plumes by seam, the potential for CO<sub>2</sub> breakthrough at offset wells, and the amount of CO<sub>2</sub> stored if the injection wells are flowed back. Finally, the paper will present an assessment of the potential of enhanced gas recovery for all wells within the study area.

### **Development of Reservoir Models**

Reservoir simulations prior to the commence of the CO<sub>2</sub> injection field test were performed to estimate the extent of the CO<sub>2</sub> plumes and identify suitable locations for monitoring wells, the storage capacity of unmineable coal seams and the potential of enhanced gas recovery of the field. The simulation covers a drainage area of approximately 1552 acres and incorporates the three selected injection wells and seventeen offset CBM wells. Table 10 shows the designations of these 20 wells as well as the date that production started at each well. The date shows that the wells in the simulated area were brought on-line at different times within a time span of sixteen years; the first well started production in 1993 and the latest producer started in 2009.

**Table 10 - Reference Names and Production Start Dates for the Coalbed Methane Wells Included in the Simulations**

State Well Name	Company Well Name	Production Start Date
BU 1480	CC6	10/1/2000
BU 3850	CC6A	06/1/2008
BU 1875	CC7	11/1/2000
BU 3335	CC7A	05/1/2007
BU 0377	CC8	02/1/1993
BU 0378	CC9	02/1/1993
BU 3388	CC9B	09/1/2007
BU 1950	DD5	06/1/2001
BU 1743	DD6	12/1/2000
BU 3893	DD6A	08/1/2008
BU 1923	DD7	12/1/2000
BU 3337	DD7A	04/1/2007
BU 1998	DD8	06/1/2001
BU 3929	DD8A	03/1/2009
BU 2092	DD9	11/1/2001
BU 4269	DD9A	09/1/2009
BU 1924	EE6	01/1/2001
BU 1922	EE7	01/1/2001
BU 2072	EE8	09/1/2001
BU 3942	EE9A	03/1/2009

The reservoir simulator employed in this study is the compositional and unconventional simulator GEM by the Computer Modeling Group Ltd. A dual porosity, single permeability model is used for modeling the coalbed reservoir, since coals consist of micro and macro pores and have a negligible matrix permeability compared to their fracture permeability (CMG, 2003).

In the reservoir models, a geologic structure for the coal seams is assumed, based on integrated data for coalbeds within the study area (VCCER, 2013). Surface elevations in the study area range from 1685- 2364 feet. The models include 18 layers at elevations ranging from 29 feet to 1201 feet with varying thicknesses between 0.01 to 4.2 feet, as shown in Table 11. It must be noted that coal seam thicknesses below 0.5 feet are based on an estimation of where the coal seam will pinch out. Layers in Table 11 are listed from top elevation to bottom elevation.

**Table 11 - Layers Number, Coal Seam Names, Thicknesses and Top Elevations for the Geologic Structure Assumed for the Study Area**

Layers Number	Coal Seam	Coal Thicknesses (ft)	Coal Elevations (ft)
1	Greasy Creek	0.03-2.90	1087-1201
2	Seaboard (20)	0.01-1.80	982-1125
3	Lower Seaboard	0.02-1.98	944-1067
4	Upper Horsepen (10)	0.37-2.85	887-992
5	Upper Horsepen (20)	0.03-1.40	829-959
6	Pocahontas No. 11	0.10-1.79	694-816
7	Pocahontas No. 10 (10)	0.01-2.07	672-780
8	Pocahontas No. 10 (20)	0.18-1.54	665-774
9	Pocahontas No. 9 (10)	1.00-3.30	593-633
10	Pocahontas No. 9 (20)	0.10-1.30	591-624
11	Pocahontas No. 7 (10)	0.12-2.47	452-564
12	Pocahontas No. 5 (10)	0.06-3.10	270-372
13	Pocahontas No. 5 (20)	0.20-4.20	234-354
14	Pocahontas No. 4 (20)	0.20-3.70	199-309
15	Pocahontas No. 3 (10)	0.06-3.00	150-266
16	Pocahontas No. 3 (40)	0.10-1.40	140-196
17	Pocahontas No. 3 (50)	0.10-1.40	125-187
18	Pocahontas No. 2 (10)	0.03-1.49	29-184

Due to the large size of the full field scale models (element-wise) and the added complexity of the multiple seams structure, in order to reduce overall simulation time two different groups of models were set up for the purposes of this investigation. A larger model (L) that includes all 20 wells within the study area and assumes a 16-layer geologic structure where seams 9, 10 and

seams 16, 17 were aggregated into single zones; a smaller model (S) incorporates the three selected injectors and the offset well, DD8A, and assumes an 18-layer structure. The input parameters and material properties shown in Table 12 were assembled utilizing data from coal sample analysis, the literature and through personal communication with Pashin (2013).

**Table 12 - Input Parameters for the Combined and Four-Well Models**

Number of Grid Blocks per Direction (combined models, (L))	I= 98, J= 69, K=16
Number of Grid Blocks per Direction (four-well models, (S))	I= 75, J= 39, K=18
Grid Block Sizes per Direction (combined models, (L)), ft	DI= 100, DJ= 100
Grid Block Sizes per Direction (four-well models, (S)), ft	DI=50, DJ=50
Coal (Matrix) Porosity (combined models, (L)), %	Layers: 1 to 6, 2 Layers: 7 to 16, 1 Dual porosity model
Coal (Matrix) Porosity (four-well models, (S)), %	Layers: 1 to 6, 2 Layers: 7 to 18, 1 Dual porosity model
Cleat (Fracture) Porosity (combined models, (L)), %	Layers: 1 to 6, 0.2 Layers: 7 to 16, 0.1 Dual porosity model
Cleat (Fracture) Porosity (four-well models, (S)), %	Layers: 1 to 6, 0.2 Layers: 7 to 18, 0.1 Dual porosity model
Matrix Permeability, mD	Not in use, single permeability model
Cleat Permeability (combined models, (L)), mD	Layers: 1 to 10, 30, Layers: 11 to 16, 10,
Cleat Permeability (four-well models, (S)), mD	Layers: 1 to 10, 30, Layers: 11 to 18, 10,
Fracture Spacing per Direction, ft	I: 0.01667 J: 0.01667, K: 0.01667
Well Radius, ft	0.13124
Formation Compressibility (Matrix & Fracture), 1/psi	2E-08 (at reference pressure 416.15 psi) (Harpalani, 2012)
Reservoir Temperature, °F	69.8
Water Density, lb/ft <sup>3</sup>	62.4779 (at reference pressure 416.15 psi)
Relative Permeability Curves Gas-Water	Figure 43
Adsorption Isotherms according to Langmuir. Langmuir Constants V <sub>L</sub> , scf/ton; P <sub>L</sub> , psi	Methane: All Layers V <sub>L</sub> = 720.003, P <sub>L</sub> = 250 Carbon Dioxide: All Layers V <sub>L</sub> = 830, P <sub>L</sub> = 300 (VCCER, 2011)
Coal Density, lb/ft <sup>3</sup>	82.65 (VCCER, 2011)
Methane Desorption Time, days	20
Pore Pressure Gradient, psi/ft	0.315
Matrix Pressure, psi	Variable, 173-717

Coal (matrix) porosity and cleat (fracture) porosity are key input parameters determining the initial volumetrics of the models and consequently affecting the ultimate methane recovery of the field. High values of matrix porosity allow for less coal volume for gas adsorption on the coal surface and thus translate to lower values of initial gas in place. High fracture porosity values suggest higher initial water in the system and higher pressure. Due to a lack of specific information on reservoirs conditions regarding both the matrix and the fracture porosity, porosity values were selected for the reservoir models in order to match the volume of the historic gas production of the field to date and to be in accordance with the estimated ultimate recovery predicted through decline curve analysis (VCCER, 2013). Cleat (fracture) porosity was assumed to be 10 percent of the coal (matrix) porosity. After personal communication with Pashin (2013), it was suggested that there is a linear decrease of matrix and fracture porosity values with depth. For this reason a coal matrix porosity of 2 percent was assumed for the first 6 shallower seams in both the combined and four wells models and 1 percent for the deeper seams.

Langmuir type isotherms were employed in the models to represent methane and carbon dioxide adsorption isotherms for coalbeds. For the specific injection site in Buchanan County, there are currently no data available on the adsorptive properties of coals. For the Russell County injection site, which is seven miles to the south-east of the current site, coal samples were sent to Pine Crest Technologies and the methane and carbon dioxide adsorption isotherms for three coal seams, Pocahontas No.3, Pocahontas No.7 and Pocahontas No.11, were determined (VCCER, 2011). Due to the close proximity of the two sites, an assumption was made that the coals would have similar properties, and by taking into account that the coals in Buchanan County have slightly higher gas contents, uniform per layer adsorption isotherms for methane and carbon dioxide were assigned to the models.

Pore pressure is a critical parameter in modeling CBM production because it essentially drives production. An initial pore pressure gradient of 0.315 psi/ft was used based on historical field data (VCCER, 2013) to reflect under-saturated conditions in the study area. The corresponding pressure values vary between 173-717 psi, depending on the depth of the coal seam in the reservoir.

As already noted, a single cleat permeability model is employed during the simulation of coalbed reservoirs (CMG, 2003). The stress field in the study area suggests similar fracture permeability values along the face and butt cleats (Pashin, 2013), and therefore isotropic cleat

permeability was assumed in the models. Cleat permeability values were determined through history matching the gas production of the field since no other laboratory or field data for the Buchanan injection site were available. It is believed that cleat permeability declines exponentially with depth; as the depths in the study area vary between approximately 1000 and 2000 feet it is assumed that cleat permeability varies between 70 mD and 10 mD (McKee et al., 1988). In the models, cleat permeability towards the lower end of the suggested range for moderate analysis was selected; 30 mD was assigned to the first 10 seams and it was reduced to 10 mD for the 8 deepest seams.

Gas and water relative permeability curves were unavailable. Relative permeability was assumed to be similar to that used by Mavor and Robinson (1993) when evaluating pressure transient data for the San Juan coals based on initially developed gas and water relative permeability curves by Gash for Fruitland coals (Gash et al., 1993). The relative permeability curves were adjusted for the specific study area through history matching gas and water well data (Figure 43).

Operational constraints are also an important modeling parameter. Initially the models were set to primarily match the historic gas rate up to year 2013, while having a secondary constraint of a minimum bottom-hole pressure of 28 psi. Even though dewatering of the coal seams is the driving force for primary methane production from coalbed wells, as previously mentioned the quality of the reported water data per well is unknown and, therefore, water production was taken into account as a secondary check point for the history matching exercise. It should be also noted that historical production data for gas and water were aggregated on a monthly basis.

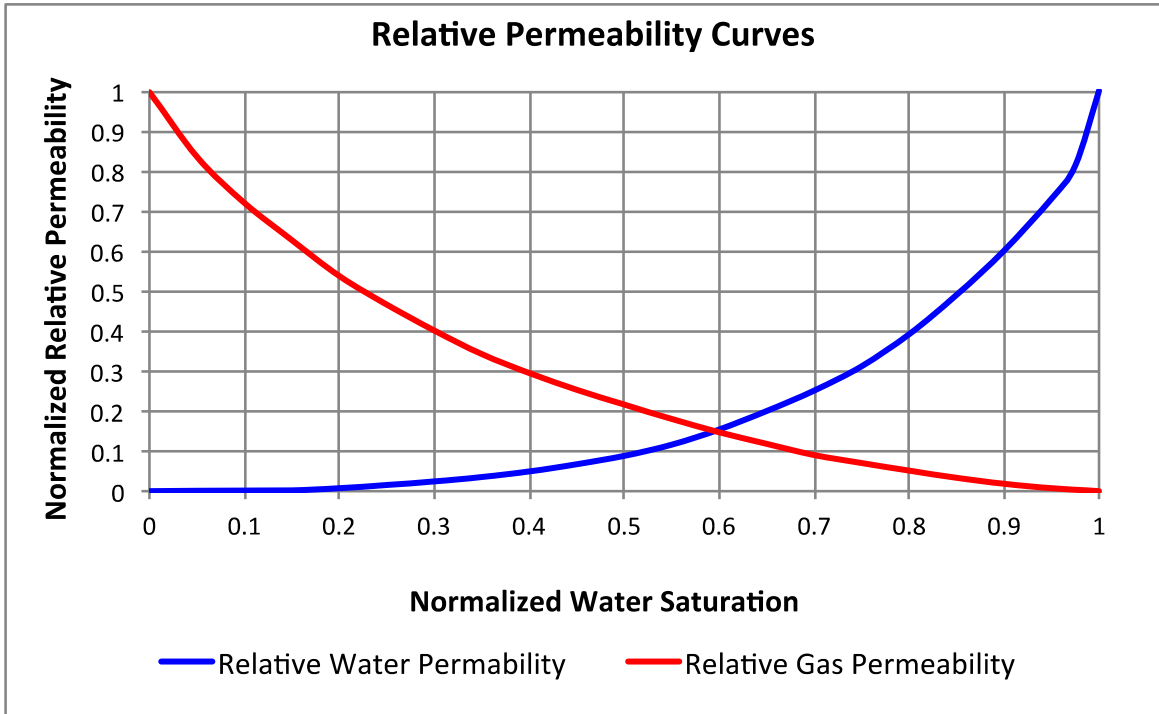


**Figure 43 - Relative Permeability Curves to Water and Gas as Determined Through History Matching Gas Production for All the Wells in the Study Area**

## Results and Discussion

Two different types of models are investigated in this paper. A larger model (L) representing the whole study area incorporating 20 wells and a smaller four-well model (S) focusing on the area around the three selected injection wells and the closest offset well, DD8A.

The main objective of the reservoir simulation efforts is to model all phases throughout the estimated life of the wells within the study area and assess the storage capacity of coalbeds and the extent of CO<sub>2</sub> plumes. More specifically, the first step is to model the initial period up to year 2013, utilizing available historical gas and water production data for all wells in order to calibrate the models. The next step is to model the one-year injection period during which it is planned to inject 20,000 tons of carbon dioxide into the three selected wells. Finally, the model will be used to forecast the behavior of all wells in the study area post injection until the end of their estimated life, year 2052.

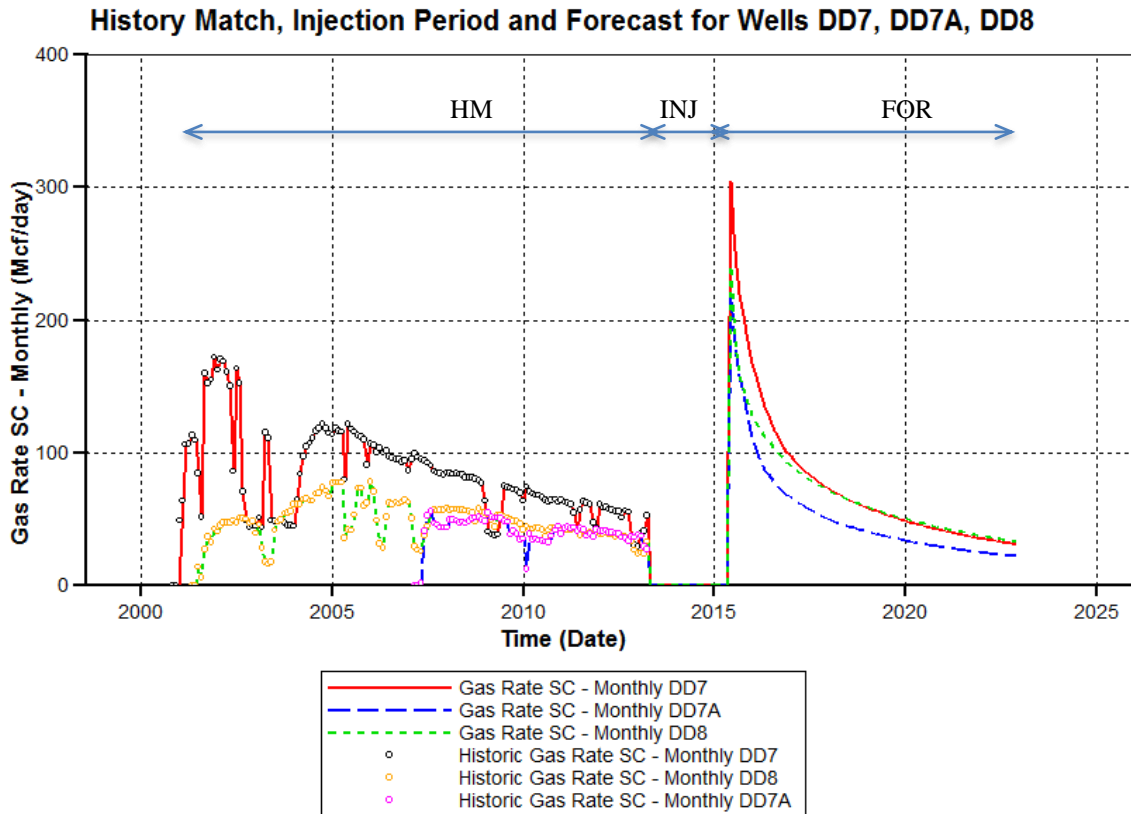


**Figure 44 - Gas Rate at Surface Conditions for the Three Injectors, DD7, DD7A, and DD8 throughout History Matching, Injection and Forecasting to Year 2023**

**S Models**

The small models (S) incorporated the three selected injectors: DD7, DD7A and DD8 and the offset well DD8A. The drainage area of the 18-seam geologic structure for the (S) models was 167.9 acres and, based on the input parameters, the original gas in place (OGIP) was estimated to be 1.84e6 standard Mcf and the original water in place 2.64e4 standard bbl.

Three different scenarios with regard to well characteristics were examined (S1, S2, S3). In scenario S1, all 18 coal seams were perforated but not hydraulically stimulated; in scenario S2 a negative skin was assigned to all four-wells to account for enhanced flow around the wellbore; and in scenario S3, the hydraulic fractures were explicitly modeled.

It is common practice in reservoir modeling to assign a negative skin factor to a well in order to account for its hydraulic fracture stimulation and, at the same time, avoid explicit modeling of the fractures, which is very computationally intensive. Therefore, to calculate the skin factor in this modeling work, equation (29) was initially used (Karacan, 2013).

$$s = -\ln\left(\frac{\alpha x_f}{r_w}\right) \quad (29)$$

where

$\alpha$ : Function of dimensionless fracture conductivity (FCD)

$x_f$ : Fracture half-length (ft)

$r_w$ : Well radius (ft)

“ $\alpha$ ” in the equation is a function of dimensionless fracture conductivity (FCD). NSI Technologies (2001) and Cunningham et al. (2003) reported that optimum well productivity occurs when FCD is around 2, and is calculated by using the expression below:

$$F_{CD} = \ln\left(\frac{k_f w_f}{k x_f}\right) \quad (30)$$

where

$k_f$ : Fracture permeability (mD)

$w_f$ : Fracture width (m)

$k$ : Permeability (mD)

$x_f$ : Fracture half-length (m)

“ $\alpha$ ” was determined as 0.3 from the dimensionless fracture conductivity versus alpha plot (Meyer, 2012) by assuming FCD as 2. Skin factor was calculated as -6.68 by assuming a 350 feet half-fracture length. However, when a skin factor of -6.68 is used in the GEM/CMG simulator, a negative well productivity index is calculated. The well productivity index for a phase should be positive and it is a function of fracture permeability, well drainage effective radius, well radius and skin factor (GEM, 2013). For the specific reservoir properties assumed in the modeling, the maximum skin factor that can be assigned to sustain a positive productivity index is -4.

Regarding hydraulic fractures, it was suggested by the operator of the wells that only 40 percent of the coal seams per completion stage have been successfully hydraulically fractured (CNX, 2013) and that the thickest seams are expected to have received most of the fractures (Pashin, 2013). For this reason, model S3, where hydraulic fractures are explicitly simulated, only includes layers 4, 6, 8, 12, 14, 16 and 18, which represent the thickest seams and account for 38 percent of the stimulated seams. A primary fracture width of 0.01042 feet (EPA, 2004) with a primary fracture permeability of 10,000 mD and 350 feet of half-length is assigned in the models. These input parameters for the hydraulic fractures translate into pseudo-fractures with

proper grid refinement that account for non-Darcy flow with an effective permeability of 82.1 mD. Hydraulic fractures were developed along the maximum horizontal stress direction in the area and thus the modeling grid was rotated to orient the maximum horizontal stress in the I direction. In addition, it was assumed that the permeability in the I direction is equal to butt cleat permeability and that in the J direction equal to face cleat permeability (Vasilikou et al., 2013).

Initially, for all three investigated scenarios S1, S2, S3 (base, skin, hydraulic fractures), history matching of the gas rate was achieved up to year 2013. Cumulative gas production of the field was similar for all scenarios at approximately 719.65 standard MMcf, accounting for almost 40 percent primary recovery of the original gas in place. The main coal seams contributing to gas commingle production in all three scenarios are listed below in order (from the largest contribution to the least): seams number 9, 15, 4, 16, 13, 8, 11, 7, and 14.

The second phase of the modeling was the injection period. The injection start date was set for the 1st of May 2013 with injection on-going until the 1st of May 2014. Wells DD7, DD7A and DD8 were shut in for one-month prior to commence of the injection and then turned into injectors. The same amount of carbon dioxide was injected into DD7, DD7A and DD8, approximately 6,667 tons per well, at a constant daily rate of 18.26 tons/day over a 1-year period. After injection of 20,000 tons of CO<sub>2</sub> was completed the three injectors remained shut in for one year until the 1st of May of 2015. Gas production for all four wells in the study area was projected to year 2023.

From the simulation results it is shown that for the three different scenarios where CO<sub>2</sub> is primarily injected into the coal seams there is a higher differential between the injection pressure at the wellhead and the flowing pressure yielded at the end of the history matching period at the specific coal seam depth. As shown in Figure 45 for scenario S3, more CO<sub>2</sub> is injected in coal layer 9 and that was also the seam most depleted during the history matching exercise. The second most depleted seam during history matching was layer 15. However, during injection layer 4, which is at a shallower depth and thus has a lower pore pressure, the seam takes up more of the injected CO<sub>2</sub> (Figure 45).

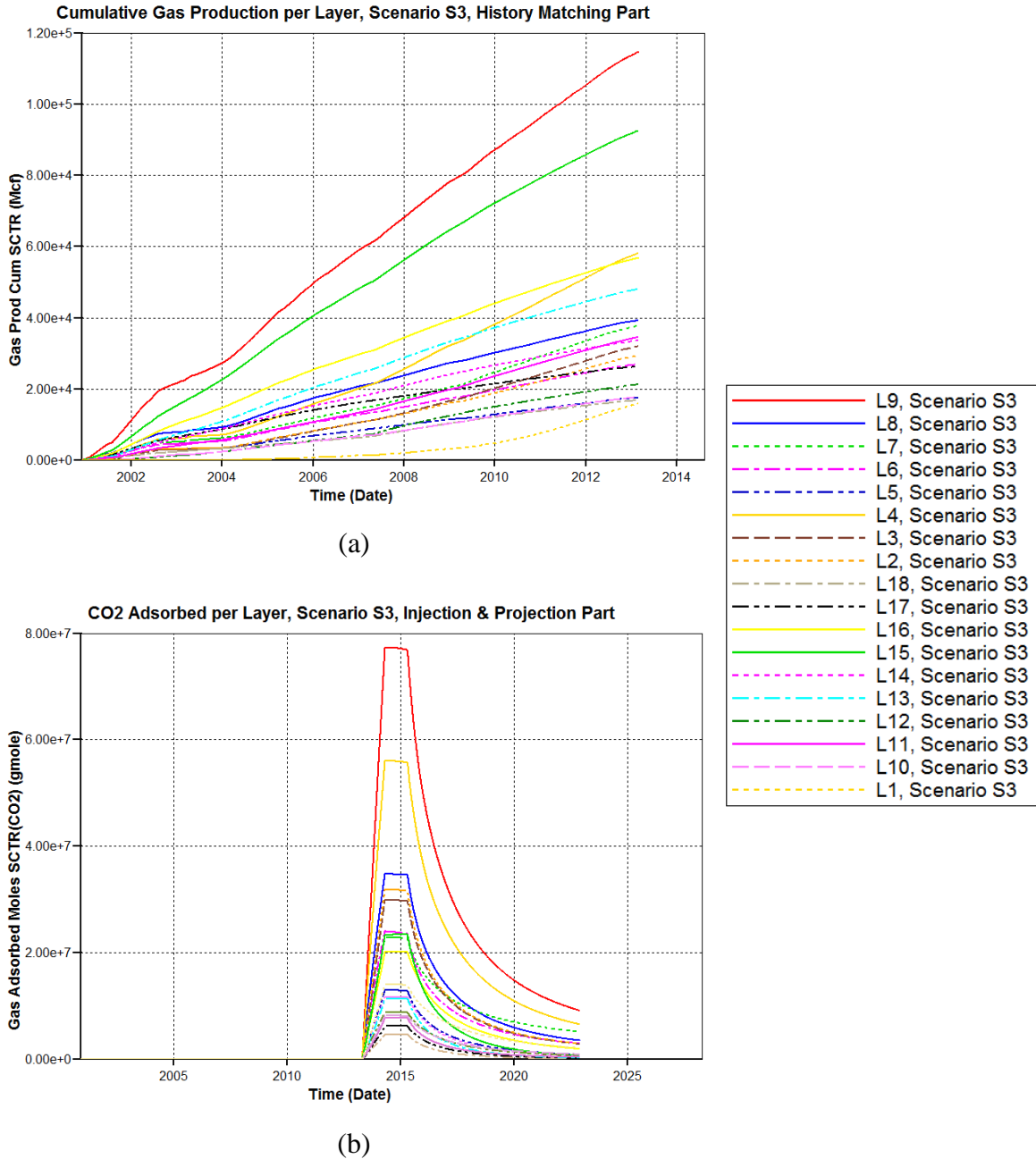


**Figure 45 - (A) Cumulative Gas Production per Layer Up to Year 2013 and (B) CO<sub>2</sub> Adsorption per Layer during Injection and Post Injection Up to Year 2023 for Scenario S3**

Scenario S3 (where hydraulic fractures were explicitly simulated) shows that the CO<sub>2</sub> plumes are more extensively developed compared to scenarios S1 and S2 (skin and base models), as shown in Figure 46, for the stimulated layers. However, since only 40 percent of the

coal seams are hydraulically stimulated the highest levels of CO<sub>2</sub> breakthrough at the offset well, DD8A, are exhibited in scenario S2 (skin scenario), where an enhanced flow zone is assigned along the wellbore for all the coal seams in the model.

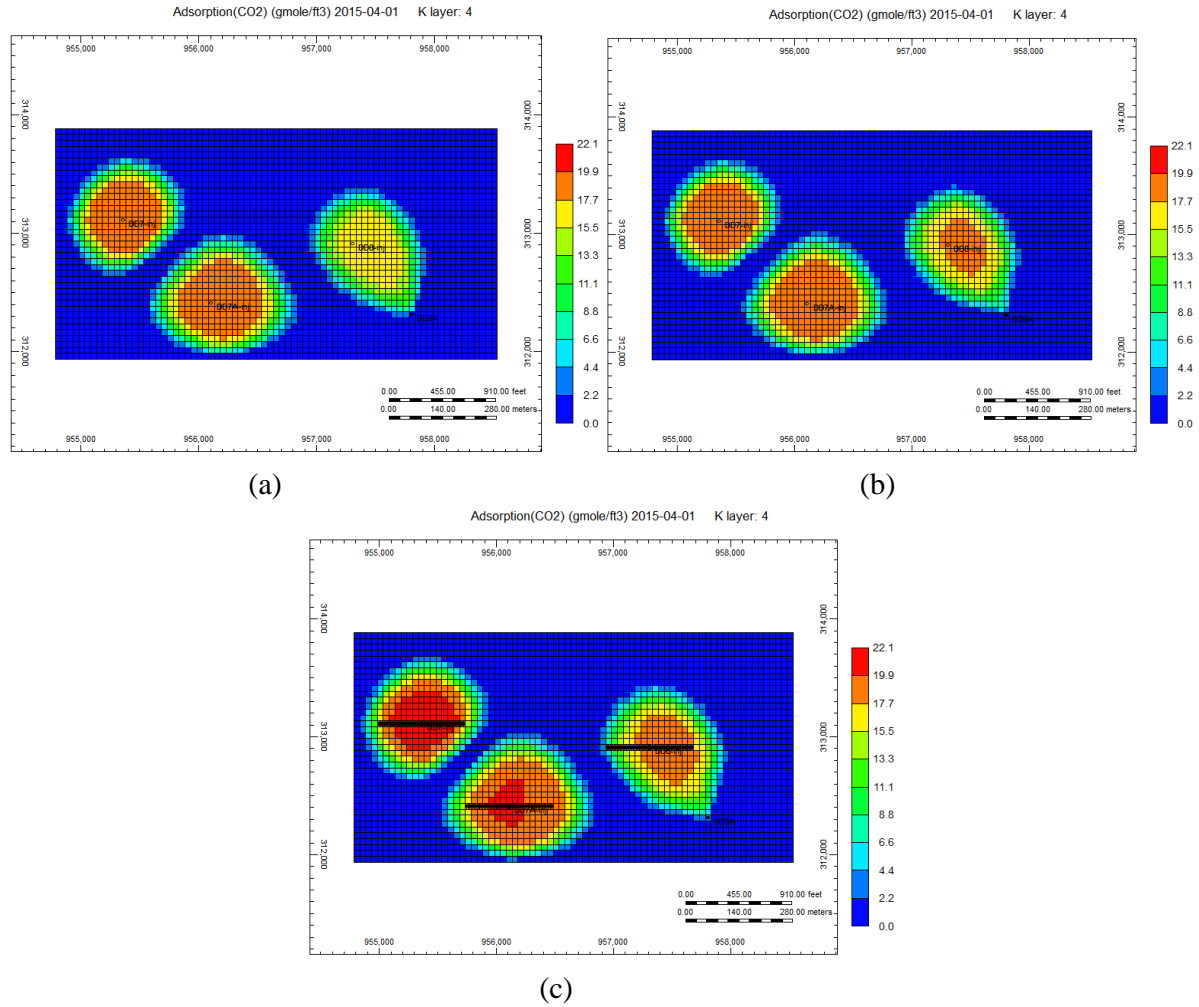


**Figure 46 - CO<sub>2</sub> Adsorption Profile in gmole/ft<sup>3</sup> at Layer 4 for Scenarios (A) S1 Base, (B) S2 Skin and (C) S3 Hydraulic Fractures Scenario**

As shown in Table 13, the results of the S model simulations show that the injection wells DD7 and DD7A produce more CO<sub>2</sub> during flowback when brought back on-line a year after injection is completed in scenario S2 compared to scenarios S1 (base model) and S3 (hydraulic fractures model). The third injector, DD8, has a higher CO<sub>2</sub> flowback in scenario S3 (hydraulic fractures model), Table 13. In all three scenarios, injector DD7 has a higher CO<sub>2</sub> flowback amount compared to DD7A and DD8; DD8 produces the least amount of CO<sub>2</sub>.

According to the modeling results of the (S) models, only 11, 6, and 10 percent of the total 20,000 tons of CO<sub>2</sub> injected in the study area is successfully (permanently) stored up to year 2023 for scenarios S1, S2 and S3, respectively. The skin model, scenario S2, which has been assigned the highest flow enhancement around the wellbore, is the one allowing for the least CO<sub>2</sub> storage and maximum flowback.

As far as ultimate field methane recovery is concerned for the (S) models, 89, 94 and 90 percent (for scenarios S1, S2 and S3, respectively) of the initial gas in place is achieved. These results are higher but still comparable to the assumption that up to more than 75 percent recovery of methane in place can be achieved with CO<sub>2</sub> injection in coalbeds (VCCER, 2011).

**Table 13 - CO<sub>2</sub> Flowback at the Injectors and CO<sub>2</sub> Breakthrough at the Offset Well for the (S) Models for Projection Time to Year 2023**

Wells	CO <sub>2</sub> Flowback at Injection Wells (Tons)		
	Base Model (S1)	Skin Model (S2)	Hydraulically Fractured Model (S3)
DD7	6,349	6,565	6,384
DD7A	5,381	5,791	5,526
DD8	5,093	4,929	5,175
	CO <sub>2</sub> Breakthrough at Offset Well (Tons)		
DD8A	963	1,462	905
CO <sub>2</sub> Total Field Production (Tons)	17,786	18,747	17,990

**Table 14 - Cumulative CH<sub>4</sub> Production for the (S) Models for the Base (S1), Skin (S2) and Hydraulic Fractures (S3) Scenarios for Projection Time to Year 2023**

Wells	Cumulative CH <sub>4</sub> Production (Std Mcf)		
	Base Model (S1)	Skin Model (S2)	HF Model (S3)
DD7	578,811	639,177	584,588
DD7A	231,607	262,101	237,485
DD8	395,162	422,485	401,668
DD8A	206,529	257,726	204,616

## **L Models**

The larger models (L) incorporated all wells within the study area. The drainage area of the 16-seam geologic structure for the (L) models was 1552 acres. Based on the input parameters, the original gas in place (OGIP) was estimated to be  $1.77e7$  standard Mcf and the original water in place to be  $2.50e5$  standard bbl.

The L models were first calibrated to match gas and water production data up to 2013. Then two different injection scenarios were applied in the simulations in order to achieve injection of 20,000 tons of CO<sub>2</sub> in wells DD7, DD7A and DD8. More specifically, in the first injection scenario (L1), 20,000 tons of CO<sub>2</sub> were equally distributed among the three injectors (approximately 6,667 tons per well) and CO<sub>2</sub> was injected at a constant daily rate of 18.26 tons/day for 365 days, in the same manner as in the (S) models. In the second injection scenario (L2), the same amount of CO<sub>2</sub> was injected per well as in scenario L1, but at a higher daily rate of 27.78 tons/day for the first 20 days of each month for a year; the injection wells were shut in during the final days of each month during injection. Figure 47 shows the CO<sub>2</sub> mass injection rate at surface conditions for injection scenarios L1 and L2 over time.

After the one-year injection period was completed, different cases were examined where the shut in period of the three injectors varied in time. The performance of all the wells within the study area was projected to year 2052.

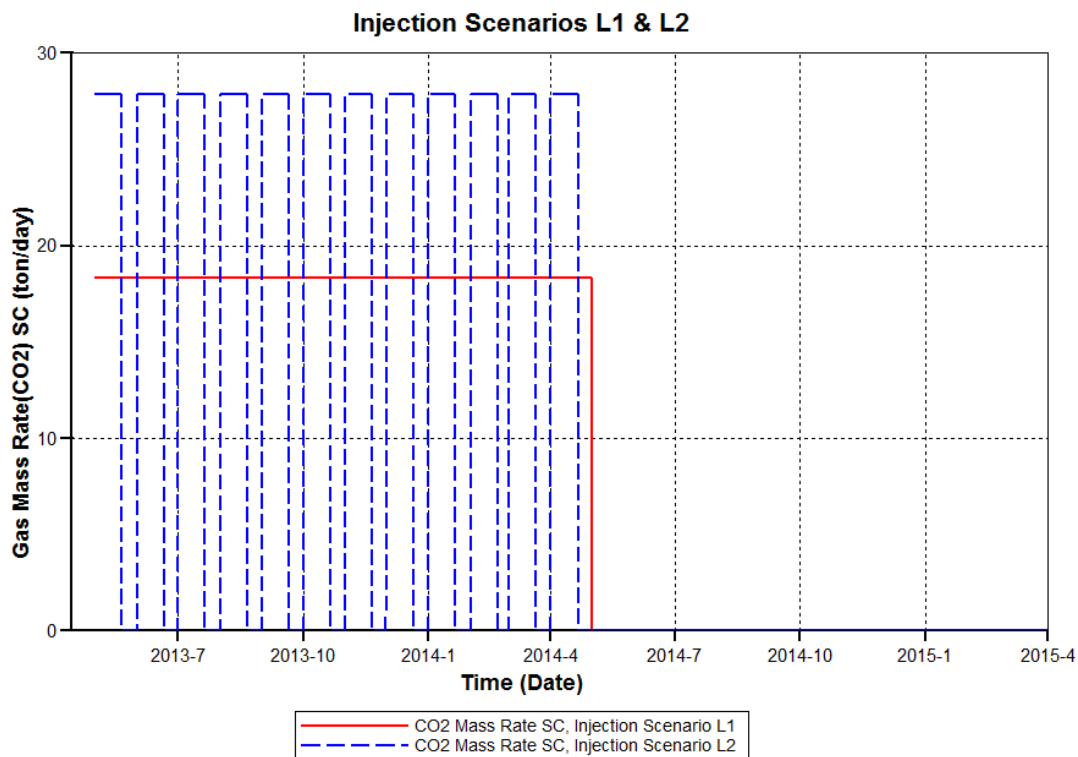


**Figure 47 - Gas Mass Rate of Injected CO<sub>2</sub> at Surface Conditions Versus Time for the Injection Scenarios L1 and L2**

Four cases with varying injection scenarios (L1, L2) and shut in periods post injection for wells DD7, DD7A and DD8 were examined. It must be noted that in all cases the well characteristics were kept constant and no skin factor or explicit simulation of hydraulic fractures was employed in the (L) models. In case L1a, injection scenario L1 was applied and the three injectors were shut in for 1 year post injection; in case L1b, injection scenario L1 was used and the injectors were shut in for 4 years; in case L2a, injection scenario L2 was employed and the selected injection wells were shut in for 1 year post injection; and in case L1c injection scenario L1 was applied and the injectors were shut in for 36 years post injection, which means they were shut in throughout the projected time of the simulation.

**During injection, for both injection scenarios L1 and L2, the bottom hole pressures in the wells did not exceed the maximum allowable pressure as indicated by a U.S. EPA class II UIC permit (VCCER, 2013). For injection scenario L1, the maximum bottom hole pressures for the three injectors DD7, DD7A and DD8 were approximately 423, 484 and 416 psi respectively; for injection scenario L2, the maximum bottom hole pressures were 482, 564 and 483 psi respectively. Also, under the specific pressure and temperature**

conditions, carbon dioxide was injected as a gas and remained in the gaseous state throughout the injection,

Figure 48.

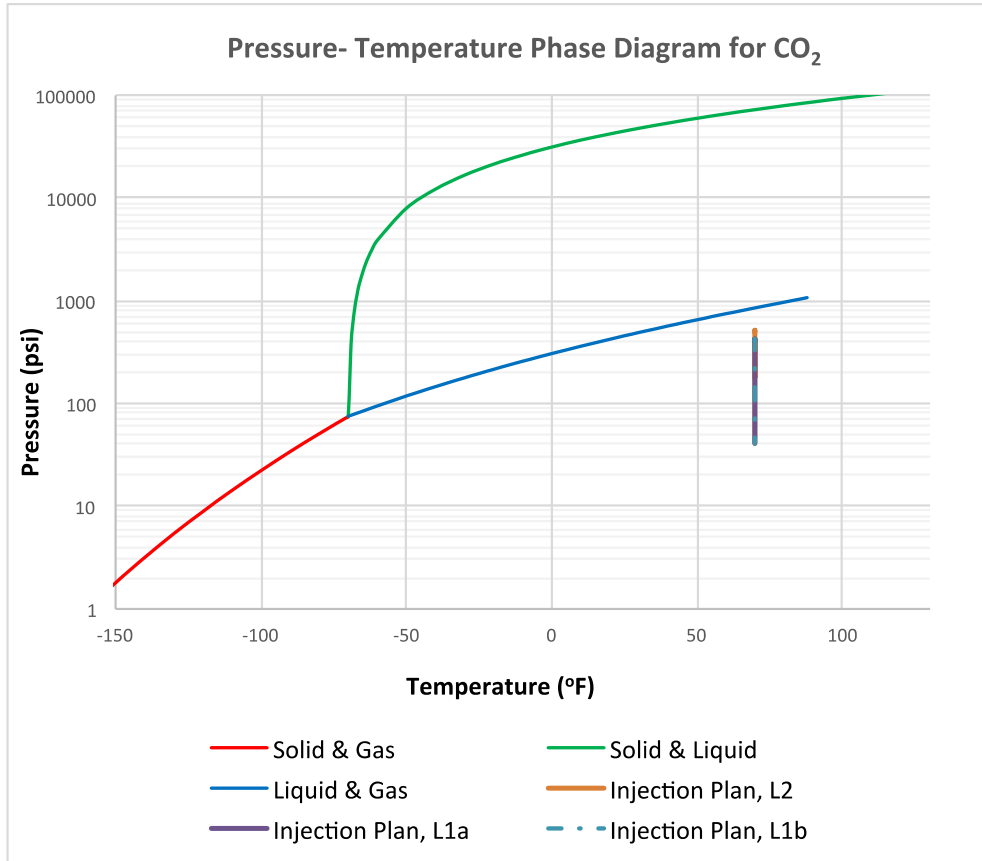
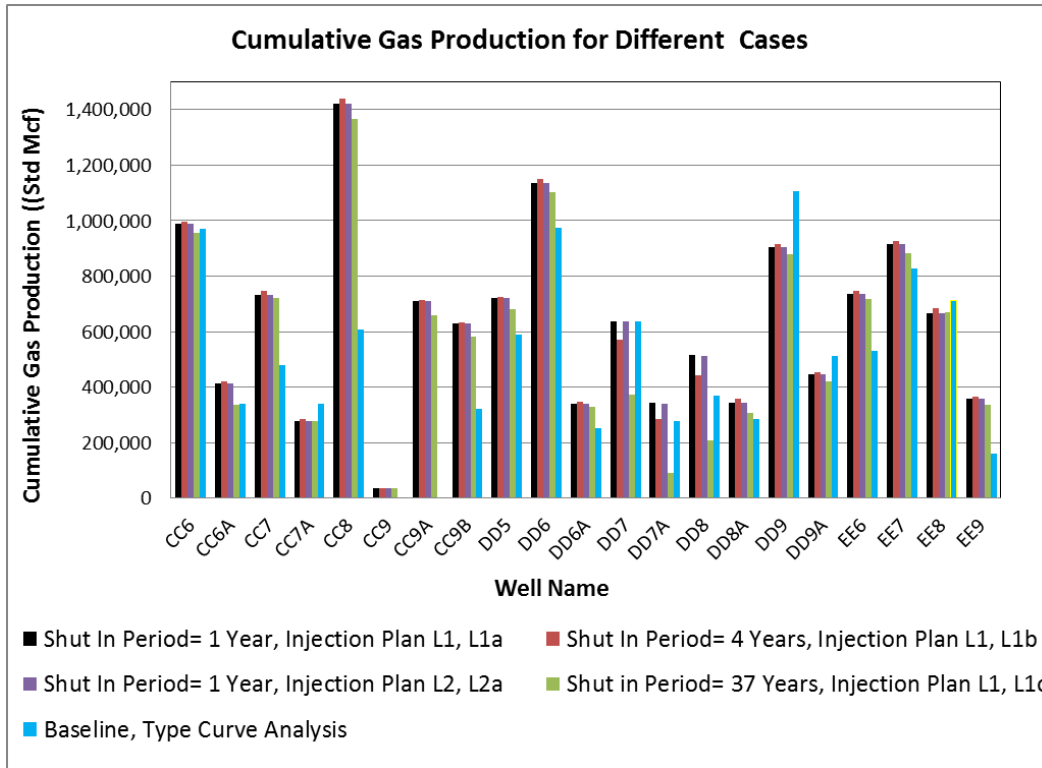


Figure 48 - Pressure-Temperature Phase Diagram for CO<sub>2</sub> and Bottom Hole Pressures at Injection Well DD7 for Injection Plans L1a, L1b, and L1



**Figure 49 - Cumulative Gas Production of All the Wells in the Study Area for All Cases Examined for the (L) Models**

The main objective of the modeling work as mentioned previously is to assess CO<sub>2</sub> storage capacity of coalbeds, examine the extent of CO<sub>2</sub> plumes and investigate the potential of enhanced gas recovery at the injectors and offset wells.

The cumulative gas production per well in the study area for all different cases (L1a, L1b, L2a, L1c) is presented in Figure 49. To estimate enhanced gas recovery of the wells, their cumulative gas production determined by the simulations is compared to the estimated ultimate recovery based on decline curve analysis. In more detail, Cardno MM&A (2013) forecasted the ultimate primary gas production of the wells within the study area without taking into account CO<sub>2</sub> injection, based solely on exponential decline curve fitting of historic gas production data (VCCER, 2013). As shown in Figure 49, for cases L1a, L1b and L2a cumulative gas production of wells CC6, CC6A, CC7, DD5, DD6, DD6A, DD8A, EE6 and EE7 is higher compared to the estimated gas production via decline curve analysis by approximately 2, 22, 53, 33, 17, 35, 15, 49 and 10 percent, respectively. For case L1c, where all three injectors remain shut in post injection until the end of the forecasted period, the cumulative gas production at wells CC7, DD5, DD6, DD6A, DD8A, EE6 and EE7 is lower than in cases L1a, L1b and L2a but it is still

enhanced in comparison to the predicted ultimate recovery of these wells without CO<sub>2</sub> injection. It must be noted that in all cases, L1a, L1b, L2a, L1c, cumulative gas production for wells CC8, CC9B and EE9 is significantly higher than what is predicted through decline curve analysis. This can be partially explained because the average pore pressure for these wells is higher due to a higher depth to the gas producing seams. In addition, the proximity of these wells to the no-flow boundary of the model should be further investigated to determine whether it contributes to the higher gas production.

Regarding CO<sub>2</sub> storage in the coal seams, it has been determined by the modeling work for cases L1a, L1b, L2a, L1c, as shown in Table 16, that 8.15, 18.2, 8.6, 81.64 percent of the total 20,000 tons were successfully sequestered up to year 2052. Comparing the two injection scenarios that have the same shut in periods for the three injectors post injection, it results that performing a type of “huff and puff” injection (scenario L2) yields slightly higher storage of CO<sub>2</sub>. With respect to case L1b, where the continuous injection plan L1 was applied and the three injectors were shut in for 4 years, less CO<sub>2</sub> as compared to cases L1a and L2a has flowed back and broken through in total. More specifically, approximately 16,354 tons of CO<sub>2</sub> versus 18,371 and 18,359 tons of CO<sub>2</sub> were produced in cases L1a, L1b and L2a, respectively. Out of all the cases investigated, the most successful regarding CO<sub>2</sub> storage - but the one with the least enhanced gas recovery - is case L1c, where the three injectors remain shut-in throughout the projected period up to year 2052.

Finally, results of the (L) models showed that ultimate field methane recovery is about 73 percent of the initial gas in place for cases L1a, L1b, L2a. For case L1c it was approximately 67 percent of the original gas in place, six percent lower than what the other models predicted.

**Table 15 - Cumulative Gas Production (CGP) for All Wells for Cases, L1a, L1b, L2a, L1c**

Wells	Different Injection Plans & Injectors Shut in Periods Models				Baseline
	CGP (Std Mcf) L1a	CGP (Std Mcf) L1b	CGP (Std Mcf) L2a	CGP (Std Mcf) L1c	EUR (Std Mcf)
CC6	987,936	994,560	987,979	954,294	971,235
CC6A	413,518	421,162	413,518	338,075	340,920
CC7	732,541	744,980	732,609	722,581	481,097
CC7A	276,046	283,501	276,089	277,727	339,373
CC8	1,422,654	1,439,308	1,422,845	1,366,867	607,132
CC9	36,651	36,651	36,651	36,651	N/A
CC9A	709,577	715,687	709,671	659,101	N/A
CC9B	629,022	633,463	629,079	580,365	320,446
DD5	720,020	723,772	720,039	682,670	588,601
DD6	1,135,585	1,146,610	1,135,673	1,102,503	972,886
DD6A	341,131	348,545	341,132	327,608	252,699
DD7	534,744	491,058	534,361	371,580	638,375
DD7A	242,935	201,746	242,843	90,420	277,865
DD8	419,415	362,923	418,783	207,072	370,263
DD8A	327,622	329,922	328,006	306,586	285,564
DD9	904,661	914,451	904,687	877,530	1,105,313
DD9A	447,732	452,743	447,714	421,883	512,732
EE6	737,057	748,151	737,105	718,395	530,887
EE7	914,234	925,790	914,227	884,206	828,465
EE8	666,874	683,045	666,752	670,343	713,174
EE9	360,081	365,278	360,108	335,567	161,065

**Table 16 - CO<sub>2</sub> Flowback and Breakthrough for Cases, L1a, L1b, L2a, L1c**

Wells	Different Injection Plans & Shut in Periods Models			
	Produced CO <sub>2</sub> (Tons) L1a	Produced CO <sub>2</sub> (Tons) L1b	Produced CO <sub>2</sub> (Tons) L2a	Produced CO <sub>2</sub> (Tons) L1c
CC6	4.95E-04	2.50E-02	9.19E-04	1.89E-01
CC6A	4.90E+00	2.23E+01	4.92E+00	6.58E+01
CC7	4.22E+00	1.72E+01	4.50E+00	5.79E+01
CC7A	5.52E-02	2.14E-01	5.88E-02	6.24E-01
CC8	1.08E-02	1.55E-01	1.61E-02	7.56E-01
CC9	0.00E+00	0.00E+00	0.00E+00	0.00E+00
CC9A	2.30E-05	2.08E-05	2.59E-05	1.87E-05
CC9B	2.70E-05	2.70E-05	2.78E-05	2.69E-05
DD5	4.16E-06	2.21E-06	3.25E-06	1.47E-06
DD6	3.10E+01	1.13E+02	3.16E+01	2.50E+02
DD6A	8.79E+00	2.54E+01	8.89E+00	5.44E+01
DD7	5.92E+03	4.70E+03	5.91E+03	0.00E+00
DD7A	5.78E+03	4.93E+03	5.77E+03	0.00E+00
DD8	5.54E+03	4.64E+03	5.56E+03	0.00E+00
DD8A	1.03E+03	1.74E+03	1.01E+03	2.85E+03
DD9	1.12E-01	7.13E-01	1.20E-01	2.21E+00
DD9A	7.60E-05	3.62E-04	7.68E-05	1.44E-03
EE6	2.25E-02	1.54E-01	2.32E-02	9.32E-01
EE7	2.86E-03	9.71E-03	2.84E-03	2.16E-03
EE8	6.44E+01	1.61E+02	6.41E+01	3.86E+02
EE9	9.99E-06	1.30E-05	1.20E-05	1.00E-05

## Conclusions

In this paper the modeling procedure for coal bed methane production and carbon dioxide injection from and into multiple seams through selected wells in Buchanan County, VA, is discussed in detail. Initially, well performance is modeled using three different modeling approaches. Results show that when a negative skin factor is assigned to the production wells, primary production during history matching, flowback of CO<sub>2</sub> at the injectors and post injection breakthrough at offset wells is possibly overestimated. When explicitly simulating hydraulic fractures, modeling is more computationally intensive but results appear more moderate compared to the case of the negative skin factor. Furthermore, when modeling the behavior of hydraulically fractured seams, the extent of the CO<sub>2</sub> plumes is more representative of actual field conditions. Nevertheless, explicit representation of hydraulic fractures introduces further modeling uncertainties on fracture parameters such as the actual width, length, effective permeability and flow properties.

The process of CO<sub>2</sub> injection into coal seams with the objective of assessing the potential enhanced gas recovery and the permanent storage of CO<sub>2</sub> was also examined.

Two different injection scenarios were examined. In the first scenario CO<sub>2</sub> was injected at a constant rate throughout the entire injection period and in the second scenario a small huff and puff injection test was performed instead, but at a higher injection rate. Results of the second scenario show that permanent CO<sub>2</sub> storage is better.

Furthermore, it was concluded CO<sub>2</sub> permanent storage is proportional to the time interval for which the injection wells are shut in post injection. Maximum CO<sub>2</sub> storage occurred when the wells were not returned to production. As a result, however, enhanced gas recovery of the field is reduced for wells with higher post injection shut in times.

## Acknowledgements

Financial assistance for this work was provided by the U.S. Department of Energy through the National Energy Technology Laboratory's Program under Contract No. DE-FC26-04NT42590 and DE-FE0006827.

## References

- CNX Gas Company LLC, 2013. Personal communication.
- Computer Modeling Group Ltd (CMG), 2003. GEM. Calgary, Canada.
- Conrad, J. M., Miller, M. J., Phillips, J., Ripepi, N. 2006. Characterization of Central Appalachian Basin CBM Development: Potential for Carbon Sequestration and Enhanced CBM Recovery, 2006 International Coalbed Methane Symposium, Preprint 0625, Tuscaloosa, AL.
- Cunningham, L., Smith, M., Miller, B., Britt, L., and Vandersypen, R. 2003. Geoscientists Provide Critical Needs for Optimal Frac Design. *Houston Geological Society Bulletin* 45:5, 45-46.
- US EPA. 2004. Evaluation of Impacts to Underground Sources June 2004 of Drinking Water by Hydraulic Fracturing of Coalbed Methane Reservoirs (Final Report). U.S. Environmental Protection Agency, EPA/816/R-04/003.
- Gash, B.W., Volz, R.F., Potter, G., and Corgan, J. M. 1993. The effects of cleat orientation and confining pressure on cleat porosity, permeability and relative permeability in coal. Paper 9321 in Proceedings of the 1993 International CoalBed Methane Symposium. Tuscaloosa: University of Alabama.
- Grimm, R. P. 2010. Seal Evaluation of the Hensley Shale for Carbon Dioxide (CO<sub>2</sub>) Enhanced Coalbed Methane Recovery in the Breathitt Group, Nora Field, Virginia. *Geological Society of America Abstracts with Programs*, 42, 137.
- Harpalani, S. 2012. Personal communication.
- Karacan, C.O. 2013. Production History Matching to Determine Reservoir Properties of Important Coal Groups in the Upper Pottsville formations, Brookwood and Oak Grove fields, Black Warrior Basin, Alabama. *Journal of Natural Gas Science and Engineering*, 10, 51-67.
- Karmis, M., Ripepi, N., Miskovic, I., Conrad, M., Miller, M., and Shea, C. 2008. CO<sub>2</sub> Sequestration in Unminable Coal Seams: Characterization, Modeling, Assessment and Testing of Sinks in Central Appalachia. Twenty-Fifth Annual International Pittsburgh Coal Conference, Pittsburgh, PA, USA, 2008. CD-ROM of Proceedings, Paper # 29-3.

- Liu, S., Harpalani, S., and Pillalamarry, M. 2012. Laboratory measurement and modeling of coal permeability with continued methane production: Part2 - Modeling Results. *Fuel*, 94, 117-124.
- Mavor, M.J. and Robinson, J.R. 1993. "Analysis of Coal Gas Reservoir Interference and Cavity Well", Paper SPE, 25860, presented at the Joint Rocky Mountain Regional and Low Permeability Reservoirs Symposium, Denver, CO, April 26-28.
- McCulloch, C.M., Deul, M., and Jeran, P.W. 1974. Cleats in bituminous coalbeds. U.S. Bur. Mines, Rept. Invest. 7910, 23.
- Mckee, C.R., Bumb, A.C., and Koenig, R.A. 1988. Stress-Dependent Permeability and Porosity of Coal. SPE-12858-PA, 3, 81-91.
- Meyer Fracturing Simulators. 2012. User's Guide Tenth Edition.
- NSI Technologies Inc. 2001. Optimum Fracture Design. *Fract Tips*. 3:1, 1-2.
- Pashin, J. 2013. Personal communication.
- Ripepi, N., Karmis, M., Miskovic, I., Shea C., and Conrad, J.M. 2009. Results from the Central Appalachian Basin Field Verification Test in Coal Seams. 26th Annual International Pittsburgh Coal Conference, Pittsburgh, PA, USA, 2009. CD-ROM of Proceedings, Paper # 33-4.
- Vasilikou, F. C., Keles, Agioutantis, Z., Ripepi, N. and Karmis, M. 2013. Model Verification of Carbon Dioxide Sequestration in Unminable Coal Seams with Enhanced Coal Bed Methane Recovery, 23rd World Mining Congress, August 11-15, Montreal, Canada.
- Virginia Center for Coal and Energy Research (VCCER). 2011. Final Technical Report: Characterization and Field Validation of the Carbon Sequestration Potential of Coal Seams in the Central Appalachian Basin, 2011: Blacksburg, VA.
- Virginia Center for Coal and Energy Research (VCCER). 2013. 6th Quarterly Report: Injecting Carbon Dioxide into Unconventional Storage Reservoir in the Central Appalachian Basin, with an Emphasis on Enhanced Coalbed Methane Recovery, to Validate Prior Geological Characterization, 2013: Blacksburg, VA.
- Virginia Center for Coal and Energy Research (VCCER). 2014. 7th Quarterly Report: Injecting Carbon Dioxide into Unconventional Storage Reservoirs in the Central Appalachian Basin, with an Emphasis on Enhanced Coalbed Methane Recovery, to Validate Prior Geological Characterization, 2014: Blacksburg, VA.

Virginia Department of Mines, Minerals and Energy (DMME). “Well Records: Completion Report”. Division of Gas and Oil Data Information System. DGO E-Forms Center. Web. 21 Dec 2011.

Virginia Department of Mines, Minerals and Energy (DMME). “Monthly Gas Production by Well”. Division of Gas and Oil Data Information System. DGO E-Forms Center. Web. 21 Dec 2013.

## SUMMARY AND CONCLUSIONS

Sequestration of carbon dioxide (CO<sub>2</sub>) into unmineable coal seams has been underway for several years as a way to mitigate the greenhouse effect with a potential of economic prosperity related to enhanced gas recovery. The Virginia Center for Coal and Energy Research (VCCER), part of the Coal Seam Group of the Southeast Regional Carbon Sequestration Partnership (SECARB), successfully completed a small scale injection project in 2009 in Russell County, VA, where 1000 tons of CO<sub>2</sub> were injected into multiple thin coal seams through one vertical well over a period of one month. In 2014, a larger scale sequestration project is scheduled, where 20,000 tons of CO<sub>2</sub> will be injected into three vertical coalbed methane wells in a coal field in Buchanan County, VA, over a one year period. The main objectives for these injection tests are to assess storage capacity of “stacked” coal seams, enhance understanding of the physical and mechanical processes taking place and examine the potential of enhanced gas recovery.

During primary coalbed methane production and enhanced production through CO<sub>2</sub> injection, a series of complex physical and mechanical phenomena occur. The ability to represent the behavior of a coalbed reservoir as accurately as possible via computer simulations yields insight into the processes taking place and is an indispensable tool for the decision process of future operations. The economic viability of projects can be assessed by predicting production, well performance can be maximized, drilling patterns can be optimized and, most importantly, associated risks with operations can be accounted for and potentially avoided.

Simulations require a large number of input parameters and high computational capabilities in order to accurately predict the behavior of the reservoir. Therefore, in current modeling practices many simplifying assumptions need to be employed. The shortcomings of the modeling approaches specific to coalbed reservoirs are:

1. In areas with complex geologic structures, it is common practice to use a simplified approach of aggregating the coal seams into zones to reduce the complexity of the model and thus the required computational intensity. However, important information with respect to the commingled production and the injection mechanism is not accounted for in this method.

2. Often to reduce modeling time in the simulation of large multi-well areas, separate single-well models are investigated, disregarding well interference of the field - one of the key parameters in coalbeds.
3. In order to minimize the computational intensity, well stimulation is either not accounted for or not representative of the in situ conditions for complex reservoirs.
4. There is an infinite solution space for history matching exercises due to the large number of unknown vs. known input parameters. Often, the calibration of the models is not constrained within an acceptable range.

In this dissertation the aforementioned shortcomings were addressed and the initial reservoir model for the Russell County site was updated. Subsequently the reservoir model for the Buchanan County test site was constructed and the preliminary simulations for CO<sub>2</sub> sequestration and enhanced gas recovery were conducted. The following were accomplished in this work:

1. Sensitivity analysis was conducted for a number of model input parameters and the key parameters and their effect identified.
2. The dynamic evolution of permeability during primary and enhanced recovery from coalbeds, which is extensively referred to in the literature, was investigated. Coupled flow and geomechanical simulations were developed to assess the significance of implementing permeability changes into full field scale simulations.
3. Well stimulation approaches, including a negative skin factor and explicit simulation of hydraulic fractures, were considered and compared.
4. Different CO<sub>2</sub> injection scenarios into multiple seams for a multi-well field area were modeled and the potential of enhanced gas recovery was assessed.

Analytical and numerical models proposed in the literature to address the phenomenon of dynamic evolution of permeability during primary and enhanced recovery in coalbeds were critically assessed. These models have been only used for single seams, single well and small area representations. An algorithm was developed to couple a reservoir simulator with a geomechanical code to examine permeability changes during methane production and CO<sub>2</sub> injection for a single coal seam. It was concluded that for relatively flat seams, where there are no areas of large stresses and strains localization, permeability changes are not significant and thus it was decided to not be considered in the full-field scale simulations.

Different modeling approaches to account for well stimulation were implemented and compared. From the analyses it was shown that assigning a negative skin factor, which is determined through history matching, often overestimates the enhanced flow properties around the wellbore and facilitates post injection flowback of CO<sub>2</sub> at the injector. Explicit simulation of hydraulic fractures can be controlled to be more representative of in situ field conditions, although more unknowns are introduced in the simulation: primary width, primary permeability, effective half-length, fracture orientation and flow regime properties. Not accounting for well stimulation can lead to unrealistic modeling results. For example, such models could not predict that during injection in the Russell County test site there would be CO<sub>2</sub> breakthrough at the monitoring well closest to the injector within hours of starting injection. More realistic modeling results were obtained where hydraulic stimulation of the injection well was included in the simulation model.

Two CO<sub>2</sub> injection scenarios for the Buchanan County, VA, site were examined. In the first scenario approximately 6,667 tons of CO<sub>2</sub> were injected into 18 coal seams at each injector at a constant rate for a year; in the second scenario a “huff and puff” type of CO<sub>2</sub> injection at a higher rate for the first twenty days per month for a year was applied. It was concluded that for the first scenario there was slightly higher CO<sub>2</sub> breakthrough at the injectors compared to the second scenario. In the second scenario there were intermediate time intervals during the one-year injection, allowing CO<sub>2</sub> to set in. From the analysis it was also shown that the time the injectors are shut in post injection is critical to the percentage of CO<sub>2</sub> successfully stored. The longer the wells are shut in the less CO<sub>2</sub> flows back at the injectors. Maximum CO<sub>2</sub> storage can be achieved when the injector well are not returned to production. CO<sub>2</sub> breakthrough at offset wells for all injection scenarios was also noted, but it was significantly less compared to flowback.

Enhanced gas recovery at the injectors and offset wells was noted in the modeling work. It was concluded that since the majority of the injected CO<sub>2</sub> flowed back, the primary mechanism for enhanced recovery for the coals in the study area is not due to the CO<sub>2</sub> preferential adsorption by the coal matrix and CH<sub>4</sub> displacement, but is because of the “renewal” of the pressures in the reservoir.

The most important conclusion for the reservoir simulation work is that it is not a straightforward process. Even though the models can provide reasonable solutions based on the

available data, it is imperative that current models are updated with new data from laboratory testing and/or field work monitoring to ensure that they remain stable and robust.

Detailed results of the aforementioned are presented in the papers included in the main body of this work.

## **Further Work**

As discussed, the main problem in reservoir modeling is the uncertainty in the magnitude and range of several input parameters. Following extensive laboratory testing related to coalbed parameters over a number of years, reservoir model input parameters have been established; however, there are still gaps in the understanding of physical processes. For improved predictions through reservoir simulations, field parameters need to be determined more accurately and at different times throughout the lifetime of a reservoir.

For instance, it is necessary to achieve better monitoring of the quantity of the water that is produced from each well during production. This would result in better history matching of the gas produced. In addition, production pressures at the well head and/or the bottom of the well should be accurately recorded.

Also, in order to better understand and “decode” commingled production from multiple seams there is a need to perform field tests where a seam or a group of seams are isolated and properties such as permeability can be determined via transient pressure testing.

Camera logging of the injectors is proposed to obtain more information regarding hydraulic fracture simulation of the well and create more representative models. In this way the modeling efforts will better capture CO<sub>2</sub> flow and potential breakthrough and storage processes.

There is a constant need to use reservoir simulators with enhanced capabilities so that less simplifying assumptions are required for the models and more details are incorporated. The next step would be to use a higher end simulator such as Eclipse by Schlumberger, where ability to model more geologic details and create larger element models is provided.

Finally, incorporating a temperature gradient in the models to better account for potential phase changes of CO<sub>2</sub> during injection and storage will be an important consideration.

## **Recommendations for Transferring Lessons Learned from Coalbed Methane Modeling to Shale Gas Modeling**

Research on primary production from coalbed reservoirs has been underway for several decades. The best practices to estimate the original gas in place are established and there is agreement within the research community on the basic methane production mechanism. Yet there are still questions which need to be answered, as previously mentioned, to further understand the production mechanism from multiple thin unmineable coal seams and the interaction with CO<sub>2</sub> injection. Currently, there is an interest in the industry to transfer the experiences and expertise from coalbed reservoir to “unlock” the great energy potential of the shale reservoirs.

In both coalbed and shale reservoirs a significant portion of the gas in place is stored via adsorption on the rock matrix. This is their main - and should be considered to be their only - similarity. There are significant differences between the geologic properties, such as initial pore pressure, porosity and adsorption isotherms that result in different initial volumetrics and production mechanisms. In addition, shale gas reservoirs are usually much deeper than coalbed methane reservoirs. The decades of coalbed methane research poses the right questions to be answered in order to identify the critical unknown parameters in hydrocarbon exploration from shale reservoirs. However, there should not be a direct transfer of properties from coalbeds to shale reservoirs since it is likely to lead to the wrong conclusions. Regarding primary production from shales, the following critical questions need to be addressed:

1. What is the effective volume activated through hydraulic stimulation, depending on the stimulation technology employed, particularly with regard to the frac-fluid composition? Further field characterization and monitoring is required.
2. What are the different flow regimes for the (i) primary artificial channels developed with hydraulic stimulation, (ii) the activated dendritic pattern perpendicular to the primary fractures, and (iii) within the shale matrix? Field determination through pressure transient testing and further laboratory-testing accounting for in situ conditions needs to be conducted to determine permeability ranges for each case.
3. What happens to the water used for hydraulic treatment? In the case where it is produced, how are the relative permeability curves affected? If it stays in the

reservoir how are the pressure profile, and the consequent gas release from the shale formation, shaped?

4. What percentage of the original estimated gas in place is recovered in relation to the well characteristics, such as lateral length, orientation to in situ stresses, proximity to other wells, frequency and intensity of hydraulic stages?
5. Could the use of CO<sub>2</sub> for well stimulation, pressure management and/or hydraulic fracturing benefit the production of both gas and condensate, specifically the ability of CO<sub>2</sub> to change the viscosity of immobile condensates and allow for their production?

There are a number of issues that need to be resolved if shale reservoirs are to be used for permanent CO<sub>2</sub> storage in a similar manner to deep coal seams. It has been determined that there is a larger affinity of CO<sub>2</sub> to the coal and the shale matrix compared to CH<sub>4</sub>, especially in shale when there is an increase of clay content. The in situ behavior of CO<sub>2</sub> and the coal matrix is still under investigation through a series of small and medium CO<sub>2</sub> sequestration projects in unmineable coal seams. The same aspects should be examined for the case of CO<sub>2</sub> sequestration in shale reservoirs with the investigation of CO<sub>2</sub> properties under the different depth and pressure conditions of shales. In addition, there is less interference between wells and different well development patterns when exploiting shale reservoirs; the potential of enhanced gas recovery at offset wells should also be examined and potentially could be negligible depending on well drilling patterns and spacing

Historic production data for coalbeds are available for in excess of 20 to 30 years, a large portion of the assumed life of a 50-year well. Type curve fitting of the historic points and development of decline curve analysis to estimate the behavior of new coalbed methane wells is well established. From the curve fitting it is concluded that for production of coalbeds there is an initial period of dewatering and increase of the gas rate, then a plateau in production due to commingle production from multi-seams and at the end a decline period which is best fitted with an exponential segment. The historic production data available for horizontal shale wells in most basins are limited to production of approximately seven years. For initial production, a sharp decline is best fitted via a hyperbolic decline segment for production of free gas in the system and for the rest of the well life an exponential decline is assumed given that desorption from the

shale matrix will be activated. Data are still not available to support this argument. However, it is evident that there is a different production mechanism in shale compared to coalbed.

To understand the physical and dynamic occurring processes in shales, all the pertinent properties need to be evaluated from the nano scale to investigate the adsorption/desorption properties, and moving toward larger scales to bridge the knowledge of the micro to the macro processes. Extensive field characterization is required by monitoring wells and with in situ properties testing. Most importantly, production data must be collected over a period of time to evaluate the basic production mechanism.